PhD

PROGRAM IN TRANSLATIONAL AND MOLECULAR MEDICINE

DIMET

UNIVERSITY OF MILANO-BICOCCA

SCHOOL OF MEDICINE AND FACULTY OF SCIENCE

Anti-amyloidogenic activity of a mutant form of Aβ: a new strategy for Alzheimer therapy

Coordinator: Prof. Andrea Biondi

Tutor: Dr. Fabrizio Tagliavini

Dr. Marcella Catania

Matr. No. 601386

XXIV CICLE

ACADEMIC YEAR

2010-2011

Table of contents

ALZHEIMER'S DISEASE

Alzheimer's Disease (AD) is the most common cause of dementia in the elderly, with current estimates reporting more than 30 million people affected worldwide. With the continuing increases in life expectancy, this number and the staggering costs associated with the care of patients debilitated by AD are expected to quadruple within the next 40 years. In the United States alone, there are more than 5 million AD patients, with 10 million caregivers, and it is the nation's third most expensive disease, already costing the US government close to $200 billion a year[1].

AD is a progressive neurologic disease that results in the irreversible loss of neurons, particularly in the cortex and hippocampus[2]. The clinical hallmarks are progressive impairment in memory, judgment, decision making, orientation to physical surroundings, and language. Diagnosis is based on neurologic examination and the exclusion of other causes of dementia; a definitive diagnosis can be made only at autopsy. The key features of AD are neuronal and synapse loss, extracellular senile plaques containing the peptide β amyloid and neurofibrillary tangles, composed of a hyperphosphorylated form of the microtubule-associated protein tau.

The aetiological events leading to AD pathogenesis are unclear. Although age and the inheritance of predisposing genetic factors appear to play a major role, more recent evidence suggests that the development and progression of AD is subject to a wide variety of both environmental and genetic modifiers[3]. In general, two subgroups

are recognized upon the age at which the first clinical symptoms become apparent: early-onset AD (onset age < 65years) and late-onset AD (onset age > 65 years). There is no single gene that accounts for AD heritability, despite some clues that have been provided by genetic analysis of rare cases of early-onset familial Alzheimer's Disease (FAD) which are caused by missense mutations in the amyloid precursor protein (APP) and presenilin-1 and -2 (PS1 and PS2) genes. The vast majority of late-onset AD cases, which account for > 99% of all AD cases, are sporadic; mutations and polymorphisms in multiple genes are likely to contribute to sporadic AD pathogenesis together with non-genetic factors[4]. Although most patients develop AD at later age, it is mainly the research performed on the rare autosomal-dominant early-onset form that provided valuable insights into disease pathogenesis.

Currently, the knowledge of the pathogenic pathway leading to the disease is largely incomplete and there is no effective treatment that delays the onset or slows the progression of AD.

There have been tremendous advances in our understanding of the scientific underpinnings of AD over the last 30 years. Major advances in genetics, cell and molecular biology, systems neuroscience, and biomarkers have set the stage for the development of the first truly effective therapies for AD. However, transitioning from scientific understanding to treatments to help AD patients has been painfully slow. Much more work is needed in the following areas: the cell and molecular biology of protein aggregate formation and neurodegeneration; genetics; developing informative biomarkers and reliable methods of early diagnosis; and the design and

implementation of new clinical trials. The stage is set to accomplish these goals and there is reason to be optimistic that truly effective disease-modifying treatments for AD can be developed in the next decade[1].

1. Clinical features

1.1 Sporadic AD

Sporadic AD is the most common form of dementia in humans over the age of 65 and affects more than 50% of individuals 85 or older. It represents the majority of AD cases (> 90% of total AD patients).

Neuropathological hallmarks of AD, identified more than 100 years ago, are the intraneuronal neurofibrillary tangles (NFT), that consist in deposits of hyperphosphorylated protein tau in the form of paired helical filaments, and the parenchymal extracellular deposits composed of both diffuse preamyloid lesions and mature amyloid plaques. Together with these features, fibrillar amyloid deposition is also commonly observed in medium-sized and small cerebral vessels. Although its significance was ignored for decades, the vascular dysfunction resulting from amyloid deposition at the cerebral vessel walls is considered today an active player in the mechanism of neurodegeneration and a major contributor to the disease pathogenesis[5].

It is diffusely accepted that clinical alterations in AD patients correlate with tau-linked pathology rather than with amyloid-related pathology. The temporal evolution of the topographic distributions of plaques and NFTs parallels the onset and progression of

neuropsychological deficits[6]. The initial typical involvement of mesial temporal structures[7] results in an early impairment of anterograde episodic memory. Usually the next cognitive domain to be involved is semantic memory, correlating with spread of NFTs to lateral temporal neocortex. Selective attention may also be disturbed at this stage[8]. In the middle stages of the disease, the spreading of pathology in the temporoparietal association cortex may manifest as impairment of comprehension, visuoperceptual dysfunction and apraxia. The prefrontal association cortex may also be affected, resulting in impairment of sequencing, planning and self-monitoring. Primary motor, sensory and visual cortices are relatively spared, correlating with a paucity of motor, somatic sensory and visual findings on neurological examination. In the later stages of the disease the patient is unable to cooperate meaningfully with standard neuropsychological assessment, although specialized cognitive batteries may still delineate residual capabilities[9].

A recent revision of the NINDS-ADRDA criteria established in 1984 has been recently done by the National Institute on Aging and the Alzheimer's Association workgroup, in an attempt of introducing diagnostic tools for the detection of early stages of the disease. Similar efforts have been recently made by Dubois and colleagues[10], which have proposed for the diagnosis of AD a group of core clinical diagnostic criteria together with supportive criteria including several biomarkers of the disease, and a group of exclusion criteria.

Among the supportive criteria, great relevance has been attributed to: (i) atrophy of medial temporal structures on MRI; (ii) abnormal cerebrospinal fluid biomarkers (particularly Aβ1-42, total

tau and phosphorylated tau); (iii) specific metabolic pattern evidenced with molecular neuroimaging methods, including PET studies with Pittsbourg Compound B or other ligands for amyloid; (iv) familial genetic mutations.

1.2 Familial AD

Despite the great progress in the field of AD genetics that has led to the discovery and confirmation of three autosomal-dominant early-onset genes and a late-onset risk-factor, a number of other additional major AD loci are predicted to exist[11].

Familial forms of AD (fAD) account for less than 5% of the total cases. They are linked to mutations in three different genes codifying for APP, PS1 and PS2, and are transmitted as autosomal dominant genetic disease with virtually complete penetrance. In addition, specific allelic combinations of the APOE gene have been identified as risk factors for the disease[12]. Late-onset Alzheimer's is conversely characterized by a considerably more multifaceted and interwoven pattern of genetic and non-genetic factors that is only poorly understood (Fig. 1).

The clinical presentation of fAD is generally very similar to that of sAD. Like sAD, most fAD cases present with an insidious onset of episodic memory difficulties followed by irreversible progression of multiple cognitive deficits. The most obvious difference between familial and sporadic cases of AD is the younger age at onset in individuals with fAD mutations, especially those carrying PSEN1 mutations. In these cases symptoms typically first appear between the ages of 30 and 50 years, but some families have individuals affected

in their 20s[13]. Patients carrying genetic defects in the APP gene usually have a later age at onset, typically in the 50s and ranging from 45 to 60 years old. fAD linked to PSEN2 mutations has a wide range of onset that includes also late-onset cases. Overall survival in fAD is also similar to that of sAD. PSEN1 mutation carriers may have slightly shorter survival.

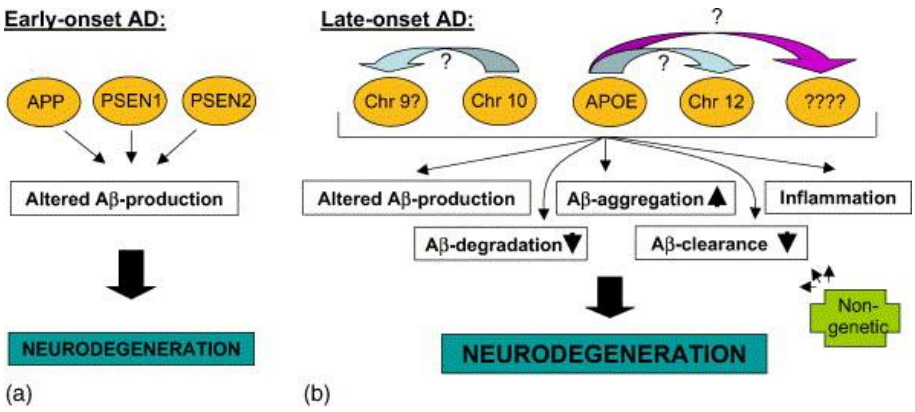

Figure 1. Scheme of contribution and interaction pattern of known and putative AD genes. (a) Mutations in the early-onset AD genes. (b) Simplified scheme of the interaction pattern of known and proposed late-onset AD genes. Likely, these risk-factor genes each affect one or more of the known pathogenic mechanisms leading to neurodegeneration in AD. Their effects are further influenced by gene–gene interactions and the contribution of non-genetic risk-factors[11].

The majority of fAD cases have an amnestic presentation very similar to that seen in sporadic disease, with the first deficits being in visual and verbal recall and recognition. Longitudinal studies of unaffected at-risk individuals have suggested that the earliest neuro psychometric findings involve a fall in verbal memory and performance IQ scores [14], with relatively preserved naming[15]. Atypical presentations with language deficits, behavioral abnormalities, focal neurological signs and symptoms are more common in familial cases.

Several PSEN1 mutations are variably associated with a spastic paraparesis, extrapyramidal and cerebellar signs. APP mutations that cluster within the Aβ coding domain around positions 692 to 694 usually exhibit a phenotype characterized by cerebral hemorrhage, probably related to extensive amyloid angiopathy. Amyloid angiopathy and seizures are also common features occurring in families carrying APP duplication[16].

2. Neuropathologic features

2.1 Diffuse ("Preamyloid") plaques

Many of the plaques found in limbic and association cortices, and almost all of those in brain regions not clearly implicated in the typical symptomatology of AD, such as thalamus, caudate, putamen, cerebellum, showed relatively light, amorphous Aβ immunoreactivity that occurred in a finely granular pattern, without a clearly fibrillar, compacted center. In most of these nonfibrillar plaques, very little of neuritic dystrophy is detected. The recognition of these amorphous plaques in the late 1980s[17,18] and their detection in regions that also contained many neuritic plaques led to the concept that they might represent precursor lesions of neuritic plaques. These lesions were thus referred to as "diffuse" plaques or "preamyloid deposits". Later, it became apparent that peptides ending at Aβ42 were the subunits of the material comprising the diffuse plaques, with little or no Aβ40 immunoreactivity, in contrast to the mixed deposits that generally were found in the fibril-rich neuritic plaques[19]. The hypothesis that diffuse plaques represent immature lesions that are precursors to the

plaques with surrounding cytopathology arose from two lines of evidence. First, diffuse plaques
were the sole form found in those brain regions that largely or entirely lacked neuritic dystrophy, glial changes and neurofibrillary tangles and were not clearly implicated in the typical clinical symptoms of AD, such as cerebellum, striatum and thalamus. Second, healthy aged humans free of AD or other dementing processes often showed diffuse plaques in limbic and association cortices, which are the same regions where Alzheimer patients showed mixtures of diffuse and neuritic plaques.

2.2 Neuritic plaques

Neuritic plaques are microscopic foci of extracellular amyloid deposition and associated axonal and dendritic injury (Fig. 2), generally found in large numbers in the limbic and association cortices[20]. These plaques contain extracellular deposits of Aβ, occurring principally in a filamentous form. Dystrophic neurites occur both within these amyloid deposits and immediately surrounding them; they are often dilated and tortuous and marked by ultrastructural abnormalities that include enlarged lysosomes, numerous mitochondria and paired helical filaments. These plaques are also intimately associated with activated microglia and they are surrounded by reactive astrocytes displaying abundant glial filaments. The microglia is usually within and adjacent to the central amyloid core of the neuritic plaque, whereas the astrocytes often ring the outside of the plaque, with some of their processes extending centripetally toward the amyloid core. The time that it takes to

develop such a neuritic plaque is unknown, but these lesions probably evolve very gradually over a substantial period of time, perhaps many months or years. Much of the fibrillar Aβ found in the neuritic plaques is composed by the species ending at amino acid 42 (Aβ42) [21], even if Aβ40 is usually colocalized with Aβ42 in the plaques.

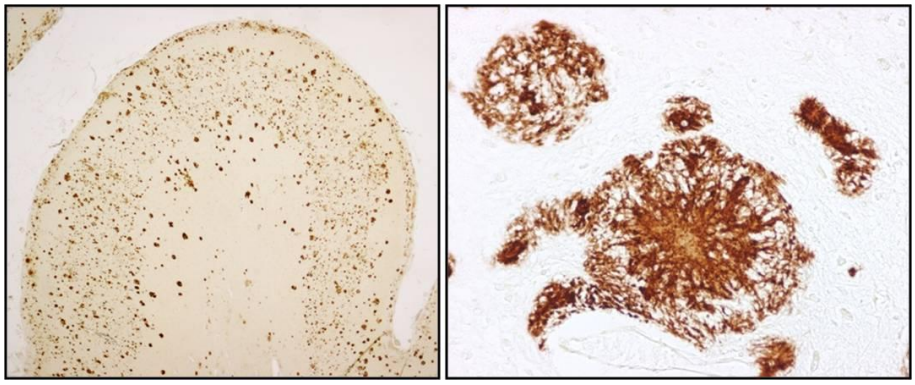

Figure 2. Neuropathology of AD brains: senile plaques.

2.3 Cerebral Amyloid Angiopathy (CAA)

Aβ was originally isolated from amyloid-laden meningeal arterioles and venules that are often found just outside of the brains of patients with AD[22]. Similarly, small arterioles, venules, and capillaries within cerebral cortex also frequently bear amyloid deposits (Fig.3). This microvascular angiopathy is characterized at the ultrastructural level by amyloid fibrils found in the abluminal basement membrane of the vessels, sometimes with apparent extension of the fibrils into the surrounding perivascular neuropil. The Aβ peptides that occur as filaments in the microvessel basement membranes appear, on the basis of immunoreactivity, to be principally Ab40 species[23].

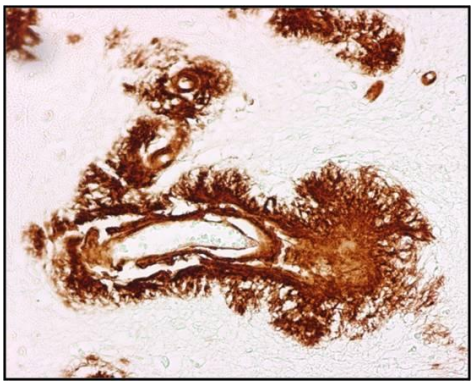

Figure 3. Neuropathology of AD brains: cerebral amyloid angiopathy.

2.4 Neurofibrillary tangles

Many neurons in the brain regions typically affected in AD (entorhinal cortex, hippocampus, parahippocampal gyrus, amygdala, frontal, temporal, parietal and occipital association cortices, and certain subcortical nuclei projecting to these regions) contain large, non-membrane bound bundles of abnormal fibers that occupy much of the perinuclear cytoplasm (Fig.4). Electron microscopy reveals that most of these fibers consist of pairs of about 10-nm filaments wound into helices (paired helical filaments or PHF), with a helical period of about 160 nm. Immunocytochemical and biochemical analyses of neurofibrillary tangles suggested that they were composed of the microtubule-associated protein tau[19,24]. This was later confirmed by isolation of a subset of PHF that could be partially solubilized in strong solvents such as SDS[25], releasing tau proteins which migrated electrophoretically at a higher molecular weight than did normal tau prepared from tangle-free human or animal brains. This slower migration was shown to result from increased phosphorylation of tau; in vitro dephosphorylation with alkaline phosphatase returned this

PHF-derived tau to essentially normal migration. Although some PHF can be solubilized by boiling in SDS, much of the tau in tangles is present in highly insoluble form[26].

The two classical lesions of AD, neuritic plaques and neurofibrillary tangles, can occur independently of each other. Tangles composed of tau aggregates that are biochemically similar to or, in some cases, indistinguishable from those in AD have been described in more than a dozen less common neurodegenerative diseases, in almost all of which no Aβ deposits and neuritic plaques have been found. Conversely, Aβ deposits can be seen in the brains of cognitively normal-aged humans in the virtual absence of tangles. There are also infrequent cases of AD itself which are "tangle poor", where only a few neurofibrillary tangles are found in the neocortex despite abundant Aβ plaques[27]. It appears that in quite a few cases, an alternate form of neuronal cytoplasmic inclusion, the Lewy body (composed principally of a-synuclein protein), is found in cortical pyramidal neurons. In other words, the Lewy body variant of AD may represent a tangle-poor form of AD that still has the usual amount of Aβ plaque formation[28]. There is growing evidence that the formation of tangles in AD represents one of several cytological responses by neurons to the gradual accumulation of Aβ and Aβ-associated molecules.

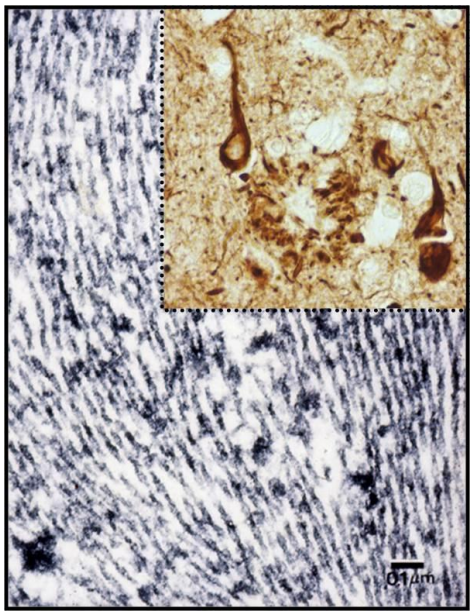

Figure 4. Neuropathology of AD brains: neurofibrillary tangles.

3. AD Pathogenesis

3.1 Amyloid Precursor Protein: synthesis, trafficking and processing

The specific accumulation of neurotoxic amyloid-β (Aβ) derived from the post-translational proteolysis of the Amyloid Precursor Protein (APP) in the Central Nervous System (CNS) is a major pathological step in the progression of AD. [29]

APP is an ubiquitously expressed type 1 membrane glycoprotein and is encoded by a single gene on chromosome 21q21. APP comprises a heterogeneous group of ubiquitously expressed polypeptides migrating between 110 and 140 kDa on electrophoretic gels [30]. This heterogeneity arises both from alternative splicing (yielding 3 major isoforms of 695, 751, and 770 residues) as well as by a variety of posttranslational modifications, including the addition

of N- and O-linked sugars, sulfation, and phosphorylation. [31]The APP splice forms containing 751 or 770 amino acids are widely expressed in non-neuronal cells throughout the body and also occur in neurons. However, neurons express even higher levels of the 695 residue isoform, which occurs at very low abundance in non-neuronal cells. [32] The difference between the 751/ 770- and 695 residue forms is the presence in the former of an exon that codes for a 56 amino acid motif that is homologous to the Kunitz-type of serine protease inhibitors (KPI), indicating one potential function of these longer APP isoforms. Indeed, the KPI-containing forms of APP found in human platelets serve as inhibitors of factor XIa, which is a serine protease in the coagulation cascade. [33] APP is highly conserved in evolution and expressed in all mammals in which it has been sought. A partial homolog of APP is found in Drosophila (referred to as APPL) [34]. Indeed, APP is a member of a larger gene family, the amyloid precursor-like proteins (APLPs)[35,36], which have substantial homology, both within the large ectodomain and particularly within the cytoplasmic tail, but are largely divergent in the Aβ region.

APP is cotranslationally traslocated into the endoplasmic reticulum by its signal peptide and matures through the central secretory pathway, with only a small percentage of holoproteins reaching the cell surface. APP has one 23-residue hydrophobic stretch near its C-terminal region that serves to anchor APP in internal membranes and in the plasmalemma[37].

Both during and after the trafficking of APP through the secretory pathway, it can undergo a variety of proteolytic cleavages to release secreted derivatives into vesicle lumens and the extracellular

space (Fig. 5). In the non-amyloidogenic pathway APP is cleaved by a proteinase-activity known as α-secretase, resulting in the production of the extracellular soluble form sAPPα, which seems to have neuroprotective activity[38], and the membrane-retained C-terminal fragment C83. Since this cleavage occurs at the lys16-leu17 bond within the Aβ domain, it prevents the deposition of intact amyloidogenic peptide. Cleavage of APP by activation of α-secretase is a relatively major and ubiquitous pathway of APP metabolism in most cells[39]. In the alternative amyloidogenic pathway APP is cleaved by β-secretase, generating the extracellular sAPPβ and the C-terminal fragment C99[4]. The final cleavage of the C83 and C99 peptides by γ-secretase produces the non-toxic p3 fragment and the amyloidogenic Aβ peptide, respectively. γ-cleavage of APP produces also an intracellular tail fragment (AICD)[40], which forms a multimeric complex with the nuclear adaptor protein Fe65 and the histone acetyltransferase TIP60. This complex potentially stimulates transcription, suggesting that release of AICD may function in gene expression[4].

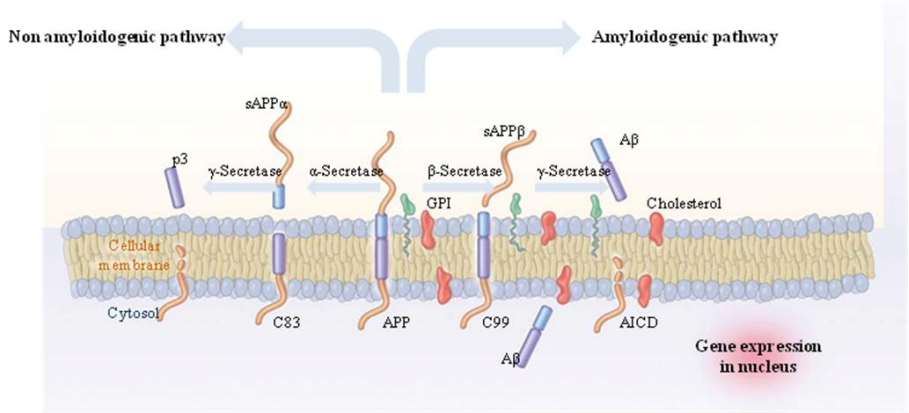

Figure 5. Processing of Amyloid Precusor Protein[41].

3.1.1 α-secretases

Several proteins with α-secretase-like activity have been identified. They are membrane-anchored disintegrin and metalloproteinases including ADAM17 (also called TACE), ADAM10 and ADAM9[42-44]. All members display a common domain organization and possess four potential functions: cell fusion, cell adhesion, intracellular signaling and proteolysis. The constitutive α-secretase activity is primarly at the cell surface, while the regulated activity is predominantly located within the Golgi apparatus[4].

3.1.2 β-secretases

Two enzymes capable of β-cleavage have been identified: the β-site APP cleavage 1 (BACE1) and 2 (BACE2) [45-47]. BACE1 is a transmembrane aspartyl protease[48,49]; its mRNA is found at very high levels in pancreas, at moderate levels in brain and at low levels in most peripheral tissues[49], but the β-secretase activity is high in brain only. Studies in BACE1 knock-out mice provide strong evidence that BACE1 is the major β-secretase in the brain and its inhibition a target for therapeutic intervention[50,51]. BACE1 is the key rate-limiting enzyme that initiates the formation of Aβ[52]. Over-expression of BACE1 in cell culture increased the amount of β-secretase cleavage products[49]. Moreover, a transgenic mouse line expressing human BACE1 in the brain induces the amyloidogenic processing of APP and elevates the steady-state levels of Aβ1-40 and Aβ1-42[53]. In addition, knock-out of the BACE1 gene completely impairs the β-secretase cleavage of APP and abolishes the generation of Aβ[50]. BACE1 generates the N-terminus of Aβ by cleavage at either Asp1 (β-site) or

Glu11 (β'-site) ultimately leading to the production of the 4KDa Aβ isoforms beginning at position Asp1 and the 3KDa Aβ species beginning with Glu11[54]. Whilst the functional significant of this N-terminal heterogeneity remains unclear, a variety of the shorter species aggregate more quickly *in vitro* than their full-length counterparts[55]. The preference of the protease for β or β' cleavage is strongly dependent on intracellular localization: within the Endoplasmic Reticulum (ER) β-site proteolysis predominates, while in the trans-Golgi network β' cleavage is favoured[56].

The related transmembrane aspartyl protease BACE2 shows similar substrate specificity[57]; its mRNA is widely expressed at low levels in peripheral tissues and at higher levels in colon, kidney, pancreas, placenta, prostate, stomach and trachea, but only at low or undetectable levels in the brain, where protein expression is also very low[58]. Therefore, it was thought that it might play a less important role in generating Aβ than BACE1. However, an increased production of Aβ from APP by BACE2, but not BACE1, was found to be associated with the Flemish mutation, suggesting that BACE2 contributes to Aβ production in these individuals[57]. Despite these observations, the precise role of BACE2 in APP processing remains unclear.

3.1.3 γ-secretases

The γ-secretase complex is composed of four core proteins, presenilin 1 (PS1)[59] or presenilin 2 (PS2)[60], anterior pharynx defective 1 (APH1)[61], nicastrin (NCT)[62], and presenilin enhancer 2 (PEN2)[61], whose presence is required for physiological activity (Fig. 6). Because APH1 exists as two separate homologues in humans and one

undergoes alternative splicing, there are six combinations of PS1 or PS2 presenilin complexes. In addition, one or more regulatory proteins, such as transmembrane trafficking protein (TMP21)[63] and c-secretase-activating protein (gSAP)[64], whose presence is not essential, interact with a subset of complexes. The presenilin complexes mediate the regulated intramembranous proteolysis of several type I transmembrane proteins[65,66].

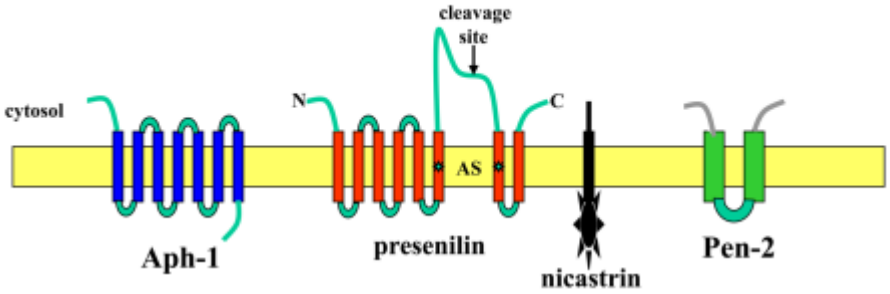

Figure 6. Structure of γ-secretase complex. γ-secretase cleaves APP within a transmembrane region; it is composed by four different proteins: presenilin, nicastrin, Aph-1 and Pen-2[67].

PS1 and PS2 are ubiquitously expressed membrane proteins comprising eight membrane-spanning regions with cytoplasmic orientation for both the N- and C-termini[46,68]. The unstable holoproteins were found to udergo constitutive endoproteolysis in many cell types and tissues and quickly converted into stable and functional heterodimers comprising the N-terminal fragment (NTF) and the C-terminal fragment (CTF). The endoproteolysis occurs within the ER vesicles with subsequent stabilization of the fragments in the Golgi[69]. The cleavage occurs within a hydrophobic portion of the cytoplasmic loop between the sixth and the seventh

transmembrane domains; thus, NTF and CTF are thought to be the biologically active forms of the proteins[70]. Excess PS holoproteins are rapidly degraded, mainly by the proteasome[71,72]. Once formed, PS fragments can associate into higher molecular mass (100–200 kDa) complexes that may represent the principal form in which presenilin functions in cells[73,74].

The biological mechanism of presenilin action is unknown; they might be involved in various biological processes, such as cell adhesion[75], G-protein mediated signaling[76], controlling transmembrane kinase/endoribonuclease Ire-1 proteolysis and unfolded protein response signaling[77] and protein trafficking[78]. PS1 is also thought to have a role in the regulation of signal transduction during development, in apoptosis, and possibly in cellular calcium ion homeostasis. The former suggestion arose because null mutations in a PS orthologue of C. elegans (sel-12) exert a suppressor effect on abnormalities in vulva progenitor cell fate decisions induced by activated Notch mutants[79]. Notch is involved in intercellular signalling during development. PS effects on Notch signalling is further supported by the fact that targeted disruption of the murine PS1 gene causes embryonic lethality around day 13 and is associated with severe developmental defects in somite formation and axial skeleton formation, the occurrence of cerebral hemorrhage and reduced Notch1 transcription in selected cell types[80,81]. Similar phenotypes have been observed in knockout mice for Notch1, also supporting this hypothesis. It has also been demonstrated that PS1 regulates the proteolytic processing of Notch in a similar manner to that of APP as well as nuclear translocation of the Notch intracellular fragment[82-84]

3.2 The Amyloid Cascade Hypothesis

The amyloid cascade hypothesis posits that the deposition of the amyloid-β peptide in the brain parenchyma is a crucial step that initiates a sequence of events that ultimately leads to Alzheimer's disease. The concept of amyloid-β-derived diffusible ligands[85] or soluble toxic oligomers[86,87] has been proposed to account for the neurotoxicity of the amyloid-β peptide. These intermediary forms lie somewhere between free, soluble amyloid-β monomers and insoluble amyloid fibrils, but the exact molecular composition of these oligomers remains elusive. The amyloid cascade hypothesis now suggests that synaptotoxicity and neurotoxicity may be mediated by such soluble forms of multimeric amyloid-β peptide species, which cause the formation of paired helical filaments (PHFs) of tau aggregates and, ultimately, result in neuronal loss[88].

3.3 Aβ aggregation: oligomers and amyloid fibrils

Amyloid β-protein is a natural product and is present in the brains and cerebrospinal fluid (CSF) of normal humans throughout life[89,90]. Thus, the mere presence of Aβ does not cause neurodegeneration; rather neuronal injury appears to ensue as a result of the ordered self-association of Aβ molecules[91]. Aβ spontaneously self-aggregates into multiple coexisting physical forms, which grow into fibrils that arrange themselves into β-pleated sheets to form the insoluble fibers of 6–10 nm diameter of advanced amyloid plaques. In vitro, synthetic Aβ can form amyloid fibrils similar to those present in human brain[92,93]. Early studies clearly demonstrated that aggregation of Aβ was essential for toxicity, but characterization of the assemblies

that formed in vitro was limited, and it was assumed that since amyloid fibrils were detectable, these assemblies mediated the observed toxicity. Yet, this ignored the concern that in patients dying with AD, there is a relatively weak correlation between the severity of dementia and the density of fibrillar amyloid plaques[94-96].

Follow-up studies by Lambert et al.[97] led directly to the biophysical and biological characterization of amyloid β-derived diffusible ligands (ADDLs), described as the neurotoxic subset of soluble, non-fibrillar Aβ oligomers. Atomic force microscopy and gel analysis revealed oligomeric structures estimated to contain 3-24 peptide monomers, with neurotoxicity manifested through compromised neuronal ability to reduce the cell-permeant dye MTT, and by rapid disruption of long term potentiation (LTP) in organotypic hippocampal slices and anesthetized rats. The acronym "ADDLs" was selected to emphasize the soluble, non-fibrillar, and ligand-like nature of these Aβ assemblies. The precise structure of the physiologically relevant oligomers is not known. Strong evidence has been published by a number of laboratories supporting the proposition that dodecameric structures are the relevant neurotoxins. In 2003 Gong et al. demonstrated the presence of dodecamers in AD brain tissue extracts and showed that ADDL levels in AD brain were elevated more than 70-fold compared with brain tissue from age-matched non-demented individuals[98]. Lesne et al. demonstrated that the appearance of dodecameric Aβ*56 in Tg2676 mice coincided with the onset of behavioral impairment[99], and Barghorn et al. demonstrated that dodecameric globulomers exhibit postsynaptic binding and LTP blocking capability identical to ADDLs[100]. Several recent studies have

suggested that Aβ dimers and trimers are the synaptotoxic structures, based on studies involving the use of 7PA2 cell culture derived material[101-103]. While the overall conclusion that ADDLs impair synaptic plasticity and memory is supported by the results of many researchers, definitive results demonstrating the exact nature of the synaptotoxic species have yet to be reported.

3.4 Effects of the Amyloid Cascade

The accumulation of misfolded Aβ in the AD brains results in different pathological events:

Synaptic failure: in mild Alzheimer's disease, there is a reduction of about 25% in the presynaptic vesicle protein synaptophysin[104]. With advancing disease, synapses are disproportionately lost relative to neurons, and this loss is the best correlate with dementia[105-107]. Basal transmission of single impulses and "long-term potentiation" (LTP), an experimental indicator of memory formation at synapses, are impaired in plaque-bearing mice with Alzheimer's disease and after Aβ peptide has been applied to brain slices[108,109]. Subsequent to this impairment, signaling molecules important to memory are inhibited. Disruptions of the release of presynaptic neurotransmitters and postsynaptic glutamate receptor ion currents[102,110] occur partially as a result of endocytosis of N-methyl-D-aspartate (NMDA) surface receptors[111] and endocytosis of α-amino-3-hydroxy-5-methyl-4-isoxazole propionic acid surface receptors[112]. The latter further weakens synaptic activity by inducing a lasting reduction in currents after a high-frequency stimulus train. Intraneuronal Aβ can trigger these synaptic deficits even earlier[113] (Fig.7).

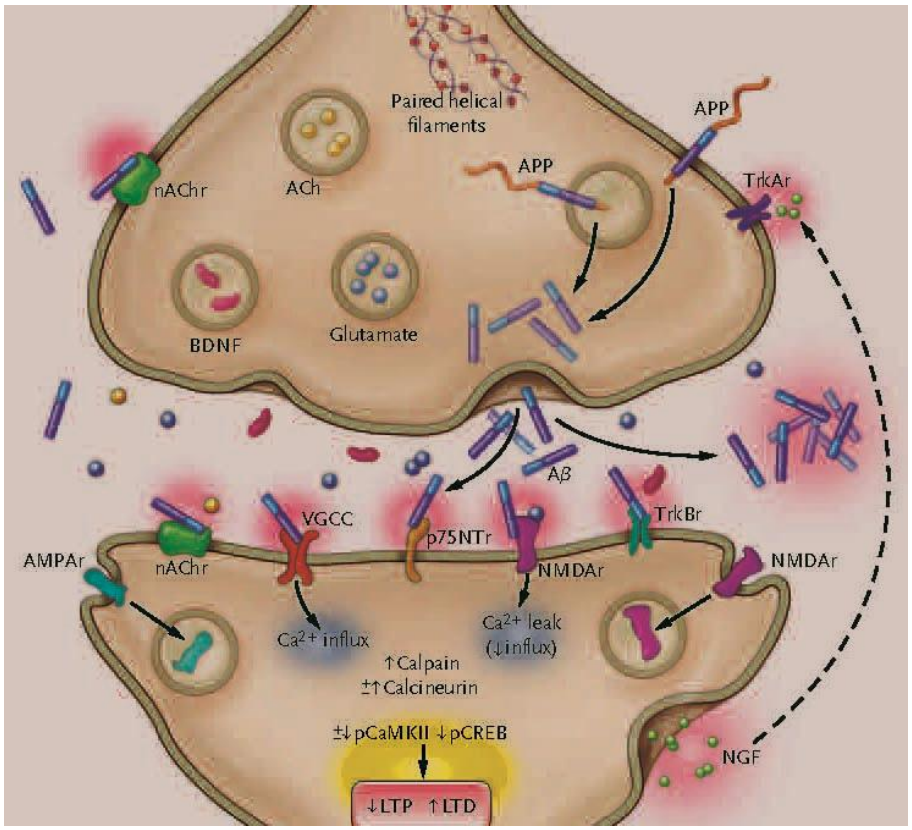

Figure 7. Synaptic Dysfunction in Alzheimer's Disease. Synaptic loss correlates best with cognitive decline in Alzheimer's disease. A control synapse is shown at the top of the figure. At the bottom of the figure, an "Alzheimer's disease synapse" depicting the pleiotropic effects of the β-amyloid peptide (Aβ) is shown. Rings represent synaptic vesicles[41].

Depletion of neurotrophin and neurotransmitters: neurotrophins promote proliferation, differentiation and survival of neurons and glia, and they mediate learning, memory and behavior. The normally high levels of neurotrophin receptors in cholinergic neurons in the basal forebrain are severely reduced in late-stage Alzheimer's disease. Moreover, the levels of brain-derived neurotrophic factor (BDNF), a member of the neurotrophin family, are depressed[114]. Presynaptic α-7

nicotinic acetylcholine receptors are essential for cognitive processing, and their levels increase in early Alzheimer's disease[115], for decreasing later[116]. Experimental studies show that Aβ binds to α-7 nicotinic acetylcholine receptors, impairing the release of acetylcholine and maintenance of LTP[117]. The level of muscarinic acetylcholine receptors is reduced in the brains of patients with Alzheimer's disease.

Mitochondrial dysfunction: exposure to Aβ inhibits key mitochondrial enzymes in the brain and in isolated mitochondria[118]. Cytochrome c oxidase is specifically attacked[119]. Consequently, electron transport, ATP production, oxygen consumption and mitochondrial membrane potential all become impaired. The increase in mitochondrial superoxide radical formation and conversion into hydrogen peroxide cause oxidative stress, release of cytochrome c, and apoptosis. Dysfunctional mitochondria release oxidizing free radicals, and in Alzheimer's disease they cause considerable oxidative stress[120]. Experimental models show that markers of oxidative damage precede pathological changes[121]and Aβ, which is a potent generator of reactive oxygen species[122] is a prime initiator of this damage. The receptor for advanced glycation end products mediates Aβ's pro-oxidant effects on neural, microglial and cerebrovascular cells[123].

Vascular effects: pathological changes include cerebral amyloid angiopathy[124], affecting more than 90% of patients with Alzheimer's disease, capillary abnormalities, disruption of the blood-brain barrier and large-vessel atheroma[125]. Another hypothesis holds that clearance of Aβ along diseased perivascular channels and through the blood–brain barrier is impeded in AD. The source of vascular Aβ (mostly 40

amino acid form) is heterogeneous, comprising neurons, degenerating myocytes, and the circulation. Amyloid deposition in the arteriolar wall enhances vasoconstriction in ex vivo studies[126]. Aβ is also cytotoxic to endothelial[127] and smooth-muscle cells[128], conferring a predisposition to lobar hemorrhage in advanced age. The "neurovascular uncoupling" hypothesis proposes that deregulation of Aβ transport across the capillary blood-brain barrier is caused by the imbalanced expression of low-density lipoprotein receptor-related proteins and receptors for advanced glycation end products, which mediate Aβ efflux and influx, respectively[129].

Inflammation: Activated microglia and reactive astrocytes localize to fibrillar plaques, and their biochemical markers are elevated in the brains of patients with Alzheimer's disease[130]. Initially, the phagocytic microglia engulf and degrade Aβ. However, chronically activated microglia release chemokines and a cascade of damaging cytokines (interleukin-1, interleukin-6 and tumor necrosis factor α) [131]. In common with vascular cells, microglia express receptors for advanced glycation end products, which bind Aβ, thereby amplifying the generation of cytokines, glutamate and nitric oxide[123]. Fibrillar Aβ and glial activation also stimulate the classic complement pathway[132].

Axonal-transport deficits: another internal derangement that is probably an effect rather than a cause of Alzheimer's disease is a reduction in the transport of critical protein cargoes to the synapse. Molecular motors of the kinesin family drive vesicles and mitochondria destined for the synaptic terminal along axonal microtubules. The kinesin superfamily heavy-chain protein 5 and its associated kinesin light chain 1 facilitate "fast" anterograde transport.

Tau forms the cross-bridges that maintain the critical spacing between microtubules. Impairment of transport causes amyloid precursor protein, vesicle, and kinesin accumulations in axonal swelling, local Aβ deposition, and neurodegeneration[133,134].

Cholesterol metabolism: a defect in cholesterol metabolism is an appealing hypothesis because it ties together the apolipoprotein E (APOE) genetic risk, amyloid production and aggregation, and vasculopathy of Alzheimer's disease. However, proof is also lacking for this hypothesis. Cholesterol is an essential component of neuronal membranes and is concentrated in sphingolipid islands termed "lipid rafts." Rafts are ordered platforms for the assembly of β-secretases and γ-secretases and processing of amyloid precursor protein into Aβ[135]. Aβ generation and aggregation are promoted and clearance from the brain is reduced when an overabundance of esterified cholesterol decreases membrane lipid turnover. Glial-derived APOE is the primary cholesterol transporter in the brain.

3.5 Aβ clearance and degradation

In all forms of AD, the accumulation of Aβ reflects an imbalance between its production and clearance, but for most of all AD cases (95-99%), which are of late-onset and sporadic in nature, the cause of that imbalance is unclear. In healthy individuals, the production and turnover of Aβ are rapid (estimated at 7.6% and 8.3%, respectively, of the total volume of Aβ per hour [136]), suggesting that small changes in Aβ production or clearance can cause its abnormal accumulation. To date, there is little evidence to suggest that an increase in the overall production of Aβ is responsible for the

development of sporadic AD [137]. Reduced catabolism may account for the unresolved mechanism of late-onset AD development.

Clearance of Aβ from the brain is mediated by multiple diverse processes. These include drainage along perivascular basement membranes, possibly to cervical lymph nodes and into the cerebrospinal fluid (CSF)[138-140]; transport across vessel walls into the circulation, mediated by low-density lipoprotein receptor-related protein 1[141] or the P-glycoprotein (PgP/MDR1/ABCB1) efflux pump (12Y14); the sequestration of Aβ by soluble low-density lipoprotein receptor-related protein 1 receptor in the circulation to promote the efflux of soluble Aβ out of the CNS[142]; microglial phagocytosis[143]; and enzyme-mediated degradation of Aβ[144-146].

Enzyme-mediated degradation of Aβ (Fig. 8) has received a great deal of attention during the past decade. Many enzymes are capable of cleaving full-length Aβ in vitro, producing fragments that are generally less neurotoxic and more easily cleared. Many proteases or peptidases have been reported with the capability of cleaving Aβ either in vitro or in vivo. These include neprilysin (NEP)[147-149], endothelin-converting enzyme (ECE)-1[150], insulin degrading enzyme (IDE)[151-153], angiotensin-converting enzyme (ACE)[154] and uPA/tPA-plasmin system[155,156].

The biologic relevance of several of these enzymes to Aβ clearance has been established in vivo in mouse models of AD: overexpression of genes encoding the relevant enzymes in mice transgenic for mutant forms of human APP (hAPP) that cause familial AD was shown to reduce Aβ accumulation and, in many cases, to ameliorate cognitive and motor deficits. Recent studies on postmortem

human brain tissue revealed elevation of the activities of several candidate Aβ-degrading enzymes late-onset AD [157]. Aβ-degrading enzyme activities were also reported to increase in hAPP mice at about the time of Aβ deposition [158-160]. Together, these data led to the hypothesis that Aβ-degrading enzymes protect against the development of AD through upregulation in response to Aβ.

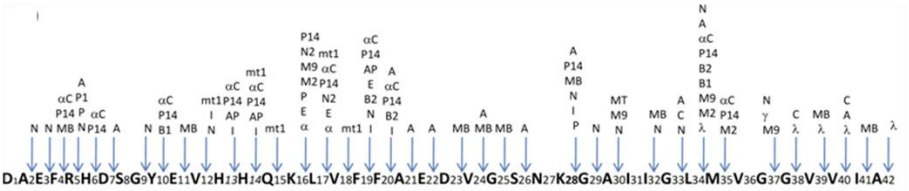

Figure 8. Sequence and structure of Aβ and known cleavage sites. N, neprilysin; E, endothelin-converting enzyme; I, insulin degrading enzyme; A, angiotensin-converting enzyme; M2, matrix metalloproteinase 2; M9, matrix metalloproteinase 9; P, plasmin; C, CTSB; Mt1, membrane-type metalloproteinase 1; MB, myelin basic protein; AP, acyl peptide hydrolase; N2, neprilysin 2; P14, protease XIV; αC, α-chymotrypsin[145].

3.5.1 Neprilysin

NEP is a plasma membrane-bound glycoprotein, composed of a short N-terminal cytoplasmic tail, a membrane-spanning domain, and a large C-terminal extracellular catalytic domain. The latter contains a HExxH zinc-binding motif [161], which facilitates the hydrolysis of extracellular oligopeptides (< 5kDa) on the amino side of hydrophobic residues, such as the small, hydrophobic Aβ40 and Aβ42 peptides. In the brain, NEP is expressed on neuronal plasma membranes, both pre- and postsynaptically [162,163], and is most abundant in the nigrostriatal pathway, as well as in brain areas vulnerable to amyloid plaque deposition, such as the hippocampus[164]. The true breakthrough demonstrating the importance of NEP was demonstration that NEP

was the rate-limiting enzyme for Aβ degradation in vivo made by Iwata et al[148]. Furthermore, it had been found that NEP was able to degrade not only monomeric, but also oligomeric forms of both Aβ40 and Aβ42[165], both intracellularly and extracellularly[166]. The role of NEP in Aβ degradation was solidified by studies in transgenic mice. In partially NEP deficient animals, the degradation of both endogenous and exogenous Aβ peptides was tightly correlated with gene dose, suggesting that even partial down-regulation of NEP activity could contribute to Aβ accumulation[148]. On the other hand, overexpression of NEP by gene transfer in amyloid-depositing transgenic mice slowed, and in some cases reversed, Aβ deposition[167-170].

Studies in human subjects have also supported the notion that NEP plays a key role in brain Aβ metabolism and AD pathogenesis. Immunohistochemical studies on AD brains have revealed NEP immunoreactivity in senile plaques[171]. Quantitative analysis showed that both NEP mRNA and protein were significantly lower in AD than in age-matched normal control brains. Reductions occurred selectively in the regions most vulnerable to AD pathology, but not in other brain areas such as cerebellum or in peripheral organs[172,173]. Interestingly, an inverse relationship between NEP and Aβ levels in AD brain vasculature has been reported. These data suggested that NEP may play a role in cerebral amyloid angiopathy (CAA), another very common pathological change found in AD brains[174].

3.5.2 Endothelin-converting enzyme-1

Endothelin (ET) is a potent vasoconstrictive peptide produced in vascular endothelial cells. ECE is a transmembrane metalloprotease that catalyzes the conversion of pro-ET into vasoactive endothelin. Two isoforms of ECE have been described; studies have suggested that ECE-1, but not ECE-2, is a possible brain Aβ-degrading enzyme[150]. ECE-1 is widely expressed in human brain, including neurons in the diencephalon, brainstem, basal nuclei, cerebral cortex, cerebellar hemisphere, amygdala and hippocampus[175,176]. Eckman and her colleagues provided the first evidence that ECE-1 may be involved in the metabolism of Aβ. They found that ECE-1 expressed in cultured Chinese hamster ovary cells that lack endogenous ECE activity reduced the concentration of extracellular Aβ by up to 90%[150]. In mice deficient for ECE-1 both Aβ40 and Aβ42 levels were significantly higher when compared with age matched wild-type littermate controls, suggesting that ECE activity might be an important factor involved in Aβ clearance in vivo[177].

3.5.3 Insulin degrading enzyme

IDE is a zinc metalloendopeptidase that hydrolyzes multiple peptides, including insulin, glucagon, atrial natriuretic factor, transforming growth factor-α, β-endorphin, amylin, and the APP intracellular domain (AICD) in addition to Aβ. Transgenic mice overexpressing IDE showed significant reductions of total amyloid burden and improved survival rates[168], while IDE knockout mice demonstrated a clear elevation of brain Aβ and the APP intracellular domain. Immunohistochemical studies showed that IDE was primarily

expressed in neurons, but was also located in senile plaques in AD brain[178]. Like NEP, IDE also showed progressively decreased expression that was age- and region dependent[173]. Thus, strong evidence exists that IDE is another important Aβ-degrading enzyme that may play a role in the amyloid pathology of AD.

3.5.4 Angiotensin-converting enzyme

ACE is a membrane-bound zinc metalloprotease, whose major function is to catalyze the conversion of angiotensin I (AngI) to angiotensin II (AngII), which plays an important role in maintaining blood pressure, body fluid, and sodium homeostasis. In the brain, ACE was found at highest levels in circumventricular organs such as the subfornical organ, area postrema, and the median eminence[179]. Most of the evidence for the potential relationship between ACE and AD has come from human genetic studies. Patients at higher AD risk had an insertion (I) polymorphism within intron 16 of the ACE gene, which was associated with AD[180]. Interestingly, patients with a deletion polymorphism had a lower risk of AD[181]. Results from preclinical and clinical studies suggested that ACE might have a role in the modulation of cognitive memory processes in the rat and in humans[182]. Hemming and Selkoe showed that ACE expression promoted the degradation of endogenous Aβ40 and Aβ42[183]. Unlike other candidate Aβ-degrading enzymes, the levels of both ACE protein and activity were elevated in postmortem brains[184].

3.5.5 uPA/tPA-plasmin system

Plasmin is a serine protease important in the degradation of many extracellular matrix components. The principal components of this system include plasminogen/plasmin, tissue plasminogen activator (tPA), urokinase-type plasminogen activator (uPA). tPA and uPA cleave plasminogen to yield the active serine protease, plasmin. In the nervous system, plasminogen and uPA are expressed in neurons, while tPA is synthesized by neurons and microglial cells[185]. The plasmin system is involved in many normal neural functions, such as neuronal plasticity, learning, and memory. Several studies showed that Aβ aggregates could substitute for fibrin aggregates in activating tPA, and suggested that tPA may be activated by Aβ in AD[186,187]. Later, it was reported that brain plasmin enhanced Aβ degradation, while plasmin and its activity were decreased in AD brains[188]. However, plasminogen deficient mice did not show increased Aβ in the brain or in the plasma and suggested that plasmin does not regulate steadystate Aβ levels in nonpathologic conditions, although it might be involved in the degradation of pathological Aβ aggregates[189].

4. Genetics of Alzheimer's Disease

Familial forms of AD account for less than 5% of the total cases. They are linked to mutations in three different genes codifying for APP, PS1 and PS2.

4.1 Amyloid Precursor Protein gene mutations

The APP gene mutations are estimated to account for less than 1% of FAD, with typical age of onset before 65 years. Several

missense mutations have been discovered in exons 16 and 17 in families with early-onset AD (Fig. 9). According to their localization, APP mutations exert their pathogenic effect through different mechanisms and often have peculiar clinical and pathological phenotypes. The mutations located near the β- or γ-secretase cleavage site alter proteolytic processing of APP, resulting in an increased production of Aβ peptides. In particular, defects occurring at the Aβ amino-terminal site induce increased cleavage by β-secretase to generate more Aβ40 and Aβ42, while substitutions occurring at the carboxy-terminal site selectively enhance the production of Aβ species ending at residue 42. Missense mutations mapping in the central region of Aβ, which has been recognized as the most important for aggregation, are thought to affect the chemico-physic properties and to enhance the fibrillogenic capability of Aβ[29].

Moreover, different APP locus duplications have been recently identified in rare families with early onset AD and Aβ-related cerebral amyloid angiopathy (CAA)[190].

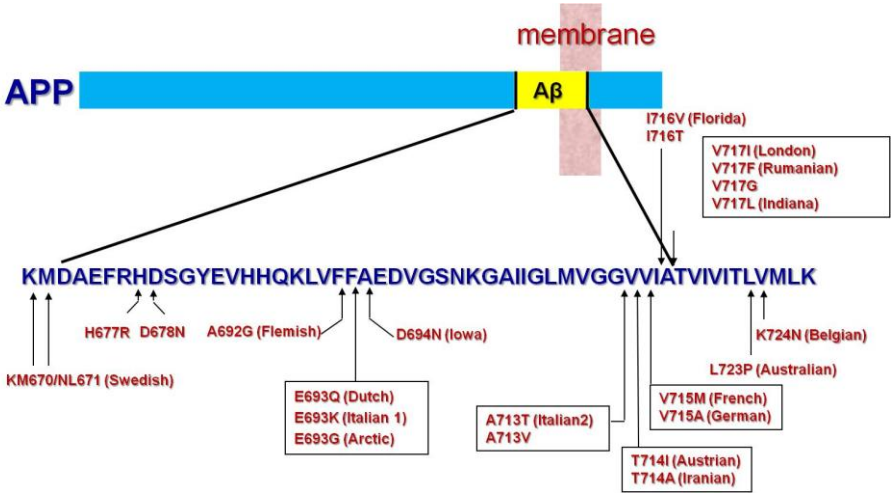

Figure 9. APP mutations.

4.2 Presenilin genes mutations

Presenilin mutations are associated with familial forms of AD, accounting for about 80% of the early-onset AD cases. Almost 200 different mutations in PS1 gene have been found in independent families and 20-25 missense mutations have been found in the PS2 gene. The phenotype associated with each genetic variant depends on the gene, type of mutation, and transmembrane domain affected [191]. All the PS mutations are linked to an autosomal dominant AD, with onset before 60 years and an almost complete penetrance. The youngest ages at onset are seen in families with PS1 mutations, which typically fall within the range 35 to 55 years. APP mutations tend to give rise to symptom onset between 40 and 65 years and PS2 mutations between 40 and 70 years[192].

These mutations generally lead to enhanced deposition of total Aβ and Aβ42 (but not Aβ40) in the brain. There is a considerable heterogeneity in the histological profiles among brains from patients with different mutations, and although some lead to predominantly parenchymal deposition of Aβ in the form of diffuse and cored plaques, others show predominantly vascular deposition, with severe amyloid angiopathy.

4.3 Apolipoprotein E4 allele: a risk factor

Apolipoprotein E (ApoE) is a plasma glycoprotein involved in the mobilization and redistribution of cholesterol during neuronal grow and after injury[193]. Zannis et al. identified by isoelectric focusing the three major isoforms of ApoE (ApoE2, ApoE3, ApoE4) and concluded that a single locus with three alleles (ε2, ε3, ε4) is

responsible for this pattern[194]. Corbo and Scacchi analysed the ApoE allele distribution in a variety of population and found that the ε3 allele is the most frequent in all human groups[195].

Many studies have demonstrated an association between ε4 allele and late-onset familial and sporadic AD. One of the first and most important of these studies is by Corder et al., who found that the effect of ε4 allele is "dose-dipendent": the risk for AD increases from 20 to 90% and the mean age of onset decreases from 84 to 68 years with increasing number of ε4 alleles[196].

Immunohistochemistry showed that inheritance of ApoE4 allele was associated with a significantly higher Aβ plaque burden than was observed in patients lacking ApoE4[197]. ApoE4 seems to enhance the steady-state levels of Aβ peptides, Aβ40 in particular, presumably by decreasing their clearance from the brain. In vitro studies quantifying the degree of Aβ fibrillogenesis using synthetic peptides suggest that the presence of the ApoE4 protein results in increased number of fibrils, compared with levels obtained in the presence of ApoE3[198]. Distinct binding properties of ApoE isoforms to Aβ peptide have suggested ways by which ApoE may mediate this action; in particular, ApoE4 isoform binds to the Aβ peptide more rapidly than ApoE3 and this binding forms novel fibrils that precipitate into dense structures[199]. Deposition of Aβ into cerebral and meningeal vessels to produce the syndrome of congophilic amyloid angiopathy is also enhanced by the gene dosage of ApoE4, even in the absence of Alzheimer-type neuropathology[200].

5. The role of Tau protein

Tau is the primary component of the neurofibrillary tangles (NFTs) in AD brain. Although AD is defined by both β-amyloid pathology and tau pathology, whether or not tau played a critical role in disease pathogenesis was a subject of discussion for many years. However, given the increasing evidence that pathological forms of tau can compromise neuronal function and that tau is likely an important mediator of Aβ toxicity, there is a growing awareness that tau is a central player in AD pathogenesis[201]. Tau is a phosphoprotein and phosphorylation plays a prominent role in regulating its physiological function. It is also clear that aberrant tau phosphorylation occurs in AD brain and is associated with pathogenesis. In AD, phosphorylation of tau at specific epitopes appears to be a progressive event, with phosphorylation at threonine 231 (T231) occurring early, at 'pretangle' stages[202,203]. Phosphorylation at this epitope appears to contribute to conformational changes in tau[204] and to a significant reduction of the ability of tau to bind microtubules[205]. Another phosphorylation site that plays a pivotal role in regulating tau function is serine 262 (S262). Phosphorylation of this site significantly decreases tau binding to microtubules[206]; increased phosphorylation at S262 was noted in pretangle neurons in AD brain suggesting that it is an early event in the pathogenic process. When considering the role of tau phosphorylation in the pathogenesis of AD, it is becoming apparent that a specific complement of phosphorylated residues enhance neurotoxicity and that phosphorylation of any one single site is likely not sufficient to convert tau to a toxic species. In addition, the

phosphorylation of one epitope on tau can influence the phosphorylation of other epitopes[207].

During the evolution of tau pathology in AD brain, tau appears to undergo sequential cleavage events[208]. Caspases, which are elevated in AD brain, are likely involved in the proteolytic processing of tau[209]. It was shown that tau is cleaved by caspases at aspartic acid 421 (D421) in AD brain and appeared to be generated early in the pathogenic process. Tau truncated at D421 is more fibrillogenic than full length tau[210,211]. In addition to being cleaved at D421, tau may also be cleaved at D13 and D402 in AD brain by caspase 6[212-214]. In one study the level of tau cleaved at D402 in NFTs and neuropil threads was associated with lower global cognitive scores in cases with no cognitive impairment, indicating that it may be an early event in the development of AD[212]. Finally, at later stages in the evolution of tau pathology, tau undergoes further processing including truncation at glutamic acid 391, along with further processing of the amino terminal. These latter cleavage events appear after tau has formed the NFTs and seem to be part of the maturation process of the tangles[215].

Abnormal phosphorylation of tau, a prominent feature of AD brain, decreases its microtubule binding ability, which may destabilize microtubules and result in cellular damage. This ‘loss of function’ model could explain several aspects of tau toxicity; however, recent research points to possible ‘gain of function’ mechanisms of tau toxicity that may not be directly dependent on its microtubule binding ability[216]. For example, tau at approximately physiological concentrations did not inhibit axonal transport; however, tau filaments at the same concentration were found to be inhibitory and this

inhibition was not due to direct microtubule binding[217]. Inhibition of anterograde axonal transport is now thought to be associated with the ability of tau to bind kinesin[218]. Tau-induced impairment of axonal transport has been implicated in the mislocalization of proteins and organelles to the soma. Pathological forms of tau have repeatedly been shown to cause abnormal somatic localization of mitochondria[219,220], which are the main source of energy production and calcium buffering in cells. Thus, sequestration of mitochondria away from axons, which contain areas of high energy demand and calcium influx, such as nodes of Ranvier and synapses, has a profound impact on cellular homeostasis[221]. For this reason, tau induced mitochondrial mislocalization may be a key component in neurodegenerative processes. Beyond impairment of mitochondrial transport, tau may disrupt several other aspects of mitochondria under pathological conditions. There is significant evidence indicating that mitochondria are compromised early in AD brain tissue[222,223]. Interestingly, stable expression of D421 truncated tau in cortical cell lines induced fragmentation of mitochondria[224], possibly replicating the imbalance of mitochondrial fission and fusion in AD brain (Fig. 10).

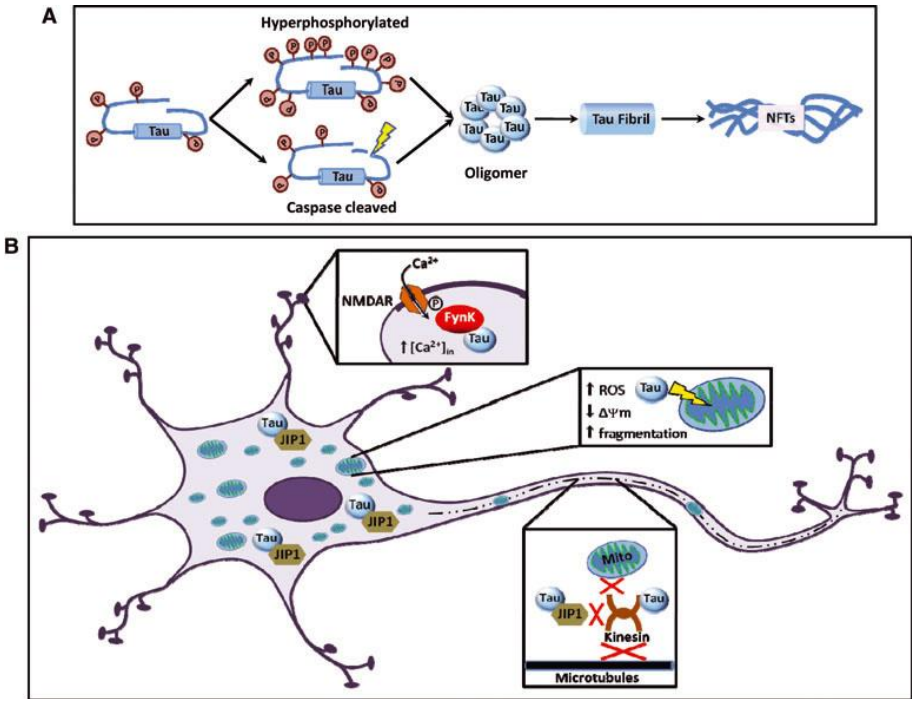

Figure 10. Cellular targets of toxic tau. (A) Tau undergoes phosphorylation in physiological conditions. However, in pathological conditions, tau becomes hyperphosphorylated and/or cleaved, which facilitates aggregation and increases the toxicity of tau. In the continuum of the aggregation process, pathologically modified tau monomers first form oligomers, which further aggregate into fibrils and finally into NFTs. Recent studies suggest that monomeric or oligomeric species of tau are the more toxic than aggregated forms. (B) Tau may manifest its toxicity by enabling or facilitating Aβ-induced excitotoxicity, mitochondrial damage and/or by disrupting axonal transport[201].

6. Therapeutic approaches to AD

At present there is no effective treatment for AD; no drug is available for the prevention, the reversal or the delay in the progression of the disease, except for memantine, which interferes with glutamate-mediated toxicity. Several evidences suggest that Aβ deposition, neuronal loss and brain atrophy start many years before the appearance of the clinical symptoms of AD; this finding explains why symptomatic treatments are not effective and the development of

drugs able to interfere with such pathogenic mechanisms is mandatory.

The identification of Aβ and tau as the principle proteinaceus component of plaques and NFTs, respectively, coupled with genetic studies implicating these protein as triggers of neurodegeneration has validated both proteins as therapeutic targets in neurodegeneration[29]. On these basis, three therapeutic strategies can be hypothesized: decrease the synthesis of Aβ or tau, prevention of misfolding and aggregation of these proteins,
neutralization or removing the toxic aggregate or misfolded forms of these proteins (Fig. 11).

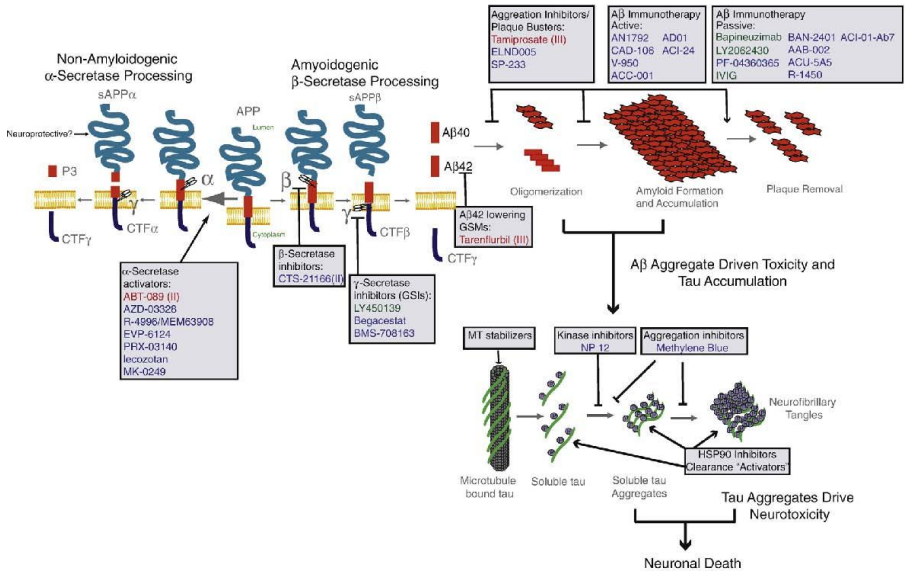

Figure 11. Aβ and tau therapies in the clinic. Aβ and tau therapeutic targets and therapeutics in the clinic are depicted the context of a schematic of the amyloid cascade hypothesis. Classes of therapeutics are shown in boxes, and below the class are therapeutics that are in, have completed, or have announced human trials (as of June 2009). Red text denotes therapies for which trials either failed to meet endpoints or were terminated for other reasons. In parenthesis is the stage of trial that the therapy completed. Green text indicates therapies in Phase III trials as of June 2009. Blue text indicates therapies in early phase trials (Phase I or II). Basic APP processing, Aβ aggregation, and tau aggregation schematics are shown[225].

6.1 Decrease of Aβ synthesis

There are currently three direct strategies targeting Aβ production that have moved to the clinic: β-secretase inhibitors and γ-secretase inhibitors (GSIs) and modulators (GSMs). Both β- and γ-secretase inhibitors block production of all species of Aβ[226,227], whereas GSMs are unique in that they shift cleavage by γ-secretase resulting in an altered profile of Aβ peptides.

β-secretase inhibitors: the development of potent β-secretase inhibitors that cross the blood-brain-barrier has been demonstrated to be very difficult. One orally bioavailable β-secretase inhibitor (CTS-21166, Comentis) has been evaluated in a Phase I study in humans (http://www.alzforum.org/new/detail.asp?id=1790).

γ-secretase inhibitors: Several GSIs are now being tested in the clinic. The most advanced of these is LY450139 (Eli Lily), a non-selective GSI that is currently in a Phase III study [228]. A potential concern regarding the first-generation GSIs is that their limited selectivity may result in target-mediated toxicity that could appear due to inhibition of Notch signaling [229]. In animal models, there is very narrow therapeutic window that allows one to significantly reduce Aβ levels in the brain without observing these side effects. Recently, two Notch-sparing GSIs have been developed (Begacestat; Wyeth; BMS-708163, Bristol-Myers Squib) (http://www.alzforum.org/new/detail.asp?id=19922008),[230]. These compounds are in or completed Phase I human studies.

γ-secretase modulators: γ-secretase inhibitors with a specific role in altering APP processing have been recently developed. They cause a decrease in Aβ1-42 production shifting APP processing

towards peptides shorter than Aβ1-40[231]. The GSM Tarenflurbil (Flurizan, R-Flurbiprofen; Myriad Genetics) has just completed a phase III study.

6.2 Increase of Aβ clearance

An approach for the reduction of Aβ levels in the brain is the activation of enzymes or cells that degrade Aβ or Aβ aggregates. However, there are two major concerns with this strategy: first, the activation of proteases with small molecules is challenging from a pharmacologic perspective; second, since there are no proteases known to selectively degrade Aβ, activating a protease may also be prone to target based toxicity. An inhibitor of plasminogen activator inhibitor-1 (PAZ-417, Wyeth) is in phase II trial for AD. PAI-1 inhibits the activation of plasmin, a protease that can degrade Aβ oligomers, monomers and fibrils. The net result is that when PAI-1 is inhibited, more plasmin is activated[232].

6.3 Aβ Immunotherapy

Active immunotherapy: the original active vaccination with fibrillar Aβ42+QS21 adjuvant, known as the AN1792 vaccine trial, was halted in Phase II due to induction of meningoencephalitis in ~6% of the vaccinated patients[233]. Despite setbacks in the AN-1792 trial, a number of alternative active anti-Aβ vaccination approaches are in early phase human testing or likely to begin human testing in the near future. Two general strategies are being employed in the effort to make a potentially safer vaccine by avoiding harmful T-cell activation. First, based on evidence in mice that full length Aβ

contains an aminoterminal B-cell epitope (residues 1–14) and a carboxyl-terminal T-cell epitope (residues 15–42), a number of vaccines comprising the amino-terminus of Aβ coupled to T-cell epitopes or conjugated to a virus-like particle have been developed (ACC-001, Elan/Wyeth; CAD- 106, Novartis; V950, Merck; ACI-24, AC Immune)[234]. Second, rather than immunize with the exact sequence of Aβ, Aβ peptide mimetics are also being developed (AD01, Affiris GmbH)[235].

Passive immunotherapy: Humanized monoclonal antibodies targeting Aβ are being actively tested in humans. The most advanced of these is the bapineuzumab (AAB-001, Elan/Wyeth), a humanized monoclonal antibody that targets the amino-terminus of Aβ and is capable of binding monomeric, oligomeric and fibrillar Aβ (http://www.alzforum.org/new/detail.asp?id=1894). A number of typical side effects associated with recombinant antibody administration were reported, and transient vasogenic edema was also noted in a subset of patients, especially among ε4 allele carriers.

6.4 Inibition of Aβ aggregation

Though inhibiting Aβ production can slow the rate of aggregate formation, it is an indirect way to target the aggregates of Aβ that are widely considered by the field to be the true triggers of AD. More direct approaches are (i) to block aggregate formation using aggregation inhibitors, (ii) to disrupt preformed aggregates, or (iii) neutralize the aggregate by direct binding. There are a number of theoretical concerns with such approaches: the poor anti-amiloidogenic activity of the molecules that could act as aggregation

inhibitors, the possibility that such compounds might convert a less toxic aggregate in a more toxic one, the impossibility to predict if these drugs will compete with endogenous molecules for the binding of Aβ. Among compounds with anti-amyloidogenic activity, Tramiprosate (3-aminopropane-1-sulfonic acid, Neurochem) is a glycosaminoglycan mimetic drug that interacts with the Aβ peptide and is reported to inhibit the transition from random structures to organized β-sheets[236]. Scyllo-inositol is another compound that has been reported to alter Aβ aggregation[237] and to directly neutralize the synaptotoxicity of oligomeric Aβ aggregates in vitro and in vivo[238]. PBT2 (Prana) is a second-generation compound related to clioquinol[239]. It is a metal chelator that is designed to alter metal-dependent Aβ aggregation and redox activity associated with Aβ–metal complexes[240].

6.5 Decrease of Tau production

Even though the exact neurotoxic species of tau has not been definitively identified, decreasing tau synthesis or a specific tau isoform is proposed to decrease the likelihood that tau will aggregate into a neurotoxic species. An approach is based on the identification of splice site mutations in tau that cause FTDP-17 which result in an imbalance between exon 10+ (4R) and exon 10− (3R) isoforms of tau, that might favor tangle pathology[241]. Such mutations lead to increased production of exon 10 containing isoforms of tau with four microtubule binding domains, and these isoforms are almost exclusively deposited in tangles in many families with FTDP-17. Thus, it may be possible to develop tau therapeutics that are designed

to enhance the mRNA splicing events resulting in exclusion of exon 10. However, therapeutics targeting tau production are still in the conceptual stage.

6.6 Interference with Tau aggregation

There is a good correlation between the propensity of mutant tau to aggregate and its toxicity to cells and in mice. However, it is not clear if the real toxic entity is aggregated tau, and not the misfolded non-aggregated protein. Nonetheless, some compounds able to inhibit tau aggregation have been proposed as anti-AD drugs; among them, methylene blue can inhibit both tau and Aβ aggregation.

6.7 Inhibition of tau phosphorilation

Tau contains multiple phosphorylation sites and phosphorylation appears to control the binding affinity for microtubules. By decreasing tau's affinity for microtubules, hyperphosphorylation of tau could play a role in the pathogenesis of AD by promoting microtubule network breakdown. The tau kinases MARK, CDK5, GSK3, PKA, and ERK1/2 have all been implicated as potential kinase targets for tau therapeutics. For example, lithium, a dual action GSK3 inhibitor, reduced tau phosphorylation, tau accumulation, and axonal degeneration in tau mice[242,243].

6.8 Targeting of Tau chaperones

Chaperone proteins, such as Heat Shock Proteins complexes, that regulate the aggregation and folding of tau or potentially mediate clearance of misfolded or aggregated tau are being explored as

therapeutic targets[244]. The main challenge to this approach is that the chaperone systems need to be upregulated, and in many cases there is no known pathway that will lead to upregulation of the specific chaperone.

6.9 Tau immunotherapy

Antibodies targeting the pathological conformers of tau might clear or suppress tau pathology. Though theoretically attractive, there are concerns that antibodies are not optimal agents for targeting intraneuronal proteins.

7. Scope of the thesis

The aims of this project are:

- the clinical, neuropathological and molecular characterization of a novel APP mutation (A673V, corresponding to position 2 of Aβ) which differs from all the other known genetic defects linked to AD, since it causes a very aggressive disease when occurring with an homozygous pattern, while is not pathogenic, and probably plays a protective role, in the heterozygous state.
- the establishment of a "proof of concept" that will allow us to demonstrate in vivo the anti-amyloidogenic effect of the mutated Aβ peptide when mixed together with the wild-type molecule, in order to evaluate the possible role of Aβ A2V as a therapeutic tool for sporadic AD.

In chapter 1 we described the clinical features of the disease caused by the APP A673V mutation and we performed genetic analysis and neuropsychological assessments to establish a correlation between the presence of the mutation in homo- or heterozygosity and the onset of the disease. Then we investigated the mechanisms by which the mutation causes the disease performing studies with synthetic peptides and cell models. Finally, we investigated the effects of the co-existence of the mutated and wild-type peptide on amyloidogenesis and cell toxicity.

In chapter 2 we performed a detailed neuropathologic characterization of the brain from the homozygous APP A673V carrier.

Chapter 3 consists of a biochemical characterization of the proband's brain homogenates, cerebrospinal fluid and amyloid. The study was then extended to other familial AD cases carrying mutations either in APP or in PS1 genes.

In chapter 4 we investigated the ability of Aβ1-40 in hindering amyloidogenesis when delivered to the brain of AD mouse models by engineered adeno-associated viruses .

8. References

1. Holtzman DM, Goate A, Kelly J, Sperling R. Mapping the road forward in Alzheimer's disease. Sci Transl Med 2011;3:114ps48.

2. McKhann G, Drachman D, Folstein M, Katzman R, Price D, Stadlan EM. Clinical diagnosis of Alzheimer's disease: report of the NINCDS-ADRDA Work Group under the auspices of Department of Health and Human Services Task Force on Alzheimer's Disease. Neurology 1984;34:939-44.

3. Tanzi RE, Bertram L. New frontiers in Alzheimer's disease genetics. Neuron 2001;32:181-4.

4. Ling Y, Morgan K, Kalsheker N. Amyloid precursor protein (APP) and the biology of proteolytic processing: relevance to Alzheimer's disease. Int J Biochem Cell Biol 2003;35:1505-35.

5. Ghiso J, Frangione B. Amyloidosis and Alzheimer's disease. Adv Drug Deliv Rev 2002;54:1539-51.

6. Storey E, Slavin MJ, Kinsella GJ. Patterns of cognitive impairment in Alzheimer's disease: assessment and differential diagnosis. Front Biosci 2002;7:e155-84.

7. Gandy S. The role of cerebral amyloid beta accumulation in common forms of Alzheimer disease. J Clin Invest 2005;115:1121-9.

8. Ghiso J, Frangione B. Cerebral amyloidosis, amyloid angiopathy, and their relationship to stroke and dementia. J Alzheimers Dis 2001;3:65-73.

9. Yamada M. Cerebral amyloid angiopathy: an overview. Neuropathology 2000;20:8-22.

10. Dubois B, Feldman HH, Jacova C, et al. Research criteria for the diagnosis of Alzheimer's disease: revising the NINCDS-ADRDA criteria. Lancet Neurol 2007;6:734-46.

11. Bertram L, Tanzi RE. The current status of Alzheimer's disease genetics: what do we tell the patients? Pharmacol Res 2004;50:385-96.

12. Hardy JA, Higgins GA. Alzheimer's disease: the amyloid cascade hypothesis. Science 1992;256:184-5.

13. Ling Y, Morgan K, Kalsheker N. Amyloid precursor protein (APP) and the biology of proteolytic processing: relevance to Alzheimer's disease. Int J Biochem Cell Biol 2003;35:1505-35.

14. Wilquet V, De Strooper B. Amyloid-beta precursor protein processing in neurodegeneration. Curr Opin Neurobiol 2004;14:582-8.

15. Zhang YW, Thompson R, Zhang H, Xu H. APP processing in Alzheimer's disease. Mol Brain 2011;4:3.

16. Rovelet-Lecrux A, Hannequin D, Raux G, et al. APP locus duplication causes autosomal dominant early-onset Alzheimer disease with cerebral amyloid angiopathy. Nat Genet 2006;38:24-6.

17. Joachim CL, Morris JH, Selkoe DJ. Diffuse senile plaques occur commonly in the cerebellum in Alzheimer's disease. Am J Pathol 1989;135:309-19.

18. Tagliavini F, Giaccone G, Frangione B, Bugiani O. Preamyloid deposits in the cerebral cortex of patients with Alzheimer's disease and nondemented individuals. Neurosci Lett 1988;93:191-6.

19. Iwatsubo T, Odaka A, Suzuki N, Mizusawa H, Nukina N, Ihara Y. Visualization of A beta 42(43) and A beta 40 in senile plaques with end-specific A beta monoclonals: evidence that an initially deposited species is A beta 42(43). Neuron 1994;13:45-53.

20. Dickson DW. The pathogenesis of senile plaques. J Neuropathol Exp Neurol 1997;56:321-39.

21. Jarrett JT, Berger EP, Lansbury PT,Jr. The carboxy terminus of the beta amyloid protein is critical for the seeding of amyloid formation: implications for the pathogenesis of Alzheimer's disease. Biochemistry 1993;32:4693-7.

22. Glenner GG, Wong CW. Alzheimer's disease: initial report of the purification and characterization of a novel cerebrovascular amyloid protein. Biochem Biophys Res Commun 1984;120:885-90.

23. Suzuki N, Iwatsubo T, Odaka A, Ishibashi Y, Kitada C, Ihara Y. High tissue content of soluble beta 1-40 is linked to cerebral amyloid angiopathy. Am J Pathol 1994;145:452-60.

24. Wood JG, Mirra SS, Pollock NJ, Binder LI. Neurofibrillary tangles of Alzheimer disease share antigenic determinants with the axonal microtubule-associated protein tau (tau). Proc Natl Acad Sci U S A 1986;83:4040-3.

25. Lee VM, Balin BJ, Otvos L,Jr, Trojanowski JQ. A68: a major subunit of paired helical filaments and derivatized forms of normal Tau. Science 1991;251:675-8.

26. Selkoe DJ, Ihara Y, Salazar FJ. Alzheimer's disease: insolubility of partially purified paired helical filaments in sodium dodecyl sulfate and urea. Science 1982;215:1243-5.

27. Terry RD, Hansen LA, DeTeresa R, Davies P, Tobias H, Katzman R. Senile dementia of the Alzheimer type without neocortical neurofibrillary tangles. J Neuropathol Exp Neurol 1987;46:262-8.

28. Hansen LA, Masliah E, Galasko D, Terry RD. Plaque-only Alzheimer disease is usually the lewy body variant, and vice versa. J Neuropathol Exp Neurol 1993;52:648-54.

29. Selkoe DJ. Alzheimer's disease: genes, proteins, and therapy. Physiol Rev 2001;81:741-66.

30. Selkoe DJ, Podlisny MB, Joachim CL, et al. Beta-amyloid precursor protein of Alzheimer disease occurs as 110- to 135-kilodalton membrane-associated proteins in neural and nonneural tissues. Proc Natl Acad Sci U S A 1988;85:7341-5.

31. Weidemann A, Konig G, Bunke D, et al. Identification, biogenesis, and localization of precursors of Alzheimer's disease A4 amyloid protein. Cell 1989;57:115-26.

32. Haass C, Hung AY, Selkoe DJ. Processing of beta-amyloid precursor protein in microglia and astrocytes favors an internal localization over constitutive secretion. J Neurosci 1991;11:3783-93.

33. Smith RP, Higuchi DA, Broze GJ,Jr. Platelet coagulation factor XIa-inhibitor, a form of Alzheimer amyloid precursor protein. Science 1990;248:1126-8.

34. Rosen DR, Martin-Morris L, Luo LQ, White K. A Drosophila gene encoding a protein resembling the human beta-amyloid protein precursor. Proc Natl Acad Sci U S A 1989;86:2478-82.

35. Slunt HH, Thinakaran G, Von Koch C, Lo AC, Tanzi RE, Sisodia SS. Expression of a ubiquitous, cross-reactive homologue of the mouse beta-amyloid precursor protein (APP). J Biol Chem 1994;269:2637-44.

36. Wasco W, Bupp K, Magendantz M, Gusella JF, Tanzi RE, Solomon F. Identification of a mouse brain cDNA that encodes a protein related to the Alzheimer disease-associated amyloid beta protein precursor. Proc Natl Acad Sci U S A 1992;89:10758-62.

37. Selkoe DJ. The cell biology of beta-amyloid precursor protein and presenilin in Alzheimer's disease. Trends Cell Biol 1998;8:447-53.

38. Kojro E, Gimpl G, Lammich S, Marz W, Fahrenholz F. Low cholesterol stimulates the nonamyloidogenic pathway by its effect on the alpha -secretase ADAM 10. Proc Natl Acad Sci U S A 2001;98:5815-20.

39. Nitsch RM, Slack BE, Wurtman RJ, Growdon JH. Release of Alzheimer amyloid precursor derivatives stimulated by activation of muscarinic acetylcholine receptors. Science 1992;258:304-7.

40. Cao X, Sudhof TC. A transcriptionally [correction of transcriptively] active complex of APP with Fe65 and histone acetyltransferase Tip60. Science 2001;293:115-20.

41. Querfurth HW, LaFerla FM. Alzheimer's disease. N Engl J Med 2010;362:329-44.

42. Blobel CP. Metalloprotease-disintegrins: links to cell adhesion and cleavage of TNF alpha and Notch. Cell 1997;90:589-92.

43. Hooper NM, Turner AJ. The search for alpha-secretase and its potential as a therapeutic approach to Alzheimer s disease. Curr Med Chem 2002;9:1107-19.

44. Slack BE, Ma LK, Seah CC. Constitutive shedding of the amyloid precursor protein ectodomain is up-regulated by tumour necrosis factor-alpha converting enzyme. Biochem J 2001;357:787-94.

45. Dingwall C. Spotlight on BACE: the secretases as targets for treatment in Alzheimer disease. J Clin Invest 2001;108:1243-6.

46. Huse JT, Doms RW. Closing in on the amyloid cascade: recent insights into the cell biology of Alzheimer's disease. Mol Neurobiol 2000;22:81-98.

47. Nunan J, Small DH. Regulation of APP cleavage by alpha-, beta- and gamma-secretases. FEBS Lett 2000;483:6-10.

48. Howlett DR, Simmons DL, Dingwall C, Christie G. In search of an enzyme: the beta-secretase of Alzheimer's disease is an aspartic proteinase. Trends Neurosci 2000;23:565-70.

49. Vassar R, Bennett BD, Babu-Khan S, et al. Beta-secretase cleavage of Alzheimer's amyloid precursor protein by the transmembrane aspartic protease BACE. Science 1999;286:735-41.

50. Cai H, Wang Y, McCarthy D, et al. BACE1 is the major beta-secretase for generation of Abeta peptides by neurons. Nat Neurosci 2001;4:233-4.

51. Luo Y, Bolon B, Kahn S, et al. Mice deficient in BACE1, the Alzheimer's beta-secretase, have normal phenotype and abolished beta-amyloid generation. Nat Neurosci 2001;4:231-2.

52. Vassar R. The beta-secretase, BACE: a prime drug target for Alzheimer's disease. J Mol Neurosci 2001;17:157-70.

53. Bodendorf U, Danner S, Fischer F, et al. Expression of human beta-secretase in the mouse brain increases the steady-state level of beta-amyloid. J Neurochem 2002;80:799-806.

54. Gouras GK, Xu H, Jovanovic JN, et al. Generation and regulation of beta-amyloid peptide variants by neurons. J Neurochem 1998;71:1920-5.

55. Pike CJ, Overman MJ, Cotman CW. Amino-terminal deletions enhance aggregation of beta-amyloid peptides in vitro. J Biol Chem 1995;270:23895-8.

56. Huse JT, Liu K, Pijak DS, Carlin D, Lee VM, Doms RW. Beta-secretase processing in the trans-Golgi network preferentially generates truncated amyloid species that accumulate in Alzheimer's disease brain. J Biol Chem 2002;277:16278-84.

57. Farzan M, Schnitzler CE, Vasilieva N, Leung D, Choe H. BACE2, a beta -secretase homolog, cleaves at the beta site and within the amyloid-beta region of the amyloid-beta precursor protein. Proc Natl Acad Sci U S A 2000;97:9712-7.

58. Bennett BD, Denis P, Haniu M, et al. A furin-like convertase mediates propeptide cleavage of BACE, the Alzheimer's beta -secretase. J Biol Chem 2000;275:37712-7.

59. Sherrington R, Rogaev EI, Liang Y, et al. Cloning of a gene bearing missense mutations in early-onset familial Alzheimer's disease. Nature 1995;375:754-60.

60. Rogaev EI, Sherrington R, Rogaeva EA, et al. Familial Alzheimer's disease in kindreds with missense mutations in a gene on chromosome 1 related to the Alzheimer's disease type 3 gene. Nature 1995;376:775-8.

61. Francis R, McGrath G, Zhang J, et al. aph-1 and pen-2 are required for Notch pathway signaling, gamma-secretase cleavage of betaAPP, and presenilin protein accumulation. Dev Cell 2002;3:85-97.

62. Yu G, Nishimura M, Arawaka S, et al. Nicastrin modulates presenilin-mediated notch/glp-1 signal transduction and betaAPP processing. Nature 2000;407:48-54.

63. Chen F, Hasegawa H, Schmitt-Ulms G, et al. TMP21 is a presenilin complex component that modulates gamma-secretase but not epsilon-secretase activity. Nature 2006;440:1208-12.

64. St George-Hyslop P, Schmitt-Ulms G. Alzheimer's disease: Selectively tuning gamma-secretase. Nature 2010;467:36-7.

65. Wolfe MS, Xia W, Ostaszewski BL, Diehl TS, Kimberly WT, Selkoe DJ. Two transmembrane aspartates in presenilin-1 required for presenilin endoproteolysis and gamma-secretase activity. Nature 1999;398:513-7.

66. Marambaud P, Robakis NK. Genetic and molecular aspects of Alzheimer's disease shed light on new mechanisms of transcriptional regulation. Genes Brain Behav 2005;4:134-46.

67. Mattson MP. Pathways towards and away from Alzheimer's disease. Nature 2004;430:631-9.

68. Mushegian A. Refining structural and functional predictions for secretasome components by comparative sequence analysis. Proteins 2002;47:69-74.

69. Zhang J, Kang DE, Xia W, et al. Subcellular distribution and turnover of presenilins in transfected cells. J Biol Chem 1998;273:12436-42.

70. Li X, Greenwald I. Additional evidence for an eight-transmembrane-domain topology for Caenorhabditis elegans and human presenilins. Proc Natl Acad Sci U S A 1998;95:7109-14.

71. Kim TW, Pettingell WH, Hallmark OG, Moir RD, Wasco W, Tanzi RE. Endoproteolytic cleavage and proteasomal degradation of presenilin 2 in transfected cells. J Biol Chem 1997;272:11006-10.

72. Steiner H, Capell A, Pesold B, et al. Expression of Alzheimer's disease-associated presenilin-1 is controlled by proteolytic degradation and complex formation. J Biol Chem 1998;273:32322-31.

73. Capell A, Grunberg J, Pesold B, et al. The proteolytic fragments of the Alzheimer's disease-associated presenilin-1 form heterodimers and occur as a 100-150-kDa molecular mass complex. J Biol Chem 1998;273:3205-11.

74. Yu G, Chen F, Levesque G, et al. The presenilin 1 protein is a component of a high molecular weight intracellular complex that contains beta-catenin. J Biol Chem 1998;273:16470-5.

75. Singh N, Talalayeva Y, Tsiper M, et al. The role of Alzheimer's disease-related presenilin 1 in intercellular adhesion. Exp Cell Res 2001;263:1-13.

76. Smine A, Xu X, Nishiyama K, et al. Regulation of brain G-protein go by Alzheimer's disease gene presenilin-1. J Biol Chem 1998;273:16281-8.

77. Katayama T, Imaizumi K, Sato N, et al. Presenilin-1 mutations downregulate the signalling pathway of the unfolded-protein response. Nat Cell Biol 1999;1:479-85.

78. Naruse S, Thinakaran G, Luo JJ, et al. Effects of PS1 deficiency on membrane protein trafficking in neurons. Neuron 1998;21:1213-21.

79. Levitan D, Greenwald I. Facilitation of lin-12-mediated signalling by sel-12, a Caenorhabditis elegans S182 Alzheimer's disease gene. Nature 1995;377:351-4.

80. Shen J, Bronson RT, Chen DF, Xia W, Selkoe DJ, Tonegawa S. Skeletal and CNS defects in Presenilin-1-deficient mice. Cell 1997;89:629-39.

81. Wong PC, Zheng H, Chen H, et al. Presenilin 1 is required for Notch1 and DII1 expression in the paraxial mesoderm. Nature 1997;387:288-92.

82. De Strooper B, Annaert W, Cupers P, et al. A presenilin-1-dependent gamma-secretase-like protease mediates release of Notch intracellular domain. Nature 1999;398:518-22.

83. Struhl G, Greenwald I. Presenilin is required for activity and nuclear access of Notch in Drosophila. Nature 1999;398:522-5.

84. Ye Y, Lukinova N, Fortini ME. Neurogenic phenotypes and altered Notch processing in Drosophila Presenilin mutants. Nature 1999;398:525-9.

85. Lambert MP, Barlow AK, Chromy BA, et al. Diffusible, nonfibrillar ligands derived from Abeta1-42 are potent central nervous system neurotoxins. Proc Natl Acad Sci U S A 1998;95:6448-53.

86. Glabe CG. Common mechanisms of amyloid oligomer pathogenesis in degenerative disease. Neurobiol Aging 2006;27:570-5.

87. Walsh DM, Klyubin I, Fadeeva JV, et al. Naturally secreted oligomers of amyloid beta protein potently inhibit hippocampal long-term potentiation in vivo. Nature 2002;416:535-9.

88. Karran E, Mercken M, De Strooper B. The amyloid cascade hypothesis for Alzheimer's disease: an appraisal for the development of therapeutics. Nat Rev Drug Discov 2011;10:698-712.

89. Haass C, Schlossmacher MG, Hung AY, et al. Amyloid beta-peptide is produced by cultured cells during normal metabolism. Nature 1992;359:322-5.

90. Walsh DM, Tseng BP, Rydel RE, Podlisny MB, Selkoe DJ. The oligomerization of amyloid beta-protein begins intracellularly in cells derived from human brain. Biochemistry 2000;39:10831-9.

91. Pike CJ, Walencewicz AJ, Glabe CG, Cotman CW. In vitro aging of beta-amyloid protein causes peptide aggregation and neurotoxicity. Brain Res 1991;563:311-4.

92. Castano EM, Ghiso J, Prelli F, Gorevic PD, Migheli A, Frangione B. In vitro formation of amyloid fibrils from two synthetic peptides of different lengths homologous to Alzheimer's disease beta-protein. Biochem Biophys Res Commun 1986;141:782-9.

93. Kirschner DA, Inouye H, Duffy LK, Sinclair A, Lind M, Selkoe DJ. Synthetic peptide homologous to beta protein from Alzheimer disease forms amyloid-like fibrils in vitro. Proc Natl Acad Sci U S A 1987;84:6953-7.

94. Katzman R. Alzheimer's disease. N Engl J Med 1986;314:964-73.

95. Terry RD, Masliah E, Salmon DP, et al. Physical basis of cognitive alterations in Alzheimer's disease: synapse loss is the major correlate of cognitive impairment. Ann Neurol 1991;30:572-80.

96. Dickson DW, Crystal HA, Bevona C, Honer W, Vincent I, Davies P. Correlations of synaptic and pathological markers with cognition of the elderly. Neurobiol Aging 1995;16:285,98; discussion 298-304.

97. Lambert MP, Barlow AK, Chromy BA, et al. Diffusible, nonfibrillar ligands derived from Abeta1-42 are potent central nervous system neurotoxins. Proc Natl Acad Sci U S A 1998;95:6448-53.

98. Gong Y, Chang L, Viola KL, et al. Alzheimer's disease-affected brain: presence of oligomeric A beta ligands (ADDLs) suggests a molecular basis for reversible memory loss. Proc Natl Acad Sci U S A 2003;100:10417-22.

99. Lesne S, Koh MT, Kotilinek L, et al. A specific amyloid-beta protein assembly in the brain impairs memory. Nature 2006;440:352-7.

100. Barghorn S, Nimmrich V, Striebinger A, et al. Globular amyloid beta-peptide oligomer - a homogenous and stable neuropathological protein in Alzheimer's disease. J Neurochem 2005;95:834-47.

101. Townsend M, Shankar GM, Mehta T, Walsh DM, Selkoe DJ. Effects of secreted oligomers of amyloid beta-protein on hippocampal synaptic plasticity: a potent role for trimers. J Physiol 2006;572:477-92.

102. Shankar GM, Bloodgood BL, Townsend M, Walsh DM, Selkoe DJ, Sabatini BL. Natural oligomers of the Alzheimer amyloid-beta protein induce reversible synapse loss by modulating an NMDA-type glutamate receptor-dependent signaling pathway. J Neurosci 2007;27:2866-75.

103. Shankar GM, Li S, Mehta TH, et al. Amyloid-beta protein dimers isolated directly from Alzheimer's brains impair synaptic plasticity and memory. Nat Med 2008;14:837-42.

104. Masliah E, Mallory M, Alford M, et al. Altered expression of synaptic proteins occurs early during progression of Alzheimer's disease. Neurology 2001;56:127-9.

105. DeKosky ST, Scheff SW. Synapse loss in frontal cortex biopsies in Alzheimer's disease: correlation with cognitive severity. Ann Neurol 1990;27:457-64.

106. Terry RD, Masliah E, Salmon DP, et al. Physical basis of cognitive alterations in Alzheimer's disease: synapse loss is the major correlate of cognitive impairment. Ann Neurol 1991;30:572-80.

107. Davies CA, Mann DM, Sumpter PQ, Yates PO. A quantitative morphometric analysis of the neuronal and synaptic content of the frontal and temporal cortex in patients with Alzheimer's disease. J Neurol Sci 1987;78:151-64.

108. Walsh DM, Townsend M, Podlisny MB, et al. Certain inhibitors of synthetic amyloid beta-peptide (Abeta) fibrillogenesis block oligomerization of natural Abeta and thereby rescue long-term potentiation. J Neurosci 2005;25:2455-62.

109. Larson J, Lynch G, Games D, Seubert P. Alterations in synaptic transmission and long-term potentiation in hippocampal slices from young and aged PDAPP mice. Brain Res 1999;840:23-35.

110. Chapman PF, White GL, Jones MW, et al. Impaired synaptic plasticity and learning in aged amyloid precursor protein transgenic mice. Nat Neurosci 1999;2:271-6.

111. Snyder EM, Nong Y, Almeida CG, et al. Regulation of NMDA receptor trafficking by amyloid-beta. Nat Neurosci 2005;8:1051-8.

112. Hsieh H, Boehm J, Sato C, et al. AMPAR removal underlies Abeta-induced synaptic depression and dendritic spine loss. Neuron 2006;52:831-43.

113. Mucke L, Masliah E, Yu GQ, et al. High-level neuronal expression of abeta 1-42 in wild-type human amyloid protein precursor transgenic mice: synaptotoxicity without plaque formation. J Neurosci 2000;20:4050-8.

114. Connor B, Young D, Yan Q, Faull RL, Synek B, Dragunow M. Brain-derived neurotrophic factor is reduced in Alzheimer's disease. Brain Res Mol Brain Res 1997;49:71-81.

115. Ikonomovic MD, Wecker L, Abrahamson EE, et al. Cortical alpha7 nicotinic acetylcholine receptor and beta-amyloid levels in early Alzheimer disease. Arch Neurol 2009;66:646-51.

116. Maelicke A, Samochocki M, Jostock R, et al. Allosteric sensitization of nicotinic receptors by galantamine, a new treatment strategy for Alzheimer's disease. Biol Psychiatry 2001;49:279-88.

117. Wang HY, Lee DH, D'Andrea MR, Peterson PA, Shank RP, Reitz AB. beta-Amyloid(1-42) binds to alpha7 nicotinic acetylcholine receptor with high affinity. Implications for Alzheimer's disease pathology. J Biol Chem 2000;275:5626-32.

118. Hauptmann S, Keil U, Scherping I, Bonert A, Eckert A, Muller WE. Mitochondrial dysfunction in sporadic and genetic Alzheimer's disease. Exp Gerontol 2006;41:668-73.

119. Caspersen C, Wang N, Yao J, et al. Mitochondrial Abeta: a potential focal point for neuronal metabolic dysfunction in Alzheimer's disease. FASEB J 2005;19:2040-1.

120. Smith MA, Perry G, Richey PL, et al. Oxidative damage in Alzheimer's. Nature 1996;382:120-1.

121. Nunomura A, Perry G, Aliev G, et al. Oxidative damage is the earliest event in Alzheimer disease. J Neuropathol Exp Neurol 2001;60:759-67.

122. Hensley K, Carney JM, Mattson MP, et al. A model for beta-amyloid aggregation and neurotoxicity based on free radical

generation by the peptide: relevance to Alzheimer disease. Proc Natl Acad Sci U S A 1994;91:3270-4.

123. Yan SD, Chen X, Fu J, et al. RAGE and amyloid-beta peptide neurotoxicity in Alzheimer's disease. Nature 1996;382:685-91.

124. Greenberg SM, Gurol ME, Rosand J, Smith EE. Amyloid angiopathy-related vascular cognitive impairment. Stroke 2004;35:2616-9.

125. Roher AE, Esh C, Rahman A, Kokjohn TA, Beach TG. Atherosclerosis of cerebral arteries in Alzheimer disease. Stroke 2004;35:2623-7.

126. Price JM, Chi X, Hellermann G, Sutton ET. Physiological levels of beta-amyloid induce cerebral vessel dysfunction and reduce endothelial nitric oxide production. Neurol Res 2001;23:506-12.

127. Paris D, Patel N, DelleDonne A, Quadros A, Smeed R, Mullan M. Impaired angiogenesis in a transgenic mouse model of cerebral amyloidosis. Neurosci Lett 2004;366:80-5.

128. Van Nostrand WE, Melchor JP, Ruffini L. Pathologic amyloid beta-protein cell surface fibril assembly on cultured human cerebrovascular smooth muscle cells. J Neurochem 1998;70:216-23.

129. Deane R, Zlokovic BV. Role of the blood-brain barrier in the pathogenesis of Alzheimer's disease. Curr Alzheimer Res 2007;4:191-7.

130. Wyss-Coray T, Mucke L. Inflammation in neurodegenerative disease--a double-edged sword. Neuron 2002;35:419-32.

131. Akiyama H, Barger S, Barnum S, et al. Inflammation and Alzheimer's disease. Neurobiol Aging 2000;21:383-421.

132. McGeer EG, Yasojima K, Schwab C, McGeer PL. The pentraxins: possible role in Alzheimer's disease and other innate inflammatory diseases. Neurobiol Aging 2001;22:843-8.

133. Kamal A, Almenar-Queralt A, LeBlanc JF, Roberts EA, Goldstein LS. Kinesin-mediated axonal transport of a membrane compartment containing beta-secretase and presenilin-1 requires APP. Nature 2001;414:643-8.

134. Stokin GB, Lillo C, Falzone TL, et al. Axonopathy and transport deficits early in the pathogenesis of Alzheimer's disease. Science 2005;307:1282-8.

135. Ehehalt R, Keller P, Haass C, Thiele C, Simons K. Amyloidogenic processing of the Alzheimer beta-amyloid precursor protein depends on lipid rafts. J Cell Biol 2003;160:113-23.

136. Bateman RJ, Munsell LY, Morris JC, Swarm R, Yarasheski KE, Holtzman DM. Human amyloid-beta synthesis and clearance rates as measured in cerebrospinal fluid in vivo. Nat Med 2006;12:856-61.

137. Zhao J, Fu Y, Yasvoina M, et al. Beta-site amyloid precursor protein cleaving enzyme 1 levels become elevated in neurons around amyloid plaques: implications for Alzheimer's disease pathogenesis. J Neurosci 2007;27:3639-49.

138. Weller RO, Preston SD, Subash M, Carare RO. Cerebral amyloid angiopathy in the aetiology and immunotherapy of Alzheimer disease. Alzheimers Res Ther 2009;1:6.

139. Weller RO, Massey A, Kuo YM, Roher AE. Cerebral amyloid angiopathy: accumulation of A beta in interstitial fluid drainage pathways in Alzheimer's disease. Ann N Y Acad Sci 2000;903:110-7.

140. Preston SD, Steart PV, Wilkinson A, Nicoll JA, Weller RO. Capillary and arterial cerebral amyloid angiopathy in Alzheimer's disease: defining the perivascular route for the elimination of amyloid beta from the human brain. Neuropathol Appl Neurobiol 2003;29:106-17.

141. Shibata M, Yamada S, Kumar SR, et al. Clearance of Alzheimer's amyloid-ss(1-40) peptide from brain by LDL receptor-related protein-1 at the blood-brain barrier. J Clin Invest 2000;106:1489-99.

142. Deane R, Bell RD, Sagare A, Zlokovic BV. Clearance of amyloid-beta peptide across the blood-brain barrier: implication for therapies in Alzheimer's disease. CNS Neurol Disord Drug Targets 2009;8:16-30.

143. Rogers J, Lue LF. Microglial chemotaxis, activation, and phagocytosis of amyloid beta-peptide as linked phenomena in Alzheimer's disease. Neurochem Int 2001;39:333-40.

144. Saido TC, Iwata N. Metabolism of amyloid beta peptide and pathogenesis of Alzheimer's disease. Towards presymptomatic diagnosis, prevention and therapy. Neurosci Res 2006;54:235-53.

145. Miners JS, Baig S, Palmer J, Palmer LE, Kehoe PG, Love S. Abeta-degrading enzymes in Alzheimer's disease. Brain Pathol 2008;18:240-52.

146. Leissring MA. The AbetaCs of Abeta-cleaving proteases. J Biol Chem 2008;283:29645-9.

147. Howell S, Nalbantoglu J, Crine P. Neutral endopeptidase can hydrolyze beta-amyloid(1-40) but shows no effect on beta-amyloid precursor protein metabolism. Peptides 1995;16:647-52.

148. Iwata N, Tsubuki S, Takaki Y, et al. Identification of the major Abeta1-42-degrading catabolic pathway in brain parenchyma:

suppression leads to biochemical and pathological deposition. Nat Med 2000;6:143-50.

149. Iwata N, Tsubuki S, Takaki Y, et al. Metabolic regulation of brain Abeta by neprilysin. Science 2001;292:1550-2.

150. Eckman EA, Reed DK, Eckman CB. Degradation of the Alzheimer's amyloid beta peptide by endothelin-converting enzyme. J Biol Chem 2001;276:24540-8.

151. Kurochkin IV, Goto S. Alzheimer's beta-amyloid peptide specifically interacts with and is degraded by insulin degrading enzyme. FEBS Lett 1994;345:33-7.

152. McDermott JR, Gibson AM. Degradation of Alzheimer's beta-amyloid protein by human and rat brain peptidases: involvement of insulin-degrading enzyme. Neurochem Res 1997;22:49-56.

153. Qiu WQ, Walsh DM, Ye Z, et al. Insulin-degrading enzyme regulates extracellular levels of amyloid beta-protein by degradation. J Biol Chem 1998;273:32730-8.

154. Hu J, Igarashi A, Kamata M, Nakagawa H. Angiotensin-converting enzyme degrades Alzheimer amyloid beta-peptide (A beta); retards A beta aggregation, deposition, fibril formation; and inhibits cytotoxicity. J Biol Chem 2001;276:47863-8.

155. Sasaki H, Saito Y, Hayashi M, Otsuka K, Niwa M. Nucleotide sequence of the tissue-type plasminogen activator cDNA from human fetal lung cells. Nucleic Acids Res 1988;16:5695.

156. Verde P, Boast S, Franze A, Robbiati F, Blasi F. An upstream enhancer and a negative element in the 5' flanking region of the human urokinase plasminogen activator gene. Nucleic Acids Res 1988;16:10699-716.

157. Miners JS, Baig S, Tayler H, Kehoe PG, Love S. Neprilysin and insulin-degrading enzyme levels are increased in Alzheimer disease in relation to disease severity. J Neuropathol Exp Neurol 2009;68:902-14.

158. Yin KJ, Cirrito JR, Yan P, et al. Matrix metalloproteinases expressed by astrocytes mediate extracellular amyloid-beta peptide catabolism. J Neurosci 2006;26:10939-48.

159. Tucker HM, Kihiko M, Caldwell JN, et al. The plasmin system is induced by and degrades amyloid-beta aggregates. J Neurosci 2000;20:3937-46.

160. Leal MC, Dorfman VB, Gamba AF, et al. Plaque-associated overexpression of insulin-degrading enzyme in the cerebral cortex of aged transgenic tg2576 mice with Alzheimer pathology. J Neuropathol Exp Neurol 2006;65:976-87.

161. Turner AJ, Isaac RE, Coates D. The neprilysin (NEP) family of zinc metalloendopeptidases: genomics and function. Bioessays 2001;23:261-9.

162. Barnes K, Turner AJ, Kenny AJ. Membrane localization of endopeptidase-24.11 and peptidyl dipeptidase A (angiotensin converting enzyme) in the pig brain: a study using subcellular fractionation and electron microscopic immunocytochemistry. J Neurochem 1992;58:2088-96.

163. Fukami S, Watanabe K, Iwata N, et al. Abeta-degrading endopeptidase, neprilysin, in mouse brain: synaptic and axonal localization inversely correlating with Abeta pathology. Neurosci Res 2002;43:39-56.

164. Iwata N, Takaki Y, Fukami S, Tsubuki S, Saido TC. Region-specific reduction of A beta-degrading endopeptidase, neprilysin, in mouse hippocampus upon aging. J Neurosci Res 2002;70:493-500.

165. Kanemitsu H, Tomiyama T, Mori H. Human neprilysin is capable of degrading amyloid beta peptide not only in the monomeric form but also the pathological oligomeric form. Neurosci Lett 2003;350:113-6.

166. Hama E, Shirotani K, Iwata N, Saido TC. Effects of neprilysin chimeric proteins targeted to subcellular compartments on amyloid

beta peptide clearance in primary neurons. J Biol Chem 2004;279:30259-64.

167. Marr RA, Guan H, Rockenstein E, et al. Neprilysin regulates amyloid Beta peptide levels. J Mol Neurosci 2004;22:5-11.

168. Leissring MA, Farris W, Chang AY, et al. Enhanced proteolysis of beta-amyloid in APP transgenic mice prevents plaque formation, secondary pathology, and premature death. Neuron 2003;40:1087-93.

169. Mohajeri MH, Kuehnle K, Li H, Poirier R, Tracy J, Nitsch RM. Anti-amyloid activity of neprilysin in plaque-bearing mouse models of Alzheimer's disease. FEBS Lett 2004;562:16-21.

170. Marr RA, Rockenstein E, Mukherjee A, et al. Neprilysin gene transfer reduces human amyloid pathology in transgenic mice. J Neurosci 2003;23:1992-6.

171. Akiyama H, Kondo H, Ikeda K, Kato M, McGeer PL. Immunohistochemical localization of neprilysin in the human cerebral cortex: inverse association with vulnerability to amyloid beta-protein (Abeta) deposition. Brain Res 2001;902:277-81.

172. Yasojima K, Akiyama H, McGeer EG, McGeer PL. Reduced neprilysin in high plaque areas of Alzheimer brain: a possible relationship to deficient degradation of beta-amyloid peptide. Neurosci Lett 2001;297:97-100.

173. Caccamo A, Oddo S, Sugarman MC, Akbari Y, LaFerla FM. Age- and region-dependent alterations in Abeta-degrading enzymes: implications for Abeta-induced disorders. Neurobiol Aging 2005;26:645-54.

174. Carpentier M, Robitaille Y, DesGroseillers L, Boileau G, Marcinkiewicz M. Declining expression of neprilysin in Alzheimer disease vasculature: possible involvement in cerebral amyloid angiopathy. J Neuropathol Exp Neurol 2002;61:849-56.

175. Naidoo V, Naidoo S, Raidoo DM. Immunolocalisation of endothelin-1 in human brain. J Chem Neuroanat 2004;27:193-200.

176. Funalot B, Ouimet T, Claperon A, et al. Endothelin-converting enzyme-1 is expressed in human cerebral cortex and protects against Alzheimer's disease. Mol Psychiatry 2004;9:1122,8, 1059.

177. Eckman EA, Watson M, Marlow L, Sambamurti K, Eckman CB. Alzheimer's disease beta-amyloid peptide is increased in mice deficient in endothelin-converting enzyme. J Biol Chem 2003;278:2081-4.

178. Bernstein HG, Ansorge S, Riederer P, Reiser M, Frolich L, Bogerts B. Insulin-degrading enzyme in the Alzheimer's disease brain: prominent localization in neurons and senile plaques. Neurosci Lett 1999;263:161-4.

179. Saavedra JM, Chevillard C. Angiotensin-converting enzyme is present in the subfornical organ and other circumventricular organs of the rat. Neurosci Lett 1982;29:123-7.

180. Kehoe PG, Russ C, McIlory S, et al. Variation in DCP1, encoding ACE, is associated with susceptibility to Alzheimer disease. Nat Genet 1999;21:71-2.

181. Lehmann DJ, Cortina-Borja M, Warden DR, et al. Large meta-analysis establishes the ACE insertion-deletion polymorphism as a marker of Alzheimer's disease. Am J Epidemiol 2005;162:305-17.

182. Sudilovsky A, Turnbull B, Croog SH, Crook T. Angiotensin converting enzyme and memory: preclinical and clinical data. Int J Neurol 1987;21-22:145-62.

183. Hemming ML, Selkoe DJ. Amyloid beta-protein is degraded by cellular angiotensin-converting enzyme (ACE) and elevated by an ACE inhibitor. J Biol Chem 2005;280:37644-50.

184. Barnes NM, Cheng CH, Costall B, Naylor RJ, Williams TJ, Wischik CM. Angiotensin converting enzyme density is increased in temporal cortex from patients with Alzheimer's disease. Eur J Pharmacol 1991;200:289-92.

185. Strickland S, Gualandris A, Rogove AD, Tsirka SE. Extracellular proteases in neuronal function and degeneration. Cold Spring Harb Symp Quant Biol 1996;61:739-45.

186. Kingston IB, Castro MJ, Anderson S. In vitro stimulation of tissue-type plasminogen activator by Alzheimer amyloid beta-peptide analogues. Nat Med 1995;1:138-42.

187. Wnendt S, Wetzels I, Gunzler WA. Amyloid beta peptides stimulate tissue-type plasminogen activator but not recombinant prourokinase. Thromb Res 1997;85:217-24.

188. Ledesma MD, Da Silva JS, Crassaerts K, Delacourte A, De Strooper B, Dotti CG. Brain plasmin enhances APP alpha-cleavage and Abeta degradation and is reduced in Alzheimer's disease brains. EMBO Rep 2000;1:530-5.

189. Tucker HM, Simpson J, Kihiko-Ehmann M, et al. Plasmin deficiency does not alter endogenous murine amyloid beta levels in mice. Neurosci Lett 2004;368:285-9.

190. Cabrejo L, Guyant-Marechal L, Laquerriere A, et al. Phenotype associated with APP duplication in five families. Brain 2006;129:2966-76.

191. Cadavid D, Mena H, Koeller K, Frommelt RA. Cerebral beta amyloid angiopathy is a risk factor for cerebral ischemic infarction. A

case control study in human brain biopsies. J Neuropathol Exp Neurol 2000;59:768-73.

192. Ryan NS, Rossor MN. Correlating familial Alzheimer's disease gene mutations with clinical phenotype. Biomark Med 2010;4:99-112.

193. Mahley RW. Apolipoprotein E: cholesterol transport protein with expanding role in cell biology. Science 1988;240:622-30.

194. Zannis VI, Just PW, Breslow JL. Human apolipoprotein E isoprotein subclasses are genetically determined. Am J Hum Genet 1981;33:11-24.

195. Corbo RM, Scacchi R. Apolipoprotein E (APOE) allele distribution in the world. Is APOE*4 a 'thrifty' allele? Ann Hum Genet 1999;63:301-10.

196. Corder EH, Saunders AM, Strittmatter WJ, et al. Gene dose of apolipoprotein E type 4 allele and the risk of Alzheimer's disease in late onset families. Science 1993;261:921-3.

197. Schmechel DE, Saunders AM, Strittmatter WJ, et al. Increased amyloid beta-peptide deposition in cerebral cortex as a consequence of apolipoprotein E genotype in late-onset Alzheimer disease. Proc Natl Acad Sci U S A 1993;90:9649-53.

198. Ma J, Yee A, Brewer HB,Jr, Das S, Potter H. Amyloid-associated proteins alpha 1-antichymotrypsin and apolipoprotein E promote assembly of Alzheimer beta-protein into filaments. Nature 1994;372:92-4.

199. Sanan DA, Weisgraber KH, Russell SJ, et al. Apolipoprotein E associates with beta amyloid peptide of Alzheimer's disease to form novel monofibrils. Isoform apoE4 associates more efficiently than apoE3. J Clin Invest 1994;94:860-9.

200. Greenberg SM, Rebeck GW, Vonsattel JP, Gomez-Isla T, Hyman BT. Apolipoprotein E epsilon 4 and cerebral hemorrhage associated with amyloid angiopathy. Ann Neurol 1995;38:254-9.

201. Pritchard SM, Dolan PJ, Vitkus A, Johnson GV. The toxicity of tau in Alzheimer disease: turnover, targets and potential therapeutics. J Cell Mol Med 2011;15:1621-35.

202. Augustinack JC, Schneider A, Mandelkow EM, Hyman BT. Specific tau phosphorylation sites correlate with severity of neuronal cytopathology in Alzheimer's disease. Acta Neuropathol 2002;103:26-35.

203. Luna-Munoz J, Chavez-Macias L, Garcia-Sierra F, Mena R. Earliest stages of tau conformational changes are related to the appearance of a sequence of specific phospho-dependent tau epitopes in Alzheimer's disease. J Alzheimers Dis 2007;12:365-75.

204. Luna-Munoz J, Garcia-Sierra F, Falcon V, Menendez I, Chavez-Macias L, Mena R. Regional conformational change involving phosphorylation of tau protein at the Thr231, precedes the structural change detected by Alz-50 antibody in Alzheimer's disease. J Alzheimers Dis 2005;8:29-41.

205. Cho JH, Johnson GV. Primed phosphorylation of tau at Thr231 by glycogen synthase kinase 3beta (GSK3beta) plays a critical role in regulating tau's ability to bind and stabilize microtubules. J Neurochem 2004;88:349-58.

206. Biernat J, Gustke N, Drewes G, Mandelkow EM, Mandelkow E. Phosphorylation of Ser262 strongly reduces binding of tau to microtubules: distinction between PHF-like immunoreactivity and microtubule binding. Neuron 1993;11:153-63.

207. Steinhilb ML, Dias-Santagata D, Fulga TA, Felch DL, Feany MB. Tau phosphorylation sites work in concert to promote neurotoxicity in vivo. Mol Biol Cell 2007;18:5060-8.

208. Basurto-Islas G, Luna-Munoz J, Guillozet-Bongaarts AL, Binder LI, Mena R, Garcia-Sierra F. Accumulation of aspartic acid421- and glutamic acid391-cleaved tau in neurofibrillary tangles correlates with progression in Alzheimer disease. J Neuropathol Exp Neurol 2008;67:470-83.

209. Rohn TT, Rissman RA, Davis MC, Kim YE, Cotman CW, Head E. Caspase-9 activation and caspase cleavage of tau in the Alzheimer's disease brain. Neurobiol Dis 2002;11:341-54.

210. Gamblin TC, Chen F, Zambrano A, et al. Caspase cleavage of tau: linking amyloid and neurofibrillary tangles in Alzheimer's disease. Proc Natl Acad Sci U S A 2003;100:10032-7.

211. Rissman RA, Poon WW, Blurton-Jones M, et al. Caspase-cleavage of tau is an early event in Alzheimer disease tangle pathology. J Clin Invest 2004;114:121-30.

212. Albrecht S, Bourdeau M, Bennett D, Mufson EJ, Bhattacharjee M, LeBlanc AC. Activation of caspase-6 in aging and mild cognitive impairment. Am J Pathol 2007;170:1200-9.

213. Guo H, Albrecht S, Bourdeau M, Petzke T, Bergeron C, LeBlanc AC. Active caspase-6 and caspase-6-cleaved tau in neuropil threads, neuritic plaques, and neurofibrillary tangles of Alzheimer's disease. Am J Pathol 2004;165:523-31.

214. Horowitz PM, Patterson KR, Guillozet-Bongaarts AL, et al. Early N-terminal changes and caspase-6 cleavage of tau in Alzheimer's disease. J Neurosci 2004;24:7895-902.

215. Binder LI, Guillozet-Bongaarts AL, Garcia-Sierra F, Berry RW. Tau, tangles, and Alzheimer's disease. Biochim Biophys Acta 2005;1739:216-23.

216. Mi K, Johnson GV. The role of tau phosphorylation in the pathogenesis of Alzheimer's disease. Curr Alzheimer Res 2006;3:449-63.

217. LaPointe NE, Morfini G, Pigino G, et al. The amino terminus of tau inhibits kinesin-dependent axonal transport: implications for filament toxicity. J Neurosci Res 2009;87:440-51.

218. Dubey M, Chaudhury P, Kabiru H, Shea TB. Tau inhibits anterograde axonal transport and perturbs stability in growing axonal neurites in part by displacing kinesin cargo: neurofilaments attenuate tau-mediated neurite instability. Cell Motil Cytoskeleton 2008;65:89-99.

219. Ebneth A, Godemann R, Stamer K, Illenberger S, Trinczek B, Mandelkow E. Overexpression of tau protein inhibits kinesin-dependent trafficking of vesicles, mitochondria, and endoplasmic reticulum: implications for Alzheimer's disease. J Cell Biol 1998;143:777-94.

220. Tatebayashi Y, Haque N, Tung YC, Iqbal K, Grundke-Iqbal I. Role of tau phosphorylation by glycogen synthase kinase-3beta in the regulation of organelle transport. J Cell Sci 2004;117:1653-63.

221. Ittner LM, Ke YD, Gotz J. Phosphorylated Tau interacts with c-Jun N-terminal kinase-interacting protein 1 (JIP1) in Alzheimer disease. J Biol Chem 2009;284:20909-16.

222. Baloyannis SJ. Mitochondrial alterations in Alzheimer's disease. J Alzheimers Dis 2006;9:119-26.

223. Bubber P, Haroutunian V, Fisch G, Blass JP, Gibson GE. Mitochondrial abnormalities in Alzheimer brain: mechanistic implications. Ann Neurol 2005;57:695-703.

224. Quintanilla RA, Matthews-Roberson TA, Dolan PJ, Johnson GV. Caspase-cleaved tau expression induces mitochondrial dysfunction in immortalized cortical neurons: implications for the pathogenesis of Alzheimer disease. J Biol Chem 2009;284:18754-66.

225. Golde TE, Petrucelli L, Lewis J. Targeting Abeta and tau in Alzheimer's disease, an early interim report. Exp Neurol 2010;223:252-66.

226. Vassar R. Beta-secretase (BACE) as a drug target for Alzheimer's disease. Adv Drug Deliv Rev 2002;54:1589-602.

227. Wolfe MS. Inhibition and modulation of gamma-secretase for Alzheimer's disease. Neurotherapeutics 2008;5:391-8.

228. Bateman RJ, Siemers ER, Mawuenyega KG, et al. A gamma-secretase inhibitor decreases amyloid-beta production in the central nervous system. Ann Neurol 2009;66:48-54.

229. De Strooper B, Annaert W, Cupers P, et al. A presenilin-1-dependent gamma-secretase-like protease mediates release of Notch intracellular domain. Nature 1999;398:518-22.

230. Mayer SC, Kreft AF, Harrison B, et al. Discovery of begacestat, a Notch-1-sparing gamma-secretase inhibitor for the treatment of Alzheimer's disease. J Med Chem 2008;51:7348-51.

231. Weggen S, Eriksen JL, Das P, et al. A subset of NSAIDs lower amyloidogenic Abeta42 independently of cyclooxygenase activity. Nature 2001;414:212-6.

232. Jacobsen JS, Comery TA, Martone RL, et al. Enhanced clearance of Abeta in brain by sustaining the plasmin proteolysis cascade. Proc Natl Acad Sci U S A 2008;105:8754-9.

233. Orgogozo JM, Gilman S, Dartigues JF, et al. Subacute meningoencephalitis in a subset of patients with AD after Abeta42 immunization. Neurology 2003;61:46-54.

234. Schenk DB, Seubert P, Grundman M, Black R. A beta immunotherapy: Lessons learned for potential treatment of Alzheimer's disease. Neurodegener Dis 2005;2:255-60.

235. Schneeberger A, Mandler M, Otawa O, Zauner W, Mattner F, Schmidt W. Development of AFFITOPE vaccines for Alzheimer's disease (AD)--from concept to clinical testing. J Nutr Health Aging 2009;13:264-7.

236. McLaurin J, Franklin T, Zhang X, Deng J, Fraser PE. Interactions of Alzheimer amyloid-beta peptides with glycosaminoglycans effects on fibril nucleation and growth. Eur J Biochem 1999;266:1101-10.

237. McLaurin J, Golomb R, Jurewicz A, Antel JP, Fraser PE. Inositol stereoisomers stabilize an oligomeric aggregate of Alzheimer amyloid beta peptide and inhibit abeta -induced toxicity. J Biol Chem 2000;275:18495-502.

238. Townsend M, Cleary JP, Mehta T, et al. Orally available compound prevents deficits in memory caused by the Alzheimer amyloid-beta oligomers. Ann Neurol 2006;60:668-76.

239. Lannfelt L, Blennow K, Zetterberg H, et al. Safety, efficacy, and biomarker findings of PBT2 in targeting Abeta as a modifying therapy for Alzheimer's disease: a phase IIa, double-blind, randomised, placebo-controlled trial. Lancet Neurol 2008;7:779-86.

240. Bush AI, Tanzi RE. Therapeutics for Alzheimer's disease based on the metal hypothesis. Neurotherapeutics 2008;5:421-32.

241. Hutton M, Lendon CL, Rizzu P, et al. Association of missense and 5'-splice-site mutations in tau with the inherited dementia FTDP-17. Nature 1998;393:702-5.

242. Nakashima H, Ishihara T, Suguimoto P, et al. Chronic lithium treatment decreases tau lesions by promoting ubiquitination in a mouse model of tauopathies. Acta Neuropathol 2005;110:547-56.

243. Noble W, Planel E, Zehr C, et al. Inhibition of glycogen synthase kinase-3 by lithium correlates with reduced tauopathy and degeneration in vivo. Proc Natl Acad Sci U S A 2005;102:6990-5.

244. Gendron TF, Petrucelli L. The role of tau in neurodegeneration. Mol Neurodegener 2009;4:13.

Chapter 1

A Recessive Mutation in the APP Gene with Dominant-Negative Effect on Amyloidogenesis

Giuseppe Di Fede, **Marcella Catania**, Michela Morbin, Giacomina Rossi, Silvia Suardi, Giulia Mazzoleni, Marco Merlin, Anna Rita Giovagnoli, Sara Prioni, Alessandra Erbetta, Chiara Falcone, Marco Gobbi, Laura Colombo, Antonio Bastone, Marten Beeg, Claudia Manzoni, Bruna Francescucci, Alberto Spagnoli, Laura Cantù, Elena Del Favero, Efrat Levy, Mario Salmona, Fabrizio Tagliavini

Science, 2009 Mar 13;323(5920):1473-7

1. Abstract

Amyloid-β precursor protein (APP) mutations cause familial Alzheimer's disease with virtually complete penetrance. We found an APP mutation (A673V) that causes disease only in the homozygous state, while heterozygous carriers were unaffected, consistent with a recessive Mendelian trait of inheritance. The A673V mutation affected APP processing, resulting in enhanced amyloid β (Aβ) production and formation of amyloid fibrils in vitro. Co-incubation of mutated and wild-type peptides conferred instability on Aβ aggregates and inhibited amyloidogenesis and neurotoxicity. The highly amyloidogenic effect of the A673V mutation in the homozygous state and its anti-amyloidogenic effect in the heterozygous state account for the autosomal recessive pattern of inheritance, and have implications for genetic screening and the potential treatment of Alzheimer's disease.

2. Introduction

A central pathological feature of Alzheimer's disease (AD) is the accumulation of amyloid β protein (Aβ) in the form of oligomers and amyloid fibrils in the brain[1]. Aβ is generated by sequential cleavage of the amyloid β precursor protein (APP) by β- and γ-secretases, and exists as short and long isoforms, Aβ1-40 and Aβ1-42[2]. Aβ1-42 is especially prone to misfolding and builds up aggregates that are thought to be the primary neurotoxic species involved in AD pathogenesis[2,3]. AD is usually sporadic, but a small fraction of cases is familial[4]. The familial forms show an autosomal dominant pattern of inheritance with virtually complete penetrance,

and are linked to mutations in the APP, presenilin 1 or presenilin 2 genes[5]. The APP mutations close to the sites of β- or γ-secretase cleavage flanking the Aβ sequence overproduce total Aβ or only Aβ1-42, respectively, while those that alter amino acids within Aβ result in greater propensity to aggregation in vitro[6,7].

3. Results

We have identified an APP mutation (A673V) that causes disease only in the homozygous state. The mutation consists of C-to-T transition resulting in alanine-to-valine substitution at position 673 (APP770 numbering) corresponding to position 2 of Aβ (Figs. 1A and S1). The genetic defect was found in a patient with early-onset dementia and in his younger sister who now shows multiple-domain mild cognitive impairment (MCI). Six relatives aged between 20 and 88 years, from both parental lineages, carrying the A673V mutation in the heterozygous state, were not affected, as deduced by formal neuropsychological assessment (supporting online text, fig. S2, table S1), consistent with a recessive Mendelian trait of inheritance. The A673V mutation was not found in 200 healthy individuals and 100 sporadic AD patients. Both mutated and wild-type APP mRNA were expressed in heterozygous carriers.

In the patient, the disease presented with behavioural changes and cognitive deficits at the age of 36 years, and evolved towards severe dementia with spastic tetraparesis, leading to complete loss of autonomy in about eight years (supporting online text). Serial magnetic resonance imaging showed progressive cortico-subcortical atrophy (Fig. S3). Cerebrospinal fluid analysis evidenced decreased

Aβ1-42 and increased total and 181T-phosphorylated tau compared to non-demented controls, similarly to AD subjects (Table S2, fig. S4). In the plasma of the patient and his A673V homozygous sister, Aβ1-40 and Aβ1-42 were higher than in non-demented controls, while the six A673V heterozygous carriers had intermediate levels (Table S2, fig. S4).

In conditioned media of fibroblasts prepared from skin biopsies Aβ1-40 and Aβ1-42 were 2.1- and 1.7-fold higher in the patient than in four age-matched controls with no change in Aβ1-42:Aβ1-40 ratio (Table S2, fig. S4), suggesting that the A673V variant alters APP processing, promoting an increase in Aβ formation. To confirm this, we transiently transfected CHO and COS7 cells with either mutant or wild-type APP cDNA and measured Aβ in conditioned media by ELISA. Cells expressing A673V APP had significantly higher levels of both Aβ1-40 and Aβ1-42 than cells transfected with wild-type APP, with no change in Aβ1-42:Aβ1-40 ratio (Table S2). CHO and COS7 cells with the A673V mutation also had increased secretion of amino-terminally truncated Aβ species, including Aβ11-40, Aβ11-42, and AβN3pE-42 (Table S2). These differences were paralleled by differences in the production of soluble forms of APP (sAPPβ and sAPPα), and of APP carboxy-terminal fragments (C99 and C83), derived from the amyloidogenic β-secretase or non-amyloidogenic α-secretase processing. Fibroblasts of the patient showed increased secretion of sAPPβ and 2.5-fold increase in sAPPβ:sAPPα ratio (mean of three determinations: 0.5) as compared to four age-matched controls (0.2±0.01) as deduced by ELISA. Similarly, the sAPPβ:sAPPα ratio was significantly higher in media

from CHO cells expressing the A673V mutation (0.4±0.1) than in control cells (0.1±0.03, p=0.03) (Fig. 1B). Immunoblot analysis of cell lysates with an antibody to the carboxy-terminal region of APP showed a 1.9±0.2 increase in C99:C83 ratio in patient's fibroblasts (mean of three determinations: 0.67) compared to control fibroblasts (0.35±0.02), and 2.5±0.2 increase in mutated CHO cells (0.52±0.10) compared to control cells (0.21±0.05, p=0.0001) (Fig. 1C,D).

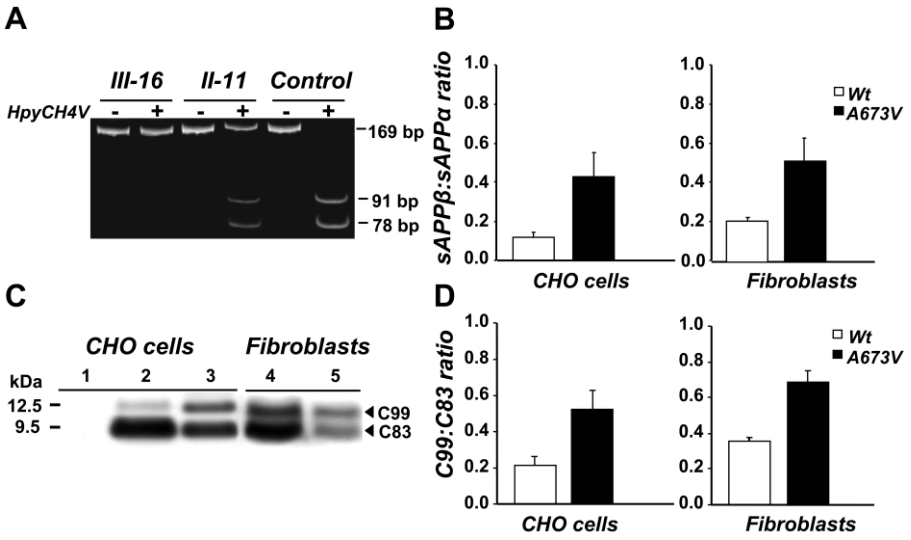

Figure 1. Analysis of APP gene and APP processing. (A) APP gene analysis by restriction fragment length polymorphism of 169—base pair (bp) polymerase chain reaction (PCR) products amplified from homozygous (III-16), heterozygous (II-11), and control subjects. In the absence of the A673V mutation, the enzyme HpyCH4V generates two fragments of 91 and 78 bp. The mutation abolishes the restriction site, and the PCR product remains uncut. (B) sAPPβ:sAPPα ratio in conditioned media from CHO cells transfected with wild-type or A673V-mutated APP and fibroblasts of the proband and four controls. Error bars represent means ± SD. (C) APP carboxy-terminal fragments C99 and C83 (arrowheads) in CHO cells transfected with wild-type (lane 2) or A673V-mutated (lane 3) APP and fibroblasts from a control (lane 4) and the proband (lane 5), as shown by immunoblot analysis. Lane 1 corresponds to lysates from nontransfected CHO cells. (D) Densitometric analysis of immunoblots, showing a significant increase in the C99:C83 ratio ($P = 0.0001$) in cells carrying the A673V mutation. Error bars represent means ± SD.

We then investigated the effects of the A673V mutation on the aggregation and amyloidogenic properties of Aβ using synthetic peptides homologous to residues 1-40 with and without the A-to-V substitution at position 2 (Aβ1-40mut and Aβ1-40wt). Laser light scattering measurements over short periods (first 24 h after sample preparation) showed that the aggregation kinetics was faster for Aβ1-40mut than Aβ1-40wt, the time constants of the exponential increase being 1.3 h and 5.8 h, respectively (Fig. 2A). Furthermore, while the initial size distribution of particles generated by the two peptides was similar, after 24 h Aβ1-40mut assemblies were much larger than Aβ1-40wt aggregates (Fig. 2B). Polarized-light and electron microscopy showed that Aβ1-40mut aggregates with the tinctorial properties of amyloid (i.e., birefringence after Congo red staining) ultrastructurally formed by straight, unbranched, 8 nm-diameter fibrils, were already apparent after 4 h. Amyloid progressively increased up to five days, when the samples contained only fibrils organized in dense meshwork (Fig. 3B,E,H,K). Aβ1-40wt followed a qualitatively similar assembly path but with much slower kinetics. Eight-nm-diameter amyloid fibrils were first observed after 72 h, mingled with oligomers and protofibrils (Fig. 3A,G), and the size and density of congophilic aggregates reached a plateau only after 20 days (Fig. 3D,J). Similar differences were observed between wild-type and mutated peptides homologous to residues 1-42 of Aβ (Fig. 3M,N), although the aggregation kinetics was faster as compared to Aβ1-40.

The finding that the A673V mutation strongly boosts Aβ production and fibrillogenesis raises the question why heterozygous carriers do not develop disease, so we analyzed the effects of the interaction between Aβ1-40mut and Aβ1-40wt. Laser light scattering showed that the time constant of aggregate formation of equimolar mixtures of wild-type and mutated peptides was higher (8.3 h) than either Aβ1-40mut (1.3 h) or Aβ1-40wt alone (5.8 h) (Fig. 2A), and the size distribution of particles was lowest both at time 0 and after 24 h (Fig. 2B). Furthermore, the aggregates formed by peptide mixtures were far more unstable than those generated by either Aβ1-40wt or Aβ1-40mut following dilution with buffer, with a characteristic dissolution time of 8 min. At the same time, no dissolution kinetics was observed for samples of Aβ1-40wt and Aβ1-40mut alone (Fig. 2C). This was confirmed by urea denaturation studies of peptide aggregates. Size exclusion chromatography showed that the elution profiles of Aβ1-40wt and Aβ1-40mut were marked by a single peak corresponding to the dimer, while the mixture gave a smaller peak area corresponding to the dimer and a second small peak corresponding to the monomer (Fig. 4A). Polarized-light and electron microscopy showed that the peptide mixture built up much less congophilic aggregates not only than Aβ1-40mut but also than Aβ1-40wt (Fig. 3C,F,I,L). Similar results were observed with Aβ1-42 peptides (Fig. 3M,N,O). Amyloid formation was also inhibited when Aβ1-40wt was incubated with a hexapeptide homologous to residues 1-6 containing the A-to-V substitution in position 2 (Aβ1-6mut) at 1:4 molar ratio (Fig. S5).

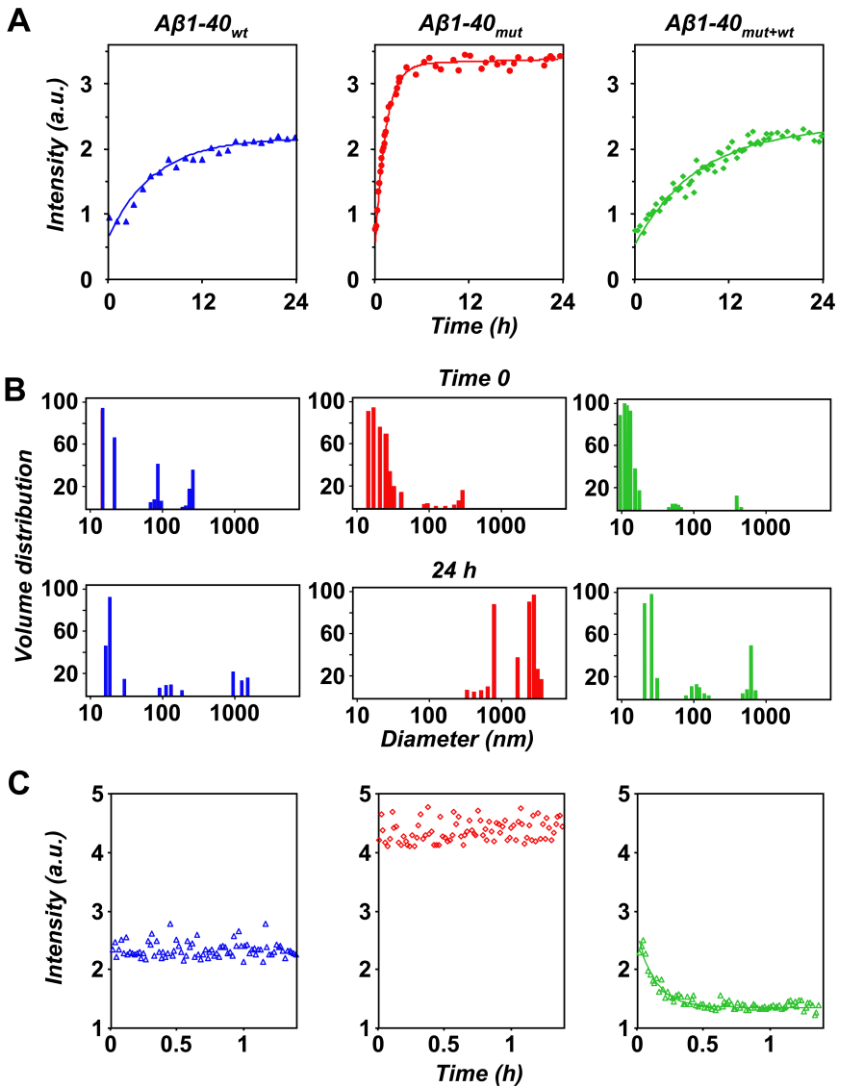

Figure 2. Short-time kinetics of Ab assembly and disassembly, determined by laser light scattering. (A) Courseof the light intensity scattered by solutions of Ab1-40wt (blue), Ab1-40mut (red), and their equimolar mixture (green). The corresponding exponential fits are indicated by full lines. (B) Particle size distribution of Ab1-40wt (blue), Ab1-40mut (red), and the peptidemixture (green) immediately after sample preparation (time 0) and after 24 hours. (C) Shorttime dissolution kinetics of 48-hour-aged peptide aggregates after fivefold dilution with buffer. a.u., arbitrary units.

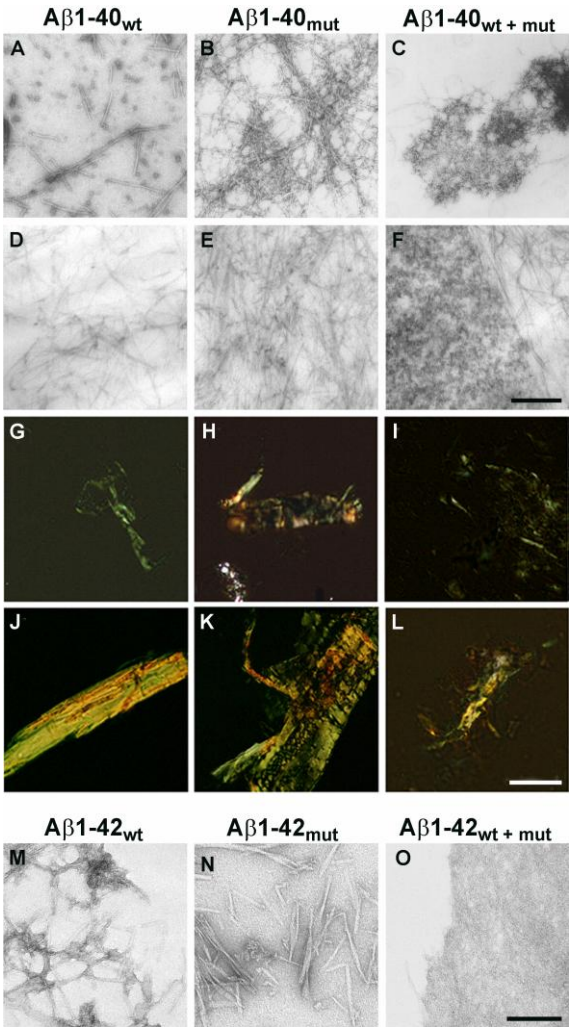

Figure 3. Aggregation properties of mutated and wild-type Aβ peptides. (A to F) Electron micrographs of aggregates generated by Aβ1-40wt, Aβ1-40mut, and equimolar mixtures after 72 hours [(A) to (C), negative staining] and 20 days incubation [(D) to (F), positive staining]. (G to L) Polarized light microscopy of Aβ aggregates stained with Congo red after 72 hours [(G) to (I)] and 20 days [(J) to (L)]. (M to O) Electron micrographs of negatively stained aggregates generated by Aβ1-42wt (M), Aβ1-42mut (N), and equimolar mixtures (O) after 5 days incubation. The peptide mixture contains mainly amorphous material (O), whereas wild-type and mutated Aβ1-42 are assembled in fibrillary structures. Scale bars indicate 250 nm [(A) to (F)], 50 mm [(G) to (L)], and 125 nm [(M) to (O)].

We analyzed the binding of Aβ peptides with and without the A673V mutation to Aβ1-40wt using surface plasmon resonance. In addition to Aβ1-40wt and Aβ1-40mut, we used the hexapeptides Aβ1-6wt and Aβ1-6mut, to evaluate the independent contribution of the amino-terminal sequence containing the mutation. No difference in binding was observed between Aβ1-40wt and Aβ1-40mut to immobilized Aβ1-40wt fibrils, consistent with the finding that Aβ aggregation is primarily driven by hydrophobic stretches in the central and carboxy-terminal parts of the peptide (Fig. 4B)[9]. However, the amino-terminal fragment Aβ1-6mut showed greater ability to bind to wild-type Aβ1-40 than Aβ1-6wt (Fig. 4C), indicating that the A-to-V substitution at position 2 favors the interaction between mutant and wild-type Aβ.

Finally, we treated human neuroblastoma SH-SY5Y cells with Aβ1-42wt, Aβ1-42mut or mixtures thereof at 5 μM for 24 h, and assessed cell viability by MTT[8]: Aβ1-42mut was more toxic than Aβ1-42wt, and the mixture was significantly less toxic than either peptide alone (Fig. 4D).

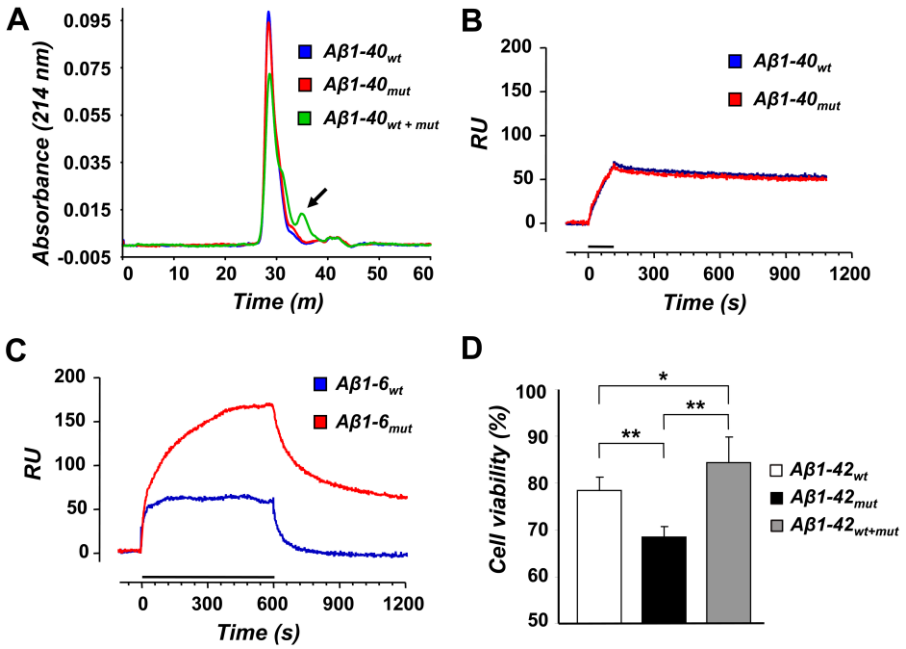

Figure 4. Physicochemical and biological properties of mutated and wild-type Aβ peptides. (A) Size exclusion chromatograms of Aβ1-40wt, Aβ1-40mut, and equimolar peptide mixture aggregates after treatment with 1 M urea for 24 hours. Monomeric species (arrow) are only seen in the peptide mixture. (B and C) Binding of wild-type and mutated Aβ1-40 (B) or Aβ1-6 (C) to amyloid fibrils of Aβ1-40wt determined by surface plasmon resonance. Solutions of Aβ1-40 (1 mM) or Aβ1-6 (500 mM) were injected onto Aβ1-40wt fibrils immobilized on the sensor chip for the time indicated by the bars. (D) Viability of human neuroblastoma cells after 24 hours exposure to 5 mM Aβ1-42wt, Aβ1-42mut, and the equimolar mixture. Error bars represent SD of the mean of eight replicates. *P = 0.026, **P < 0.001.

4. Discussion

We have identified a mutation in the APP gene showing a recessive Mendelian trait of inheritance. Recently, a homozygous APP mutation (A693Δ) was detected in three AD patients from two Japanese pedigrees[10]. Since one out of four heterozygous individuals had MCI, in the absence of experimental studies mimicking the situation in heterozygotes, it is hard to establish whether A693Δ is a recessive mutation or a dominant APP variant with incomplete penetrance.

The A673V APP mutation has two pathogenic effects: (i) it shifts APP processing towards the amyloidogenic pathway and (ii) enhances the aggregation and fibrillogenic properties of Aβ. However, the interaction between mutant and wild-type Aβ, favored by the A-to-V substitution at position 2, interferes with nucleation or nucleation-dependent polymerization, or both, hindering amyloidogenesis and neurotoxicity, and thus protecting the heterozygous carriers.

Until recently, the importance of the amino-terminal sequence of Aβ in misfolding and disease was underestimated since this region is highly disordered in the fibrillar form of the peptide[11]. However, the amino-terminal domain of Aβ is selectively perturbed in amyloidogenesis and, most significantly, changes in its primary sequence trigger peptide assembly and fibril formation[12,13]. The importance of this domain is further supported by the finding that antibodies against it are optimal for plaque clearance in animal models[14]. A previous study reported a distinct heterozygous APP mutation at codon 673 (A673T) in a subject without clinical signs of

dementia[15]. Histological analysis did not detect amyloid deposits in the brain. However, when the A673T mutation was introduced in a synthetic Aβ1-40 peptide, it increased the propensity to aggregate, with a much shorter lag-phase than the wild-type peptide[16]. These observations, together with our results, suggest that mutations at position 2 of Aβ confer amyloidogenic properties that lead to AD only in the homozygous state. The finding that the interaction between A673V-mutated and wild-type Aβ hinders amyloidogenesis, and especially the anti-amyloidogenic properties of the mutated six-residue peptide, may offer grounds for the development of therapeutic strategies based on modified Aβ peptides or peptido-mimetic compounds[17,18] for both sporadic and familial AD.

The present data highlight the importance of screening demented and non-demented human populations for mutations of the Aβ encoding region of APP. Genetic variants that could be regarded as normal polymorphisms may turn out to be pathogenic in homozygous individuals. The identification of such mutations would help to prevent the occurrence of the disease in their carriers.

5. References

1. Hardy J, Selkoe DJ. The amyloid hypothesis of Alzheimer's disease: progress and problems on the road to therapeutics. Science 2002;297:353-6.

2. Selkoe DJ. Alzheimer's disease: genes, proteins, and therapy. Physiol Rev 2001;81:741-66.

3. Walsh DM, Klyubin I, Fadeeva JV, et al. Naturally secreted oligomers of amyloid beta protein potently inhibit hippocampal long-term potentiation in vivo. Nature 2002;416:535-9.

4. Bertram L, Tanzi RE. The genetic epidemiology of neurodegenerative disease. J Clin Invest 2005;115:1449-57.

5. Rocchi A, Pellegrini S, Siciliano G, Murri L. Causative and susceptibility genes for Alzheimer's disease: a review. Brain Res Bull 2003;61:1-24.

6. St George-Hyslop PH. Molecular genetics of Alzheimer's disease. Biol Psychiatry 2000;47:183-99.

7. Levy E, Carman MD, Fernandez-Madrid IJ, et al. Mutation of the Alzheimer's disease amyloid gene in hereditary cerebral hemorrhage, Dutch type. Science 1990;248:1124-6.

8. Petersen RC, Doody R, Kurz A, et al. Current concepts in mild cognitive impairment. Arch Neurol 2001;58:1985-92.

9. Cecchini M, Curcio R, Pappalardo M, Melki R, Caflisch A. A molecular dynamics approach to the structural characterization of amyloid aggregation. J Mol Biol 2006;357:1306-21.

10. Tomiyama T, Nagata T, Shimada H, et al. A new amyloid beta variant favoring oligomerization in Alzheimer's-type dementia. Ann Neurol 2008;63:377-87.

11. Williams AD, Portelius E, Kheterpal I, et al. Mapping abeta amyloid fibril secondary structure using scanning proline mutagenesis. J Mol Biol 2004;335:833-42.

12. Lim KH. A weakly clustered N terminus inhibits Abeta(1-40) amyloidogenesis. Chembiochem 2006;7:1662-6.

13. Hori Y, Hashimoto T, Wakutani Y, et al. The Tottori (D7N) and English (H6R) familial Alzheimer disease mutations accelerate Abeta fibril formation without increasing protofibril formation. J Biol Chem 2007;282:4916-23.

14. Bard F, Barbour R, Cannon C, et al. Epitope and isotype specificities of antibodies to beta -amyloid peptide for protection against Alzheimer's disease-like neuropathology. Proc Natl Acad Sci U S A 2003;100:2023-8.

15. Peacock ML, Warren JT,Jr, Roses AD, Fink JK. Novel polymorphism in the A4 region of the amyloid precursor protein gene in a patient without Alzheimer's disease. Neurology 1993;43:1254-6.

16. Meinhardt J, Tartaglia GG, Pawar A, et al. Similarities in the thermodynamics and kinetics of aggregation of disease-related Abeta(1-40) peptides. Protein Sci 2007;16:1214-22.

17. Soto C, Sigurdsson EM, Morelli L, Kumar RA, Castano EM, Frangione B. Beta-sheet breaker peptides inhibit fibrillogenesis in a rat brain model of amyloidosis: implications for Alzheimer's therapy. Nat Med 1998;4:822-6.

18. Adessi C, Frossard MJ, Boissard C, et al. Pharmacological profiles of peptide drug candidates for the treatment of Alzheimer's disease. J Biol Chem 2003;278:13905-11.

This work was supported by grants from the Italian Ministry of Health (533F/Q/1 to F.T. and M.S., and 71.6/2006 and RFPS 2007/02 to F.T.), CARIPLO Foundation (Guard) to F.T. and M.S., ERA-Net Neuron (nEUROsyn) to F.T., Negri-Weizmann Foundation to M.S., the National Institute of Neurological Disorders and Stroke (NS42029) to E.L., and the American Heart Association (0040102N) to E.L. A patent application related to this work has been filed by Fondazione IRCCS Istituto Nazionale Neurologico “Carlo Besta”.

6. Supporting Online Material

6.1 Materials and Methods

6.1.1 Neuropsychological evaluation

General intellectual function was assessed using Raven's Progressive Colored Matrices, and visuospatial perception by the Street's Completion Test. Auditory and visual memory were investigated using the immediate and delayed recall (Short Story Recall, Verbal Selective Reminding, Corsi Supraspan and Rey Figure Delayed Reproduction). Attention capabilities were assessed using the Attentive Matrices, Digit Span and the Trail Making. Language skills were measured by the Word Fluency, the Boston Naming Test and the Token Test. Executive functioning was evaluated by the Tower of London, the Weigl Sorting Test and Cognitive Estimation Test. Praxies were analyzed using the Imitating Gestures and Orofacial Expression Test and the Rey Figure Copying. Theory of Mind was evaluated by the Faux Pas Test. All tests were administered according to standardized procedures.

6.1.2 Genetic analysis

The exons 16 and 17 of the APP gene were amplified using the polymerase chain reaction (PCR) with previously described primers[S1]. Sequencing of both sense and complementary strand of the PCR product was performed with ABI PRISM model 310 using the ABI PRISM BigDyeTM terminator cycle sequencing ready reaction kit (Perkin-Elmer). The mutation A673V was confirmed by restriction fragment length polymorphism analysis. The exon 16 of APP was

amplified by PCR with the following primers: 5'-TACTTTAATTATGATGTAATAC-3' and 5'-GGCAAGACAAACAGTAGTGG-3'. The PCR product was digested with HpyCH4 V (New England Biolabs) and resolved using 10% polyacrilamide gels. The normal allele was characterised by two fragments of 91 and 78 bp, and the mutant allele by one fragment of 169 bp.

The Apoliprotein E (ApoE) genotype was determined using restriction isotyping, as described[S2]. Briefly, genomic DNA was amplified by PCR using the following primers: 5'-TCCAAGGAGCTGCAGGCGGCGCA-3' and 5'-ACAGAATTCGCCCCGGCCTGGTACACTGCC A-3'. The PCR products were digested with CfoI enzyme (Roche) and the resulting fragments were resolved by electrophoresis on 15% polyacrilamide gels.

The proband was also subjected to the analysis of the entire coding sequence of PSEN1, PSEN2, and the genes encoding the microtubule-associated protein tau, progranulin, prion protein and huntingtin as described[S3-7].

Total RNA was extracted from whole blood of the proband, a A673V heterozygous carrier and a control individual using the QIAamp RNA blood Mini Kit, according to the manufacturer's protocol. The RNA was reverse-transcribed with the Cloned AMV First-Strand cDNA Synthesis Kit using random primers. A 240-bp cDNA fragment comprising the mutated region was obtained by PCR with the following primers: 5'-CTGGGTTGACAAATATCAAGACGG-3' (forward) and 5'-

CCACACCATGATGAATGGATGTG-3’ (reverse). The amplified fragment was purified and subjected to direct sequencing in both directions.

6.1.3 Generation of DNA constructs and cell transfections

Human APP751 cDNA was HindIII subcloned into pcDNA3.1(-) plasmid vector (Invitrogen) and mutagenized using QuickChange site-directed mutagenesis kit (Stratagene) according to the manufacturer’s instructions with the following primers to introduce the A673V substitution: 5’-GATCTCTGAAGTGAAGATGGATGTAGAATTCCGACA TGAC-3’ (forward) and 5’-GTCATGTCGGAATTCTACATCCATCTTCACTTCAGAGATC-3’(reverse).

COS7 and CHO cells were maintained in D-MEM (Gibco) and ALPHA-MEM (Cambrex), respectively and both supplemented with 10% foetal bovine serum (FBS). When a 80% confluency was reached, the cells were transiently transfected with either wild-type or A673V APP by electroporation. Six h post-transfection, media were changed with OPTIMEM (Gibco) that was conditioned for 48 h and then collected for ELISA assays in the presence of a protease inhibitor cocktail (Roche). The efficacy of transfections was determined by immunoblot analysis of transfected cell lysates using the antibodies 22C11 (Chemicon, 1:10,000 dilution) and A8717 (Sigma, 1:2,000 dilution) that recognize all three isoforms of APP[S8,9]. CHO or COS7 cells expressing the wild-type or mutated APP were lysed 48 h after transfection in a cold lysis buffer (100 mM NaCl, 10 mM EDTA,

0.5% Nonidet P-40, 0.5% sodium deoxycholate, 10 mM Tris-HCl, pH 7.4) containing protease inhibitors (Roche), briefly sonicated, and boiled for 10 min. Fibroblasts were grown until reaching 80% confluence, conditioned for 5 days in highly enriched OPTIMEM and then lysed following the same protocol. Equal amounts of protein were separated on a 12.5% Tris-Tricine gel and transferred to PVDF membranes (Millipore), which were blocked in Tris-buffered saline with 0.1% tween-20 (TBST) containing 5% non-fat dry milk, and incubated with the appropriate primary antibody. The signal intensity of APP was evaluated by densitometric analysis of blots, that were developed using enhanced chemoluminescence (Amersham) and visualized on autoradiography films.

6.1.4 sAPP, Aβ, total tau and phospho-tau determinations

Plasma levels of Aβ1-40 and Aβ1-42 were determined in the proband, his A673V homozygous sister, six A673V heterozygous carriers, three family members without the A673V mutation and six unrelated healthy subjects. Plasma samples were collected and stored at -80°C until use. The plasma levels of Aβ1-40 and Aβ1-42 were measured by ELISA (The Genetics Company) following manufacturer's instructions. CSF levels of Aβ1-42, total tau and T181-phosphorylated tau were measured in the proband, 10 sporadic AD patients and 10 control subjects by ELISA (Innogenetics) as described[S10]. All determinations were performed in triplicate and were replicated six times.

sAPPα, sAPPβ, and Aβ peptides, including Aβ1-40, Aβ1-42 and N-terminal truncated Aβ species, were measured in conditioned media

from APP-transfected COS7 and CHO cells and fibroblasts obtained by skin biopsies from the proband and four unaffected unrelated subjects using ELISA (Immuno-Biological Laboratories and The Genetics Company). The conditioned media were stored at -80°C in presence of a protease inhibitor cocktail (Roche) until analysis. The experiments were performed in triplicate and repeated three times in fibroblasts and seven times in transfected cells, following manufacturer's instructions.

6.1.5 Immunoblot analysis of APP C-terminal fragments

Lysates of fibroblasts and transfected cells were analyzed by immunoblot with the A8717 antibody, to determine the levels of APP carboxy-terminal fragments C99 and C83. The blots were developed using enhanced chemoluminescence (Amersham) and visualized on autoradiography films.

Quantification of immunoreactive bands was carried out by densitometry of the scanned autoradiograms under conditions of non-saturated signal, using the Quantity One-image software (Biorad Laboratories Inc.). The experiments were repeated six times for transfected cells and three times for fibroblasts, and the densitometric values in each experiment were the mean of three determinations.

6.1.6 Aβ peptide synthesis and purification

Synthetic peptides homologous to residues 1-40, 1-42 and 1-6 of Aβ either with or without the A-to-V substitution in position 2 (Aβ1-40mut, Aβ1-40wt, Aβ1-42mut, Aβ1-42wt, Aβ1-6mut, Aβ1-6wt) were prepared by solid-phase synthesis and purified as described[S11]. The

purity and identity of peptides were determined by reverse-phase HPLC, amino acid sequencing and MALDI-TOF analysis. The purity of peptides was above 95%.

6.1.7 Laser light scattering

Aβ1-40mut, Aβ1-40wt and equimolar mixtures thereof were dissolved in 10 mM NaOH and then diluted in an equal volume of 100 mM Tris-HCl, pH 7.0, to the final concentration of 0.125 mM. The short-time (0-24 h) kinetics of aggregate formation was analyzed by laser light scattering, using an equipment designed at the Department of Medical Chemistry, Biochemistry and Biotechnology, University of Milan, that has been described in detail previously[S12]. Both independent static (SLS) and dynamic (QELS) laser light scattering measurements were performed on the same samples at 37°C. The average scattered intensity (SLS) increases with the average molecular mass of macromolecules in solution. The scattered intensity correlation function (QELS) decays are proportional to the translational diffusion coefficients of macromolecules and then, via the Stokes-Einstein relation, their hydrodynamic diameter can be obtained[S13]. To assess the stability of aggregates generated by Aβ1-40mut, Aβ1-40wt and peptide mixtures, the samples were diluted five folds after 48 h incubation using 50 mM Tris-HCl, pH 7.0, and light intensity scattered by peptide assemblies was recorded for 90 min.

6.1.8 Polarized-light microscopy and electron microscopy

Aβ1-40mut, Aβ1-40wt and equimolar mixtures thereof were dissolved in 10 mM NaOH and then diluted in an equal volume of 100

mM Tris-HCl, pH 7.0, to final concentrations of 0.250 and 0.125 mM. The samples were incubated at 37°C, and the tinctorial and ultrastructural properties of peptide assemblies were determined at various interval of times ranging from 1 h to 20 days[S14]. At each time point (1, 4, 8 h, and 1, 2, 3, 4, 5, 7, 10, 15 and 20 days) 10 µl aliquots of peptide suspensions were air-dried on poli-L-lysine-coated slides (Bio-Optica) stained with the amyloid-binding dye Congo red and viewed under polarized light (Nikon Eclipse E-800 microscope). At the same time points, 5 µl aliquots were applied on Formvar-Carbon 200 mesh nickel grids for 5 min, negatively stained with uranyl acetate, and observed with electron microscope (EM109 Zeiss) operating at 80 KV at a standard magnification, calibrated with an appropriate grid. At day 20, samples were centrifuged at 13,000 x g for 30 min. The pellets were fixed in 2.5% glutaraldehyde in 50 mM phosphate buffer, pH 7.4, post-fixed in 1% acqueous solution of osmium tetroxide, dehydrated in graded acetone and embedded in epoxy resin (Spurr, Electron Microscopy Sciences). Ultrathin sections (500 Å) were collected on 200-mesh copper grids, positively stained with uranyl acetate and lead citrate, and observed with the electron microscope. The experiments were repeated five times. A similar study was carried out with the synthetic peptides Aβ1-42mut, Aβ1-42wt and equimolar mixtures thereof. Peptides solutions were prepared as described above at final concentration of 0.125 mM, and analysed at different time points ranging from 1 h to 10 days. To assess the anti-amyloidogenic effect of the hexapeptide Aβ1-6 carrying the A-to-V substitution in position 2, we prepared solutions of Aβ1-6mut and Aβ1-40wt in 50 mM Tris-HCl, pH 7.0, at final

concentration of 0.125 mM, as well as mixture of Aβ1-6mut and Aβ1-40wt at 1:1 (0.125 mM concentration of each peptide) or 4:1 (0.5 mM Aβ1-6mut, 0.125 mM Aβ1-40wt) molar ratio. The solutions were incubated at 37°C and sample aliquots were analyzed by polarized light and electron microscopy after 4, 8 and 24 h, and 3, 5 and 7 days as described above.

6.1.9 Surface plasmon resonance (SPR)

Binding of Aβ1-40mut, Aβ1-40wt, Aβ1-6mut or Aβ1-6wt to Aβ1-40wt fibrils was assessed by SPR using the Proteon XPR36 equipment (Bio-Rad Laboratories, Inc.). Fibrils were obtained following incubation of 50 μM Aβ1-40wt in 50 mM phosphate buffer, pH 7.4, for three days at 37°C under agitation. The fibrillary structure of Aβ1-40wt assemblies was determined by atomic force microscopy. Fibrils were covalently immobilized on a sensor chip using amine-coupling chemistry (immobilization level ≈ 2000 resonance units)[S15]. Reference cells were prepared in parallel using the same immobilization procedure but without addition of peptide[S16]. Freshly prepared solutions of Aβ1-40wt (1 μM concentration), Aβ1-40mut (1 μM), Aβ1-6wt (500 μM) and Aβ1-6mut (500 μM) in phosphate buffered saline, pH 7.4, were injected onto the immobilized fibrils for 2-10 min at a flow rate of 30 μl/min. These solutions did not contain aggregates as assessed by atomic force and electron microscopy. The sensorgrams -i.e. the time course of the SPR signal, expressed in resonance units (RU)- observed in the cell with covalently bound Aβ1-40wt peptide were corrected by subtracting the response detected in the reference cells [16]. The experiments were replicated three times.

6.1.10 Size Exclusion Chromatography

Aβ1-40mut, Aβ1-40wt and equimolar mixtures thereof were dissolved in 10 mM NaOH and then diluted in an equal volume of 100 mM Tris-HCl, pH 7.0, to final concentration of 0.125 mM. To determine size and concentration of the peptide aggregates prior and following denaturation with urea, three set of samples were analyzed by size exclusion chromatography: (i) freshly-prepared peptide solutions; (ii) samples after 72 h incubation at 37°C; (iii) samples prepared as in (ii) and then incubated for 24 h after addition of urea at final concentration of 1M. Size exclusion chromatography was performed using an FPLC apparatus (Biologic FPLC system, Biorad) equipped with a precision column pre-packed with Superdex 75 with a separation range of 3-70 kDa (GE Healthcare). The mobile phase flow rate was set at 0.5 ml/min and the elution peaks were detected at UV absorbance 214 and 280 nm. The composition of the mobile phase was 1M urea in 50 mM Tris-HCl, pH 7.0. The column was calibrated using insulin chain B (3.5 kDa), D-JNK1 (3.8 kDa), ubiquitin (8.5 kDa), ribonuclease A (13.7 kDa), carbonic anydrase (29.0 kDa), ovalbumin (43.0 kDa) and BSA (67.0 kDa). The void volume was determined by Blue dextrane 2000 (200 kDa).

6.1.11 Neurotoxicity and MTT assay

The SH-SY5Y human neuroblastoma cell line was grown in D-MEM/F12 culture medium supplemented with 2 mM glutamine, 100 U/ml penicillin, 100 μg/ml streptomycin and 10% foetal bovine serum (FBS). Cells were plated at 2×104 cells/well into 48-well plates, and differentiated for seven days by the addition of 10 μM retinoic acid in

cell culture medium containing 0.5% DMSO. Freshly-prepared solutions of Aβ1-42wt, Aβ1-42mut and equimolar mixtures thereof in 50 mM Tris-HCl, pH 7.4, were then added to the culture medium to the final concentration of 5 μM. After peptide treatment for 24 h, cell viability was determined by MTT assay (Sigma) following manufacturer's instructions. Results were expressed as percentage of the values obtained for control cells.

6.1.12 Statistical analysis

Student t-test was used to calculate the statistical difference of experimental versus control values in ELISA tests, immunoblot analysis of APP-transfected cells, and MTT assay. A difference was considered statistically significant if $P < 0.05$. The Prism program (GraphPad Software) was used to analyze the correlation and draw the standard curve in all the ELISA tests.

6.2 Supporting Text

6.2.1 Clinical and genetic study

The study was approved by the ethical committee of Carlo Besta Institute and written informed consent was obtained from the legal representative of the proband and participating relatives.

6.2.2 Case Report

The proband is a 44-year-old man with no family history of neurological disorders. At the age of 36 years, he developed progressive memory deficits, impairment of verbal initiative, difficulties in daily planning, mood depression and irritability with

episodic aggressiveness. Three years later, neuropsychological assessment revealed severe impairment of attention, working memory, episodic memory, and executive functions (initiative, fluency, abstraction, set shifting, and planning). The Mini-Mental State Examination gave an adjusted score of 17/30, and the Wechsler Adult Intelligence Scale provided a total IQ of 47, with all sub-test scores under cut-off values. The clinical picture evolved towards a severe dementia, with loss of self-awareness, awareness of disease and interpersonal cognition, and disturbances of behavioural control including disinhibition, perseverations and echolalia. Myoclonic jerks, spastic tetraparesis and sphincteric incontinence were later additional features. The patient showed complete loss of autonomy in about eight years from clinical onset, and is presently unable to communicate, stand and walk.

Serial EEG recordings showed progressive slowing of background activity and occurrence of pseudoperiodic triphasic complexes. Serial Magnetic Resonance Imaging documented progressive cortico-subcortical atrophy, mainly involving the frontal, temporal, insular and parietal cortex, anterior cinguli and basal ganglia, with enlargement of the lateral ventricles (Fig. S3 A,B,C). The atrophy was more pronounced on the right hemisphere, and was associated with moderate hyperintensity in the subcortical white matter on T2-weighted and Fluid Attenuated Inversion Recovery (FLAIR) images (Fig. S3 D,E).

Genetic analysis

ApoE genotyping showed that the patient and the family members whose DNA was available (Fig. S2) were ε3/ε3 homozygous except for an A673V heterozygous carrier who had the ε2/ε4 genotype.

In addition to APP and ApoE genotyping, the patient was subjected to the analysis of PSEN1, PSEN2, and the genes encoding the microtubule-associated protein tau, progranulin, prion protein and huntingtin. No defects were found in any of these genes.

Neuropsychological evaluation of the patient's relatives

The A673V homozygous sister of the patient (Fig. S2, subject III-18) as well as five heterozygous (II-11, III-1, III-6, III-24, and III-26) and two non-mutated (III-14 and III-22) family members underwent neuropsychological assessment. At the interview, the proband's sister complained of mild attention and memory deficits, such as retaining newspaper articles or short novels. These difficulties became apparent in the last year, as confirmed by her cousins. The neuropsychological tests revealed that she had significant deficits in delayed recall of new verbal stimuli, picture naming and "theory of mind", i.e. the ability to attribute mental states, such as believes, intents and desires, to oneself and others. Moreover, her performances in word fluency and verbal episodic memory were at lower limits of normal values. Overall these features were consistent with the diagnosis of multiple domain MCI[S17]. By contrast, the five A673V heterozygous and the two non-mutated relatives performed well on all tests (Table S1). Of particular significance was the excellent

performance of the 88-year-old aunt of the proband (Fig. S2, II-11), despite she was non-educated. Moreover, the interview of several members of family A enabled us to rule out the presence of progressive cognitive decline in the expected obligatory heterozygous carriers belonging to the I (I-1 or I-2) and II generation (II-1).

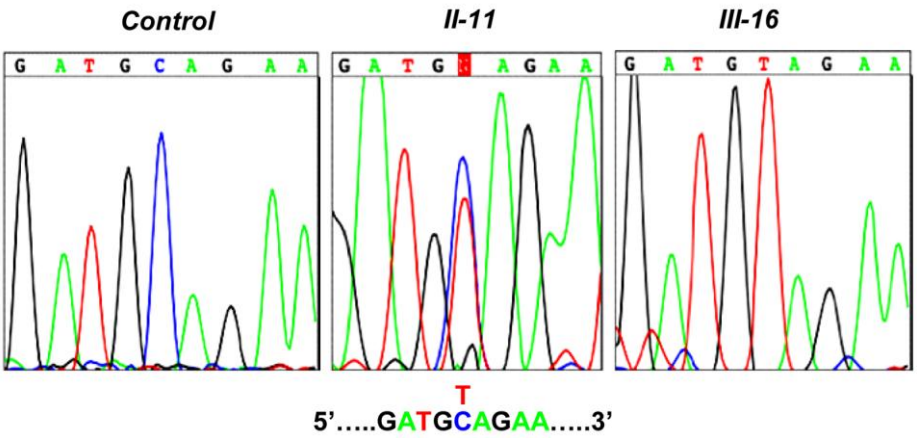

Figure S1. Sequencing of the APP gene. Chromatograms of APP exon 16 showing the C-to-T transition resulting in A673V mutation in heterozygous (II-11) and homozygous (III-16) carriers, and the wild-type sequence in a control subject.

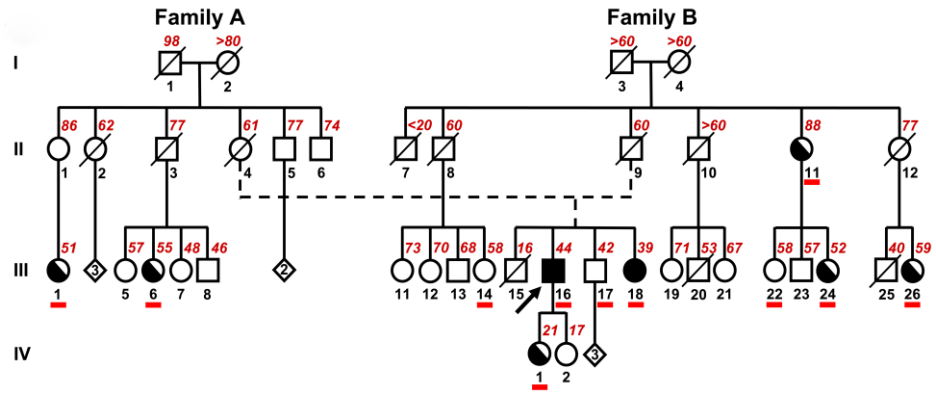

Figure S2. Family trees of patient's (arrow) parental lineages showing the A673V homozygous (filled symbols) and heterozygous (half-filled symbols) carriers. Underscored numbers denote individuals whose DNA was analyzed. Red numbers indicate the age.

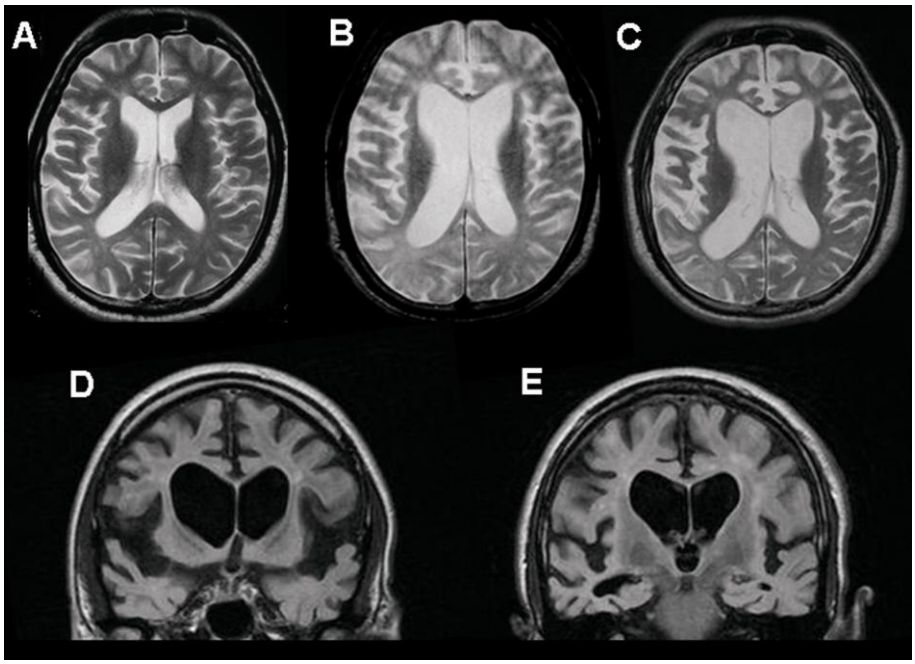

Figure S3. Brain Magnetic Resonance Imaging of the proband. (**A**,**B**,**C**) Axial T2-weighted images in the early clinical stage of disease (**A**), after three years (**B**), and after eight years from onset (**C**). (**D**,**E**) Coronal FLAIR images eight years after the onset of symptoms. The scans show the progression of the cortico-subcortical atrophy and subcortical white matter changes.

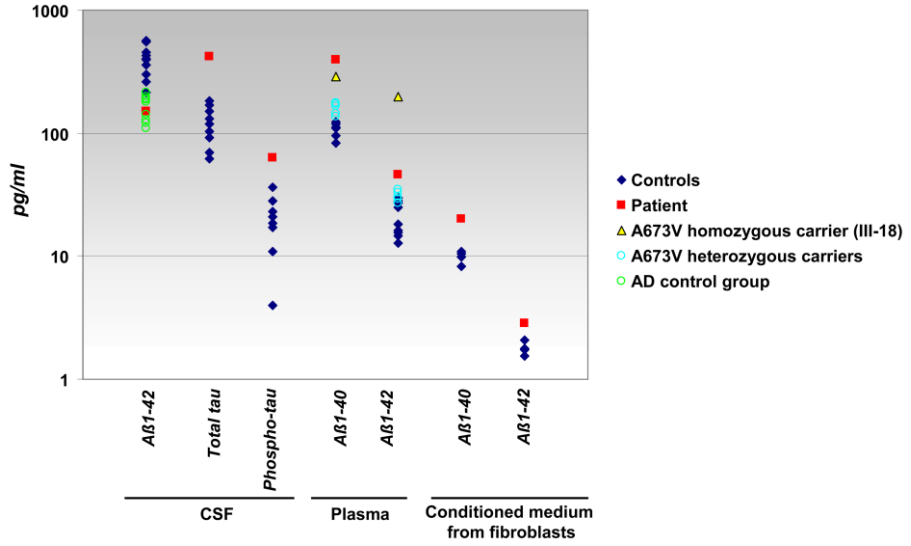

Figure S4. Levels of Aβ, total tau and phospho-tau in CSF, and Aβ measurements in plasma and conditioned medium from cultured fibroblasts. The values of controls (N = 10 for CSF analysis, N = 9 for plasma analysis, and N = 4 for fibroblasts analysis), sporadic AD patients (N = 10) and A673V heterozygous carriers (N = 6) represent each the mean of three determinations. The values of the proband and his homozygous sister are the mean of 6 single determinations. The data are reported on a logarithmic scale.

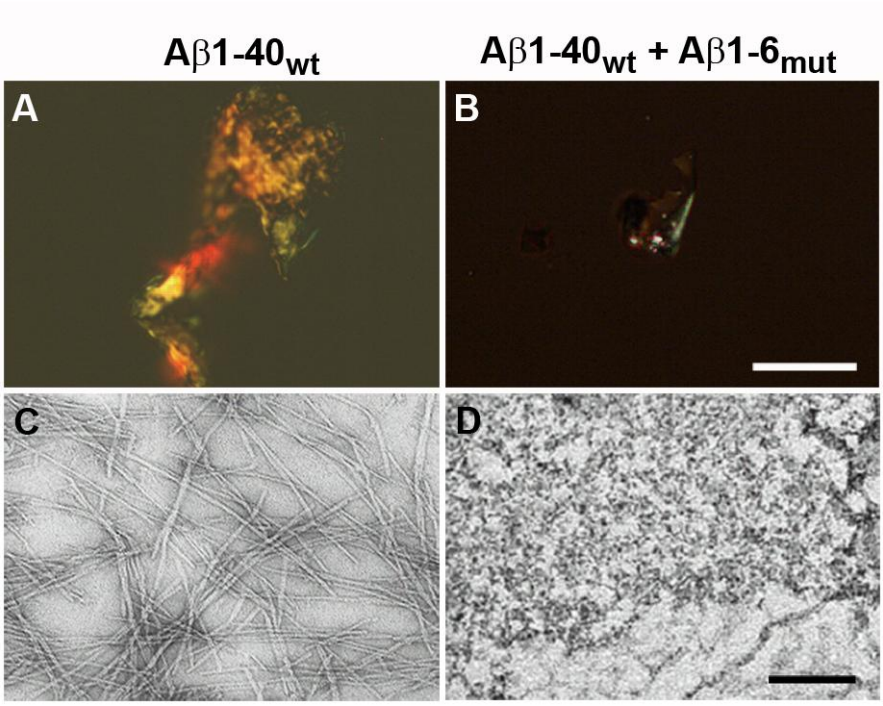

Figure S5. Effects of Aβ1-6_{mut} on the aggregation properties of Aβ1-40_{wt}. (**A**,**B**) Polarized light microscopy after Congo red staining and (**C**,**D**) electron microscopy after negative staining of Aβ1-40_{wt} after 5-day incubation in the absence (**A**,**C**) or the presence (**B**,**D**) of Aβ1-6_{mut} at 1:4 molar ratio. In the absence of Aβ1-6_{mut}, Aβ1-40_{wt} generates large congophilic aggregates (**A**), that are formed by long, straight, unbranched fibrils (**C**). Amyloidogenesis is hindered by the presence of Aβ1-6_{mut} (**B**,**D**).

Supplementary table 1

Test	Subject III-18 *Age:39y* *Schooling: 8y*			Subject III-1 *Age:51y* *Schooling: 13y*			Subject III-6 *Age:55y* *Schooling: 8y*			Subject III-14 *Age:58y* *Schooling: 5y*		
	Raw scores	*C.S.*	*E.S.*	*Raw scores*	*C.S.*	*E.S.*	*Raw scores*	*C.S.*	*E.S.*	*Raw scores*	*C.S.*	*E.S.*
Digit Span[S18]	5	5	*3*	7	6.75	*4*	5	5	*3*	4	4.5	*2*
Attentive Matrices[S18]	59/60	52.75/60	*4*	60/60	60/60	*4*	50/60	48/60	*3*	49/60	50.75/60	*4*
Street Completion Test[S18]	6/14	4/14	*2*	10/14	7.75/14	*4*	6/14	5/14	*2*	8/14	8/14	*4*
Imitating Gestures[S18]	20/20	20/20	*4*	20/20	20/20	*4*	20/20	20/20	*4*	20/20	20/20	*4*
Imitating Orofacial Expressions[S18]	20/20	20/20	*4*	20/20	20/20	*4*	20/20	20/20	*4*	20/20	20/20	*4*
Trail Making Test Part A[S19]	33”	29”	*4*	29”	26”	*4*	84”	71”	*2*	52”	31”	*4*
Trail Making Test Part B[S19]	64”	47”	*4*	111”	95”	*4*	204”	156”	*2*	126”	50”	*4*
Tower Of London[S20]	26/36		*Cut-off 24*	30/36		*Cut-off 24*	24/36		*Cut-off 24*	26/36		*Cut-off 24*
Weigl Sorting Test[S18]	9/15	7.75/15	*2*	15/15	15/15	*4*	12/15	11.25/15	*4*	10/15	10.25/15	*4*
Rey Figure Copying[S20]	36/36	36/36	*4*	35/36	34.25/36	*4*	32/36	32.5/36	*4*	35/36	36/36	*4*

Raven's Progressive Colored Matrices[S21]	29/36	28.5/36	*3*	33/36	32/36	*4*	29/36	30/36	*3*	29/36	33.5/36	*4*
Word Fluency On Phonemic Cue[S22]	**19**	**20**	***1***	32	29	*3*	27	30	*3*	30	37	*4*
Word Fluency On Semantic Cue[S22]	33	32	*2*	42	40	*4*	29	31	*2*	40	46	*4*
Token Test[S18]	33/36	31.75/36	*3*	35/36	33/36	*4*	32/36	31.25/36	*2*	32/36	32.25/36	*3*
Corsi Bloks Span[S18]	5	5	*4*	5	4.75	*4*	4	4.25	*2*	5	5.5	*4*
Short Story[S22]	**10/28**	**8.5/28**	***1***	15.5/28	13/28	*3*	11/28	10.5/28	*2*	11.5/28	13.5/28	*4*
Rey Figure Delayed Reproduction[S19]	13.5/36	12.75/36	*2*	18/36	18.25	*4*	10/36	12.5/36	*2*	17.5/36	21.75/36	*4*
Faux Pas Test[S23]	**8/20**		***Cut-off 18***		-			-		20/20		*Cut-off 18*
Cognitive Estimation Test[S24]	14/42		*Cut-off 18*		-			-		10/42		*Cut-off 18*
Boston Naming Test (S25)	**43/60**		***Cut-off 56***		-			-		57/60		*Cut-off 56*
Verbal Selective Reminding[S18]	**17/160**	**0/160**	***0***		-			-		112/160	112/160	*4*
Corsi supraspan[S18]	22.14/29	15.39/29	*3*		-			-		15.5/29	15.5/29	*4*

Test	**Subject III-22**			**Subject III-24**			**Subject III-26**			**Subject II-11**		
	Age:58y			*Age:52y*			*Age:59y*			*Age:88y*		
	Schooling: 8y			*Schooling: 8y*			*Schooling: 5y*			*Schooling: 3y*		
	Raw scores	*C.S.*	*E.S.*	*Raw scores*	*C.S.*	*E.S.*	*Raw scores*	*C.S.*	*E.S.*	*Raw scores*	*C.S.*	*E.S.*
Digit Span[S18]	5	5	*3*	6	6	*4*	5	5.5	*4*	4	4.75	*3*
Attentive Matrices[S18]	52/60	51.25/60	*4*	58/60	54.5/60	*4*	55/60	56.75/60	*4*	27/60	37.75/60	*2*
Street Completion Test[S18]	7/14	6.5/14	*3*	9/14	7.75/14	*4*	8/14	8/14	*4*	7/14	9.5/14	*4*
Imitating Gestures[S18]	20/20	20/20	*4*	20/20	20/20	*4*	20/20	20/20	*4*	20/20	20/20	*4*
Imitating Orofacial Expressions[S18]	20/20	20/20	*4*	20/20	20/20	*4*	20/20	20/20	*4*	18/20	19/20	*3*
Trail Making Test Part A[S19]	37”	20”	*4*	20”	10”	*4*	40”	19”	*4*	102”	68”	*2*
Trail Making Test Part B[S19]	130”	72”	*4*	53”	16”	*4*	112”	36”	*4*		-	
Tower Of London[S20]	30/36		*Cut-off 24*	32/36		*Cut-off 24*	28/36		*Cut-off 24*		-	
Weigl Sorting Test[S18]	12/15	11.5/15	*4*	12/15	11/15	*4*	8/15	8.5/15	*2*	7/15	10/15	*3*
Rey Figure Copying[S19]	33.5/36	34.5/36	*4*	35/36	35.25/36	*4*	33/36	34.5/36	*4*	26/36	30.25/36	*2*

Raven's Progressive Colored Matrices[S21]	28/36	31/36	*4*	34/36	35.5/36	*4*	28/36	32.5/36	*4*	25/36	33.5/36	*4*
Word Fluency On Phonemic Cue[S22]	28	31	*3*	43	46	*4*	28	35	*4*	10	23	*2*
Word Fluency On Semantic Cue[S22]	38	40	*4*	40	42	*4*	40	46	*4*	30	44	*4*
Token Test[S18]	33/36	32.5/36	*3*	36/36	36/36	*4*	35/36	35.25/36	*4*	39/36	31.75/36	*3*
Corsi Bloks Span[S18]	5	5.5	*4*	5	5.25	*4*	5	5.5	*4*	5	6	*4*
Short Story[S21]	14.5/28	14/28	*3*	15.5/28	15/28	*4*	13.5/28	15.5/28	*4*	9.5/28	17/28	*4*
Rey Figure Delayed Reproduction[S19]	15/36	18.5/36	*4*	14/36	15.5/36	*4*	16.5/36	20.75/36	*4*	10/36	21/36	*4*
Faux Pas Test[S23]	20/20		*Cut-off 18*	20/20		*Cut-off 18*	20/20		*Cut-off 18*		-	
Cognitive Estimation Test[S24]	15/42		*Cut-off 18*	8/42		*Cut-off 18*	16/42		*Cut-off 18*		-	
Boston Naming Test (*S25*)	59/60		*Cut-off 56*	60/60		*Cut-off 56*	57/60		*Cut-off 56*		-	
Verbal Selective Reminding[S18]	132/160	123/160	*4*	150/160	127/160	*4*	156/160	156/160	*4*		-	
Corsi supraspan[S18]	27.6/29	26.94/29	*4*	21.69/29	17.94/29	*3*	24.61/29	24.61/29	*4*		-	

Supplementary Table 1. Neuropsychological assessment of patient's relatives. Data are reported as raw scores, corrected scores (C.S.) and equivalent scores (E.S.: 0= Impaired performance, 1= Lower-limit performance, 2-3-4= Normal performance). For tests where equivalent scores are not available (Tower of London, Faux Pas Test, Cognitive Estimation Test and Boston Naming Test) the cut-off values are reported. Higher raw and corrected scores indicate better performances, except for the Trial Making Test and the Cognitive Estimation Task, which are inversely associated with the level of performance. Since subject II-11 is non educated, her row scores have been corrected for the lowest educational level (3 years). Impaired scores are highlighted in red while lower-limit scores are highlighted in blue.

	CSF *(pg/ml)*	Plasma *(pg/ml)*	Conditioned medium from fibroblasts *(pg/ml)*	Conditioned medium from APP-transfected CHO cells *(pg/ml)*	Conditioned medium from APP-transfected COS7 cells *(pg/ml)*
Control*					
Aβ1-40	392 ± 115.5	109.5 ± 12.7	9.8 ± 1.0	49.8 ±11.8	572.3 ± 11.8
Aβ1-42		20.8 ± 6.7	1.7 ± 0.2	4.6 ± 1.4	54.2 ± 17.3
Aβ1-42/Aβ1-40 ratio			0.1	0.1	0.1
Aβ11-40			*nd*	13.3 ± 3.4	152.5 ± 1.6
Aβ11-42			*nd*	33.7 ± 2.5	130.9 ± 0.8
AβN3pE-42			*nd*	4.3 ± 1.1	4.2 ± 0.3
Patient					
Aβ1-40	151	426.5	20.2‡	85.3 ± 8.6 *(p=0.004)*	863.4 ± 32.6 *(p=0.002)*
Aβ1-42		45.9	2.9‡	9.9 ± 1.3 *(p=0.033)*	78.1 ± 22.9 *(p=0.006)*
Aβ1-42/Aβ1-40 ratio			0.1	0.1	0.1
Aβ11-40			*nd*	27.3 ± 2.4 *(p=0.002)*	233.8 ± 16.6 *(p=0.011)*
Aβ11-42			*nd*	45.7 ± 8.4 *(p=0.017)*	198.5 ± 6.6 *(p=0.004)*
AβN3pE-42				8.4 ± 2.2 *(p=0.028)*	9.8 ± 2.6 *(p=0.066)*
A673V homozygous patient's sister	*Nd*	287.8	*nd*	*nd*	*nd*
Aβ1-40		200.1			
Aβ1-42					
A673V heterozygous carriers†	*Nd*	155.9 ± 16.9	*nd*	*nd*	*nd*
Aβ1-40		30.8 ± 2.8			
Aβ1-42					

Supplementary Table 2. Determination of A*β* peptides in CSF, plasma and media from cultured fibroblasts and APP-transfected cells. *Controls are: 1) non demented subjects for CSF analysis (N = 10); 2) healthy subjects for plasma analysis (N = 9); 3) age-matched non-demented subjects for cultured fibroblasts (N = 4); 4) cells transfected with wild-type APP for A673V transfected CHO and COS7 (N = 7 for both CHO and COS7). Aβ values were normalized to the number of cells for Aβ determination in fibroblasts, and to the APP signal intensity for Aβ analysis in transfected CHO and COS7 cells. Statistical analysis was carried out according to Student's t test. The significance of differences between A673V and control values is reported in bracket.

†A673V heterozygous carriers: N = 6.

‡Mean of four determinations.

6.3 Supporting references

S1. Mullan M, Crawford F, Axelman K, et al. A pathogenic mutation for probable Alzheimer's disease in the APP gene at the N-terminus of beta-amyloid. Nat Genet 1992;1:345-7.

S2. Wenham PR, Price WH, Blandell G. Apolipoprotein E genotyping by one-stage PCR. Lancet 1991;337:1158-9.

S3. Cruts M, van Duijn CM, Backhovens H, et al. Estimation of the genetic contribution of presenilin-1 and -2 mutations in a population-based study of presenile Alzheimer disease. Hum Mol Genet 1998;7:43-51.

S4. Poorkaj P, Bird TD, Wijsman E, et al. Tau is a candidate gene for chromosome 17 frontotemporal dementia. Ann Neurol 1998;43:815-25.

S5. Rossi G, Giaccone G, Giampaolo L, et al. Creutzfeldt-Jakob disease with a novel four extra-repeat insertional mutation in the PrP gene. Neurology 2000;55:405-10.

S6. Novelletto A, Persichetti F, Sabbadini G, et al. Analysis of the trinucleotide repeat expansion in Italian families affected with Huntington disease. Hum Mol Genet 1994;3:93-8.

S7. Cruts M, Gijselinck I, van der Zee J, et al. Null mutations in progranulin cause ubiquitin-positive frontotemporal dementia linked to chromosome 17q21. Nature 2006;442:920-4.

S8. Hoffmann J, Twiesselmann C, Kummer MP, Romagnoli P, Herzog V. A possible role for the Alzheimer amyloid precursor protein in the regulation of epidermal basal cell proliferation. Eur J Cell Biol 2000;79:905-14.

S9. Games D, Adams D, Alessandrini R, et al. Alzheimer-type neuropathology in transgenic mice overexpressing V717F beta-amyloid precursor protein. Nature 1995;373:523-7.

S10. Iqbal K, Flory M, Khatoon S, et al. Subgroups of Alzheimer's disease based on cerebrospinal fluid molecular markers. Ann Neurol 2005;58:748-57.

S11. Salmona M, Morbin M, Massignan T, et al. Structural properties of Gerstmann-Straussler-Scheinker disease amyloid protein. J Biol Chem 2003;278:48146-53.

S12. Lago P, Rovati L, Cantù L, Corti M. A quasielastic light scattering detector for chromatographic analysis. Rev. Sci. Instr. 1993; 64:1797-802.

S13. Corti M. Physics of amphiphiles: micelles, vesicles and microemulsions. V. Degiorgio and M. Corti, Ed. (North-Holland, Amsterdam, 1985), pp122-51.

S14. Bonetto V, Massignan T, Chiesa R, et al. Synthetic miniprion PrP106. J Biol Chem 2002;277:31327-34.

S15. Jonsson U, Fagerstam L, Ivarsson B, et al. Real-time biospecific interaction analysis using surface plasmon resonance and a sensor chip technology. BioTechniques 1991;11:620-7.

S16. Gobbi M, Colombo L, Morbin M, et al. Gerstmann-Straussler-Scheinker disease amyloid protein polymerizes according to the "dock-and-lock" model. J Biol Chem 2006;281:843-9.

S17. Petersen RC, Doody R, Kurz A, et al. Current concepts in mild cognitive impairment. Arch Neurol 2001;58:1985-92.

S18. Italian standardization and classification of Neuropsychological tests. The Italian Group on the Neuropsychological Study of Aging. Ital J Neurol Sci 1987;Suppl 8:1-120.

S19. Lezak M. Ed. Neuropsychological assessment (Oxford Univ. Press, New York, 1995).

S20. Shallice T. Specific impairments of planning. Philos Trans R Soc Lond B Biol Sci 1982;298:199-209.

S21. Basso A, Capitani E, Laiacona M. Raven's coloured progressive matrices: normative values on 305 adult normal controls. Funct Neurol 1987;2:189-94.

S22. Novelli G, Papagno C, Capitani E, et al. Tre test clinici di memoria verbale a lungo termine. Taratura su soggetti normali. Arch Psicol Neurol Psichiatr. 1986;47:278–296.

S23. Stone VE, Baron-Cohen S, Knight RT. Frontal lobe contributions to theory of mind. J Cogn Neurosci 1998;10:640-56.

S24. Della Sala S, MacPherson SE, Phillips LH, Sacco L, Spinnler H. How many camels are there in Italy? Cognitive estimates standardised on the Italian population. Neurol Sci 2003;24:10-5.

S25. E. Kaplan et al. Ed. Boston naming test (Lea & Febiger, Philadelphia, PA, 1983).

S26. We are grateful to V. Bellotti for helpful discussion, C. Pasquali for help in sample collection and molecular genetic studies, M. Stravalaci for plasmon surface resonace study, A.Cagnotto for peptide synthesis, and Flamma SpA Bergamo, Italy, for the kind gift of FMOC amino acids.

Chapter 2

Neuropathology of the recessive A673V APP mutation: Alzheimer disease with distinctive features

Giorgio Giaccone, Michela Morbin, Fabio Moda, Mario Botta, Giulia Mazzoleni, Andrea Uggetti, **Marcella Catania**, Maria Luisa Moro, Veronica Redaelli, Alberto Spagnoli, Roberta Simona Rossi, Mario Salmona, Giuseppe Di Fede, Fabrizio Tagliavini

Acta Neuropathol. 2010 Dec;120(6):803-12. Epub 2010 Sep 15.

1. Abstract

Mutations of three different genes, β-amyloid precursor protein (APP), presenilin 1 and presenilin 2 are associated with Alzheimer's disease (AD). Recently, the APP mutation A673V has been identified that stands out from all the genetic defects previously reported in these three genes, since it causes the disease only in the homozygous state[7].

We here provide the account on the neuropathological picture of the proband of this family, who was homozygous for the APP A673V mutation and recently came to death. The brain has been studied by histological and immunohistochemical techniques, at the optical and ultrastructural levels.

Cerebral Aβ accumulation and tau pathology were severe and extensive. Peculiar features were the configuration of the Aβ deposits that were of large size, mostly perivascular and exhibited a close correspondence between the pattern elicited by amyloid stainings and the labelling obtained with immunoreagents specific for Aβ40 or Aβ42. Moreover, Aβ deposition spared the neostriatum while deeply affected the cerebellum, and therefore was not in compliance with the hierarchical topographical sequence of involvement documented in sporadic AD.

Therefore, the neuropathological picture of familial AD caused by the APP recessive mutation A673V presents distinctive characteristics compared to sporadic AD or familial AD inherited as a dominant trait. Main peculiar features are the morphology, structural properties and composition of the Aβ deposits as well as their topographic distribution in the brain.

2. Introduction

Alzheimer's disease (AD), whose pathogenesis involves a combination of genetic and environmental factors, is the most prevalent cause of dementia. AD is characterized neuropathologically by Aβ-amyloid deposition and intraneuronal accumulation of abnormal tau protein with neurofibrillary tangle formation[8]. AD is usually sporadic, but a small percentage of cases is familial. Familial AD (FAD) has usually an earlier age of onset than the sporadic form and is largely due to fully penetrant, autosomal dominant mutations in three genes, coding for amyloid-β-precursor protein (APP) and for two highly homologous genes, presenilin 1 and presenilin 2 (PSEN1 and PSEN2). To date, close to 30 APP mutations, almost 200 PSEN1 mutations, and more than 10 PSEN2 mutations have been found [for an overview, see http://www.molgen.ua.ac.be/ ADMutations/].

Neuropathologically, the hallmark lesions of FAD are the same found in the sporadic form, often appearing with significantly enhanced severity[27]. This fact has an high theoretical relevance since one of the major support to the amyloid cascade hypothesis of AD is that APP mutations induce full expression of the disease with Aβ deposition and tau pathology[12]. However, a subset of APP mutations (E693Q, E693K and L705V) is associated with hereditary cerebral hemorrhage with amyloidosis (HCHWA), a condition in which cerebral amyloid angiopathy (CAA) largely prevails over parenchymal Aβ deposits and neurofibrillary pathology is absent[4,21,31]. It is also noteworthy that in FAD associated with several other mutations in the APP such as A692G, E693G, D694N, A713T, and

APP duplication, CAA is unusually severe and widely distributed throughout the brain [1,5,11,23,24].

Recently, a new APP mutation (A673V) has been identified by our group that differs from all the other genetic defects inducing AD, since it causes the disease only in the homozygous state. This mutation is located in the N-terminal part of the Aβ sequence (position 2)[7].

We here provide the detailed account on the neuropathological picture of the proband of this family, who recently died. This report is therefore the first to describe the neuropathology of a patient with FAD induced by a recessive mutation.

The neuropathological picture presented several distinctive characteristics compared to sporadic or familial AD inherited as a dominant trait. Beside the marked severity of the lesions, peculiar features were the configuration of the Aβ deposits that were often of large size and perivascular and exhibited a complete correspondence between the pattern elicited by amyloid stainings and the labeling obtained with immunoreagents specific for Aβ40 or Aβ42. Moreover, the topographic distribution of Aβ deposition was not in compliance with the hierarchical regional sequence of involvement documented in sporadic AD, since it spared the neostriatum while deeply affecting the cerebellum and the brainstem.

3. Material and Methods

3.1 Clinical history and genetic analysis

At age 36 the patient developed cognitive and behavioral disturbances. Five years after the onset he was incontinent and unable

to communicate. The disease then progressed to a condition characterized by severe dementia with spastic paraparesis and the patient died at age 46.

Genetic analysis showed on both APP alleles the presence of a C-to-T transition that results in an alanine-to-valine substitution at position 673 (APP770 numbering) corresponding to position 2 of Aβ. ApoE genotype was ε3/ε3. Analysis of the genes encoding for PSEN1, PSEN2, tau protein (MAPT) and progranulin (PGRN), did not reveal mutations.

3.2 Neuropathological protocol

The brain of the patient was obtained at autopsy that was performed 20 hours after death. The right cerebral hemisphere, the cerebellum and the brainstem were fixed in 10% formalin, while the left cerebral hemisphere was dissected and partly fixed in Alcolin (a non-linking alcohol-based fixative, Diapath) and partly frozen at -80°C.

Several coronal slices of the left cerebral hemisphere were dehydrated in graded ethanol, cleared in xylene, embedded in paraffin, cut in 12-µm-thick sections using a Reichert-Jung polycut E microtome (Leica Microsystem, Germany).

For comparison, we examined the brains of 18 patients with sporadic AD at stage VI of Braak of neurofibrillary pathology[6] as well as patients with familial AD associated with the following mutations: A713T of APP[23], S169L[29] and M146L[3] of PSEN1, M239V[19] and A85V[22] of PSEN2, as well as a patient with HCHWA linked to the A693K mutation of APP[4].

Routine examination was carried out on sections stained with hematoxylin-eosin (H&E), cresyl violet for Nissl substance, Heidenhein-Woelcke for myelin, thioflavine S for amyloid and Bodian silver impregnation.

3.3 Immunohistochemistry

Immunohistochemistry was carried out with antibodies recognizing Aβ and tau protein as well as markers of accompanying secondary lesions of AD.

For Aβ, the antibodies used were either specific for Aß40 (polyclonal, Biosource, 1:2000; monoclonal, Signet, 1:500) and for Aß42 (polyclonal, Biosource, 1:1000; monoclonal, Signet, 1:500) or monoclonal antibodies against total Aβ (6E10, Signet, epitope at residues 4-9, 1:1000; 4G8, Signet, epitope at residues 17-24, 1:4000). Before Aß immunostaining, the sections were pretreated with formic acid (98%, 30 min).

For tau-immunohistochemistry, a polyclonal anti-tau antibody (1:500, DakoCytomation), several antibodies to phosphorylation-dependent epitopes including AT8 (monoclonal, 1:300, epitope at residues 199-205, Innogenetics), AD2 (monoclonal, 1:1000, epitope at residues 396-404, Biorad), Alz50 (monoclonal, 1:200, epitope at residue 231, gift of dr. P Davies, New York) were used, as well as two monoclonal antibodies that distinguish with complete specificity the tau isoforms with three (RD3, 1:1000, clone 8E6/C11, Chemicon) or with four (RD4, 1:300, clone 1E1/A6, Chemicon) microtubule-binding repeat domains.

Additional sections were immunostained with antibodies to APP: SP18 (polyclonal, raised against a synthetic peptide homologous to residues 45-62 of APP770, 1:100, gift of dr. Frangione, New York University, New York) and SP20 (monoclonal, raised against a synthetic peptide homologous to the 20 C-terminal residues of APP, 1:100, gift of dr. Frangione), α-synuclein (monoclonal, 4D6, 1:5000, Signet), ubiquitin (polyclonal, 1:500, DakoCytomation) and the related protein p62 (monoclonal, 1:1000, Signet), glial fibrillary acidic protein (polyclonal, 1:800, DakoCytomation), CR3-43, as marker of activated microglia (monoclonal, 1:200, DakoCytomation), actin (monoclonal, 1:200, Neomarkers) and collagen IV (monoclonal, 1:50, DakoCytomation). The immunoreactions were visualized by the EnVision Plus/Horseradish Peroxidase system for rabbit or mouse immunoglobulins (DakoCytomation) using 3-3'-diaminobenzidine as chromogen.

Furthermore, a morphometric analysis to evaluate the Aβ burden was carried out by using a method reported previously[6].

3.4 Electron and immunoelectron-microscopy

Electron microscopy (EM) was carried out on specimens of the frontal cortex dissected at autopsy, that were fixed in 2.5% EM grade glutaraldehyde (Fluka Chemie, AG Buchs, CH) in 0.05 M PBS at pH 7.4, cut in small blocks, post-fixed in 1% acqueous osmium tetroxide (Electron Microscopy Sciences, Fort Washington, PA) in 0.05 M PBS, dehydrated in graded acetone, and embedded in epoxy resin (Spurr, EMS).

0.5 μm-thick sections were stained with Toluidin Blue. Selected areas were chosen for EM. 500Å-thick sections were stained with 2% lead citrate and sovrasaturated uranyl acetate.

Post-embedding immunolabeling was performed as previously reported on non-osmicated sections, using antibodies against Aβ (1:100, 4G8), Aβ40 (1:100, Biosource), Aβ42 (1:100, Biosource) and a polyclonal antibody to Tau protein (1:100, DakoCytomation). Briefly, 80 nm sections placed on 200 mesh formvar-carbon coated nickel grids (EMS), were etched in 1% sodium periodate for 60 min and pretreated with 3% formic acid for 10 minutes. Residual aldehyde groups were quenched with 0.05 M glycine (Sigma, St Louis, MO) in PBS pH 4 for 5 minutes. Primary polyclonal and monoclonal antibodies, were diluted in Aurion-BSA incubation buffer (Aurion, Wageningen, The Netherlands), and were applied on grid overnight at 4°C. After rinsing in Aurion-BSA, grids were incubated for 3 hours at room temperature with goat anti-rabbit (GAR) or goat anti-mouse (GAM) secondary antibodies conjugated to 10 nm gold particles (GAR-10 Aurion, 1:30). Sections were fixed in 1% glutaraldehyde, postfixed in vapours of 1% OsO4, counterstained with uranyl acetate and lead citrate, and viewed under an Electron Microscope (Zeiss, Oberhocken,EM109).

4. Results

4.1 General neuropathologic features

Gross examination of the brain showed diffuse atrophy of the cerebral hemispheres, more marked in the frontal and temporal lobes. The lateral and third ventricles were enlarged and the substantia nigra

slightly depigmented. The total brain weight was 1100 g. The vessels of the circle of Willis showed mild focal atheroma.

At the histological examination, neuronal loss, astrogliosis, and microglial activation were very severe throughout the cerebral cortex, with thinning of the cortical ribbon and loss of distinction of the cortical layers. Focal areas of vacuolization of the neuropil were also present.

In the cerebral cortex, amyloid deposits were very abundant and easily recognized even at H&E staining both in the parenchyma and in the vessel walls (Figure 1 a,b,d). In the neuropil, amyloid deposits were unusually large, up to 150 μm in diameter (Figure 1 i,j). Many small parenchymal and leptomeningeal vessels showed thickening of the walls due to accumulation of material fluorescent after thioflavine-S (Figure 1 b,c). The phenomenon of apparent amyloid spreading through the vessel wall into the surrounding neuropil -"drusige Entartung" of Scholz[25] - was remarkable (Figure 1 m,n).

In the cerebellum, amyloid deposition was also profuse (Figure 1 d,e). Focal amyloid plaques were smaller than in the cerebral cortex. CAA and "drusige Entartung" were striking.

Parenchymal and vascular amyloid deposits were intensely immunoreactive for antibodies recognizing epitopes spanning the Aβ sequence (4G8, 6E10), as well as using immunoreagents specific for Aβ40 and Aβ42 species (see below).

Bodian silver impregnation, thioflavine S and tau immunohistochemistry revealed the presence of abundant neurofibrillary changes in the neocortex, including the primary visual cortex, and in the mesial temporal structures (Figure 2). These lesions

took the form of neurofibrillary tangles in the perikarya, neuropil threads dispersed in the cortex, and degenerating neurites surrounding Aβ amyloid deposits (Figure 1 q,r,s). Lewy bodies and α-synuclein inclusions were not present (not shown). Extracellular ("ghost") NFT were numerous both in the mesial temporal structures and in the neocortex (Figure 1r).

4.2 Topographic distribution of Aβ deposits and neurofibrillary changes

Aβ deposits and CAA were abundant in all areas of the cerebral cortex, including the mesial temporal structures, in the thalamus, the cerebellum, and in the brainstem, while they were very few in the caudate nucleus and the putamen (Figure 2 a-c, g). In the cortex Aβ deposition involved uniformly the different layers and the different lobes, with an higher density in the immediate subpial region. No difference in the amount of Aβ deposition was apparent between primary motor or sensory cortex and associative cortical areas (Figure 2). Quantification of Aβ in the superior frontal gyrus indicated that the cortical area fraction occupied by Aβ was 14.9%.

In the cerebellum, build up of amyloid was severe in the molecular layer, where Aβ-deposits were mostly in the vessel walls spreading in the perivascular neuropil, and in the granular layer, where Aβ formed focal deposits, round, stellate or irregularly shaped. Ribbon-like diffuse deposits perpendicular to the pial surface (frequently found in FAD with PS1 mutations) were not a feature of our patient.

In the caudate nucleus, putamen and globus pallidum Aβ deposits were restricted to the ventral anterior portion of the neostriatum, corresponding to the nucleus accumbens. Aβ deposition was present in the thalamus, hypothalamus, septal nuclei, in the mesencepahlon (superior colliculum and central grey with sparing of the substantia nigra), in the pons (locus coeruleus, cranial nerve nuclei and raphe nuclei with sparing of the reticular formation) and in the medulla. In the thalamus most Aβ was in the neuropil, as CAA was very scanty in this brain structure (Figure 1h).

A remarkable finding was the presence of Aβ-immunoreactive deposits in the white matter of the centrum ovale either as small focal deposits or very large (up to about 1 mm), "lake-like" deposits surrounding penetrant arteries in the subcortical white matter (U-fibers) (Figure 1f).

The extent and severity of neurofibrillary pathology were consistent with the diagnosis of definite AD by the CERAD criteria[20] and with stage VI of Braak and Braak[2] (Figure 2 d-f).

Tau-related neurofibrillary changes were present but mild in the caudate nucleus and putamen (also in areas that were free of Aβ) under the form of thin neuropil threads, grains and rare NFT. In the thalamus they were more severe with a consistent amount of neuropil threads and NFT in the latero-dorsal, the dorso medial and the reticular nuclei. In the cerebellum, very few profiles immunoreactive for AT8 were present in the molecular layer. The brainstem contained neurofibrillary pathology with a distribution largely overlapping that of Aβ deposition. Also in the white matter of the centrum ovale some

tau immunoreactivity was detected, with threads, grains, rare coiled bodies and some immunolabelled ectopic neurons.

4.3 Structure and antigenic properties of SP and CAA

The morphology and antigenic characteristics of Aβ deposition was different from those of any other FAD or sporadic AD previously reported.

In the cerebral cortex, most senile plaques (SP) showed a compact core with long, wavy amyloid bundles appearing as fringes that irradiate from it ("fringed plaques") (Figure 1 i,j). Similar fringes of Aβ amyloid extended from amyloid-laden walls of parenchymal arterioles and small arteries (Figure 1 m,n). The plaques in which a central core was not apparent were composed of thin bundles of Aβ rather than coarse or granular material. Aβ deposits were numerous immediately under the pial surface, against which they appeared to be flattened, forming often a continuous row (Figure 1l).

Aβ deposition associated with the blood vessels was very severe. The bulk of vessel-associated changes was made up by "drusige Entartung" that was pronounced both in larger penetrating arteries and in smaller arterioles of the cerebral cortex (Figure 1 c,f,,m,n). In many instances vessels with moderate CAA were bordered by bundles of amyloid irradiating from them or even surrounded by cores of amyloid adhering to the vessel wall (Figure 1k). When cut tangentially in sections stained for Aβ, amyloid-laden vessels could be followed in the sections, looking like centipedes if one wants to use imagination (Figure1o). In the cerebellum, Aβ deposition was massive (Figure 1 g,p).

The comparison of adjacent sections stained with thioflavine S and with different anti-Aβ antibodies demonstrated a very high degree of overlap between amyloid, Aβ40 and Aβ42 deposition (Figure 3). Moreover, immunoreagents that recognize total Aβ as monoclonal antibody 4G8 did not elicit significant labeling outside the structures showing the tinctorial and optical properties of amyloid. In other words, at difference from the scenario of other FAD and sporadic AD, preamyloid deposits or diffuse plaques were very scanty if any, as virtually all Aβ deposits in the neuropil and in the vessel walls displayed the tinctorial and optical properties of amyloid and were decorated by Aβ40 and Aβ42 (Figure 3).

However, slight differences could be detected: immunostaining in the cores was more intense with anti-Aβ42 compared to 4G8 and anti-Aβ 40 that marked intensely the periphery of plaques. There was occasional, tiny Aβ deposits which were not thioflavin S positive, suggesting the presence of rare, small diffuse plaques.

4.4 Associated lesions and secondary changes

Synaptophysin and MAP2 immunostaining documented marked synaptic loss and reduction of the dendritic tree of residual neurons (not shown).

Immunostaining of large hemispheric sections and of the cerebellum for GFAP showed that gliosis was diffuse and involved the gray and white matter. Reactive astrocytes clustered around SP and amyloid laden vessels in the cerebral cortex (Figure 1t) and in the cerebellum. Also the caudate nucleus and putamen were sites of intense gliosis, even if these structures were devoid of Aβ deposition.

Microglia activation was striking with high number of activated microglia cells grouped around amyloid deposits (not shown).

An intracortical laminar distribution of these changes was not evident, even if the severity of the degeneration through the neocortex, precluded the precise distinction of individual cortical layers.

APP immunoreactivity was associated with SP and the pattern was similar to that observed in sporadic AD with labelled round or rod-shaped cellular processes around amyloid deposits (not shown).

Cerebral infarct or hemorrhagic lesions were not present.

4.5 Electron and immunoelectron-microscopy

Ultrastructural examination of cerebral cortex disclosed the presence of amyloid deposits both in the neuropil and in the vessels walls. Neurons were scanty and often had shrunk cytoplasm. Reactive astrocytes were particularly abundant around plaques and amyloid laden vessels, where also activated microglial cells clustered.

Amyloid deposition was made up of typical long straight 8-10 nm unbranched fibrils.

Neuropil amyloid deposits were often unusually large, and were recognizable either in the shape of plaques or of loose or compact bundles of fibrils, intermingled with astroglial cells altering the normal organization of neuropil (Figure 4a,b). No Aβ-positive amorphous or non-fibrillar material was detected.

Vascular amyloid deposition was similar to those previously reported in cerebral amyloid angiopathy. In particular amyloid fibrils disrupting the normal vessels organization were recognizable along the entire thickness of parenchymal and small arteriolar walls.

Amyloid deposition consisted of densely packed fibrils just below the endothelial cells, whereas amyloid fibrils were dispersed in loose meshwork mixed with cellular debris towards the astroglial cells layer. Fringes of Aβ amyloid extended from amyloid-laden walls of parenchymal arterioles and small arteries.

Immunoelectron microscopy disclosed that both parenchymal and vessel-associated amyloid deposits were intensely decorated by immunoreagents specific for Aβ40 and Aβ42 (Figure 4 c-f).

Conversely tau immunohistochemistry was similar to FAD and sporadic AD, with abundant neurofibrillary changes, taking the form of neurofibrillary tangles in the perikarya, neuropil threads dispersed in the cortex, and degenerating neurites surrounding Aβ amyloid deposits.

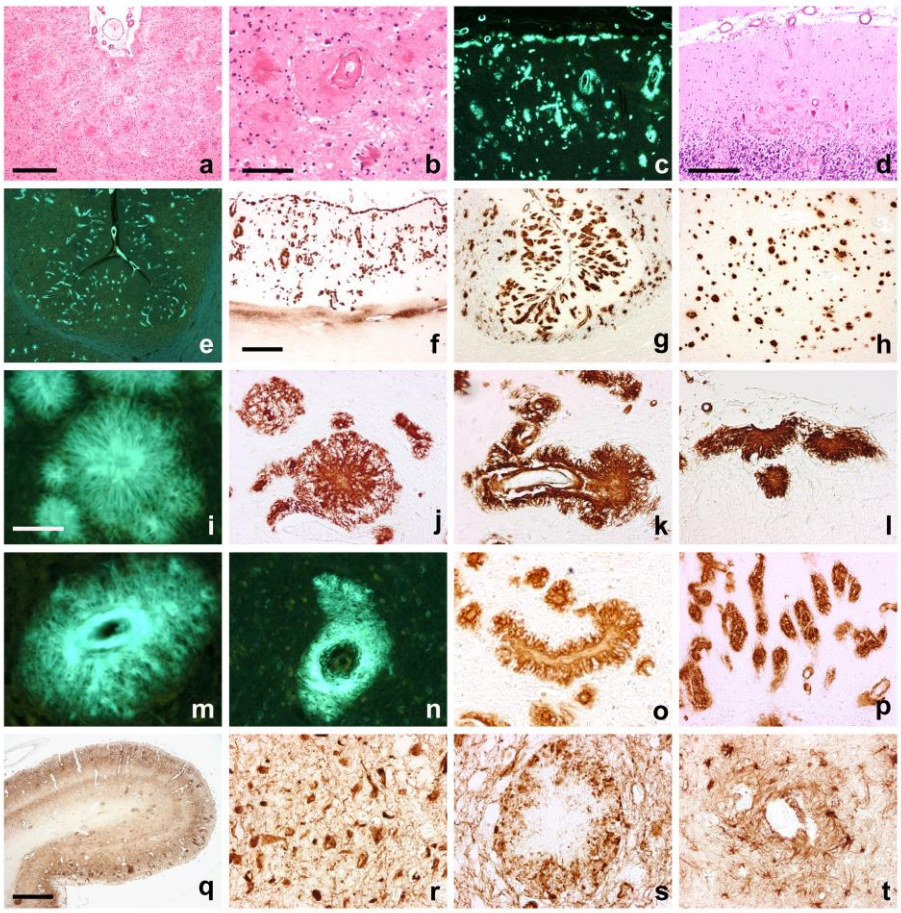

Figure 1.

Figure 1. Neuropathological lesions in the patient homozygous for the APP A673V mutation. Even at low magnification, amyloid deposits in the brain parenchyma and associated with the vessel walls can be detected in sections stained with H&E (a,b: cerebral cortex; d: cerebellum) and thioflavine S (c: cerebral cortex; e: cerebellum). The amyloid is intensely immunolabeled by anti-Aβ antibodies (f: cerebral cortex; g: cerebellum; h: thalamus. 4G8 immunostaining). Aβ is abundant in the perivascular space in the cerebral cortex and cerebellum (f,g), while in the thalamus builds up mostly in the neuropil (h). Large, "lake-like" Aβ-immuoreactive deposits are present in the cortex/white matter junction (f). Senile plaques are made up by thin bundles of Aβ-amyloid forming "fringes" irradiating from the central core (i: thioflavine S; j,k,l: 4G8 immunostaining). Cores often adhere to the vessel wall (k) or to the pial surface (l). Vascular-associated amyloid (m,n: thioflavine S) is abundant in the perivascular space of vessels with (m) or without (n) CAA. When cut tangentially, amyloid-laden vessels could be followed in the sections, looking like centipedes (o: 4G8 immunostaining). This is the most prominent form of amyloid deposition also in the molecular layer of the cerebellum (p: 4G8 immunostaining). Immunostaining for phosphorylated tau (q,s: AT8; r: AD2) reveal diffuse neurofibrillary changes in the cerebral cortex (q), where both intra- and extracellular tangles are present (r). Tau-positive neurites (s) and GFAP-positve reactive astrocytes (t) cluster around amyloid plaques. Scale bar in A = 400 μm (a,c,e,g and h are the same magnification); scale bar in b = 100 μm (b,j,k,l,o,p and t are the same magnification); scale bar in d = 200 μm; scale bar in i = 50 μm (i,m,n,r and s are the same magnification); scale bar in f = 1 mm and scale bar in q = 2 mm.

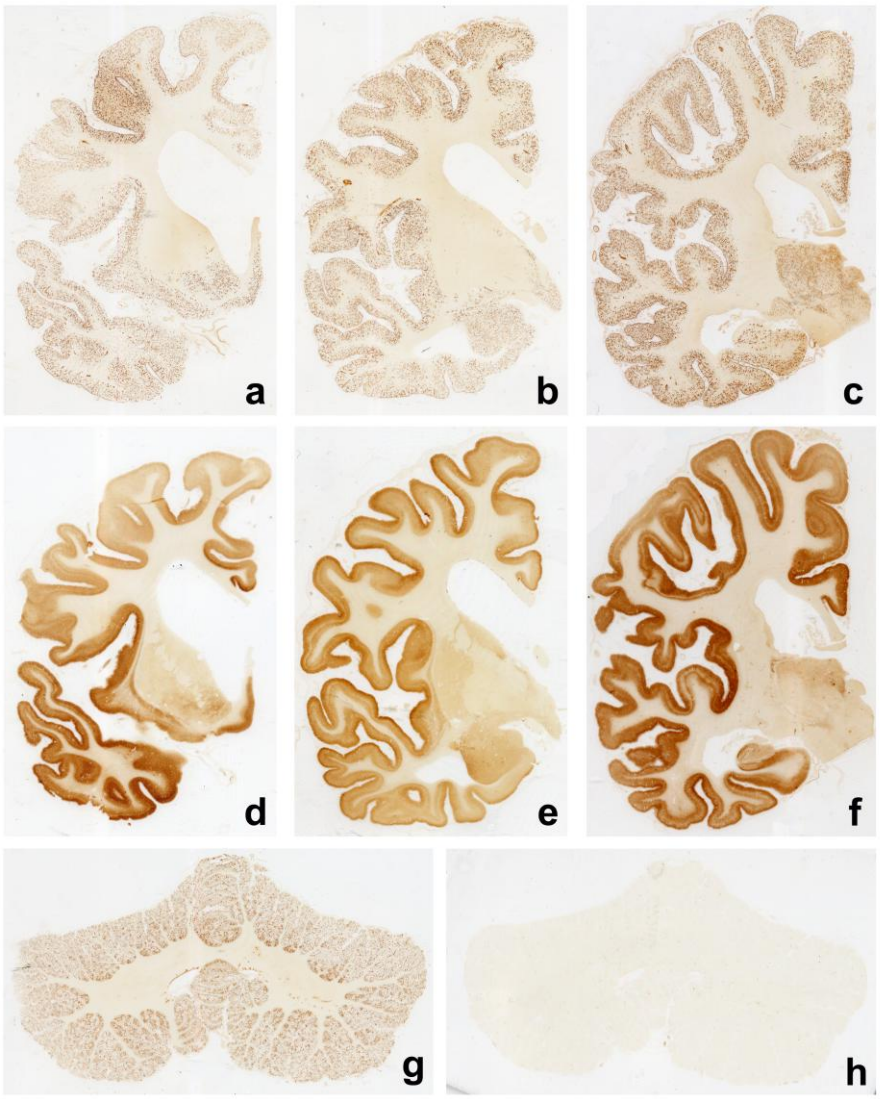

Figure 2. Topographic distribution of Aβ deposits and tau-related neurofibrillary changes. Coronal sections of the right cerebral hemisphere at level of the head of the caudate nucleus (a,d), of the amygdala (b,e) and of the lateral geniculate body (c,f) and sections of the cerebellum (g,h) immunostained for Aβ (a,b,c,g: 4G8) and for phosphorylated tau (d,e,f,h: AT8). Immunoreactivity for Aβ is abundant in all areas of the cererbral cortex, thalamus, and cerebellar cortex, while is absent in the caudate nucleus and putamen, apart from the nucleus accumbens. The deposition of hyperphosphorylated tau is widespread in the cerebral cortex, involving primary motor and sensory areas as well as associative fields, while spares the cerebellum.

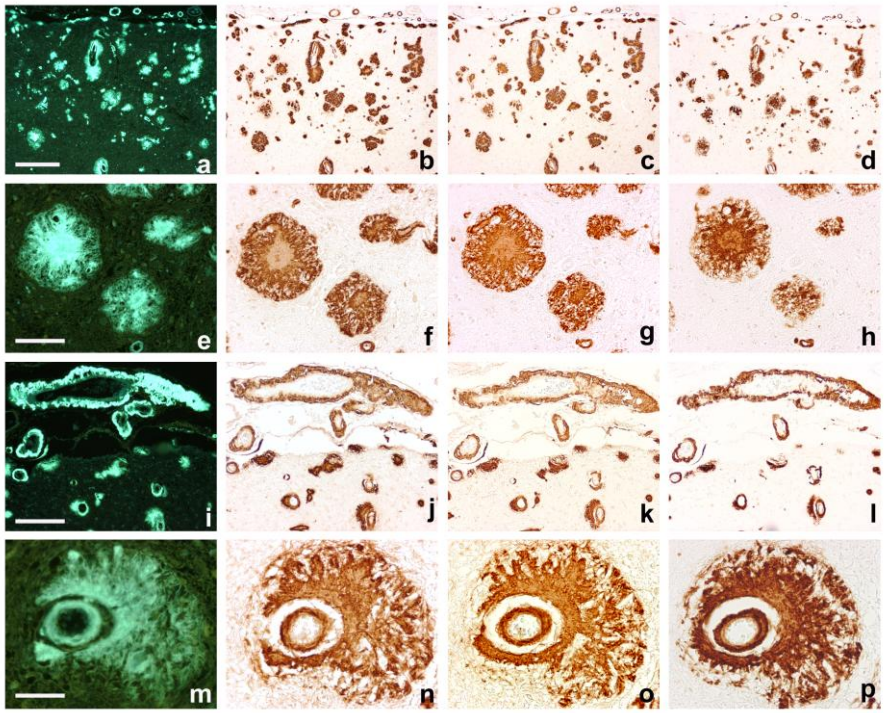

Figure 3. Tinctorial and antigenic properties of Aβ-amyloid deposits. Comparison of adjacent sections treated with thioflavine S (a,e,i,m), immunostained with an antibody to total Aβ (b,f,j,n: 4G8), with the monoclonal antibody specific for Aβ40 (c,g,k,o) or for Aβ42 (d,h,l,p). Low magnification shows that the distribution and the quantity of the lesions is very similar with the four methods employed (a,b,c,d) documenting the absence of structures immunoreactive for Aβ but not fluorescent after thioflavine S. Anti-Aβ40 (g) immunostains senile plaques with a pattern indistinguishable from that obtained with thioflavine S (e), 4G8 (f) or anti-Aβ42 (h) immunostaining. There is a close correspondence between the fluorescence elicited by thioflavine S in CAA of leptomeningeal vessels (i) and the immunolabeling obtained with 4G8 (j), anti-Aβ40 (k) and anti-Aβ42 (l). Aβ-amyloid in the vessel wall and in the perivascular space (m: thioflavine S; n: 4G8) is immunostained by both Aβ40- (o) and Aβ42 (p) antibodies. Scale bar in a = 400 μm (a,b,c and d are the same magnification); scale bar in e = 100 μm (e,f,g and h are the same magnification); scale bar in i = 200 μm (i,j,k and l are the same magnification); scale bar in m = 50 μm (m,n,o and p are the same magnification).

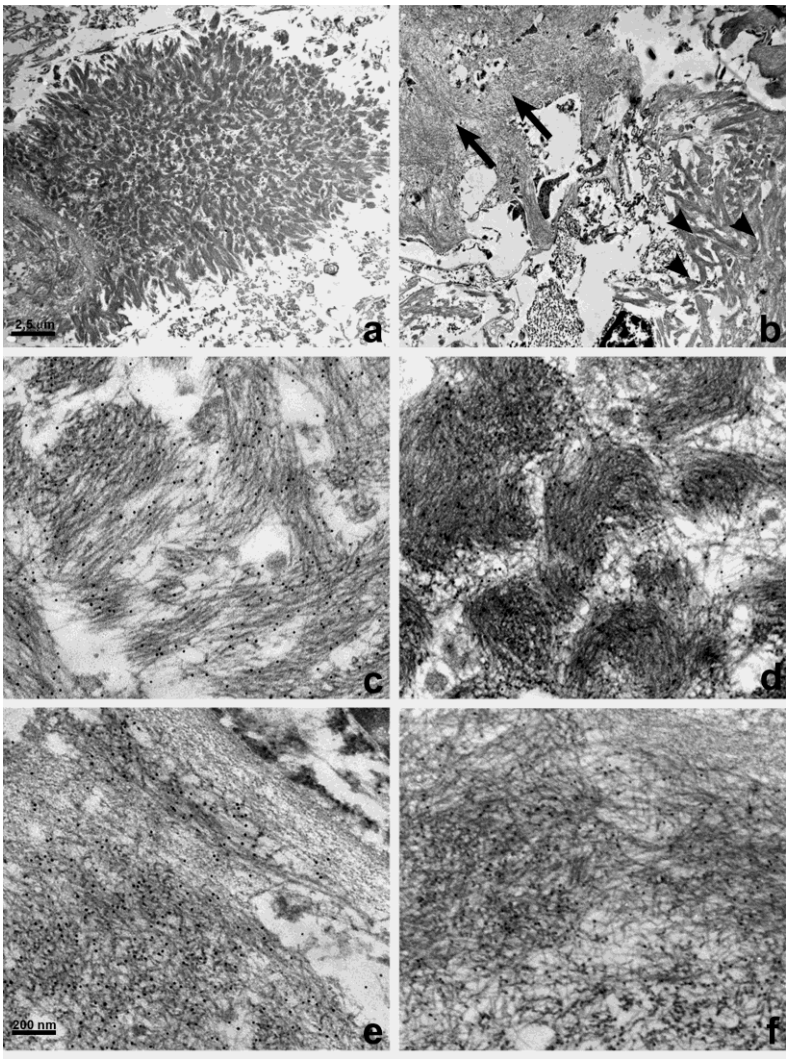

Figure 4. Ultrastructure of Aβ-amyloid deposits. Electron microscopy (a,b) and immunoelectron microscopy (c-f) of parenchymal (a-d) and vascular (e,f) amyloid depositions. Parenchymal amyloid deposits were detectable in the shape of plaques (a) or of loose (arrows) or compact bundles of fibrils (arrowheads) (b) , intermingled with astroglial cells, in absence of pre-amyloid fibrils. (Ultrathin section stained with uranyl acetate and lead citrate). Immunoelectron microscopy disclosed that both parenchymal and vessels deposits were formed by long straight unbranched 8-10 nm-thick fibrils, morphologically recognizable as amyloid. Both parenchymal (c,d) and vascular deposits (e,f) were intensely decorated using antibodies specific for both Aβ40 (c,e) and Aβ42 (d,f). Ultrathin section immunostained with antibodies specific for Aβ40 (c,e) and Aβ42 (d,f) revealed with GAR-10 and counterstained with uranyl acetate and lead citrate. Scale bar in a = 2.5 μm (a and b are the same magnification); scale bar in e = 200 nm (c,d,e and f are the same magnification).

5. Discussion

The present study confirms the diagnosis of AD at the neuropathological level in the Italian family with the APP recessive mutation A673V, documenting the presence of extensive deposition of Aβ amyloid and formation of neurofibrillary changes in the brain of the proband who was homozygous for this genetic defect.

Neurofibrillary changes were severe, but did not show distinctive characteristics, while Aβ deposits exhibited significant peculiarities in their morphological, structural and antigenic properties that allowed to differentiate this case from the patients with sporadic AD or FAD inherited as a dominant trait. Most relevant in this regard was the configuration of the Aβ deposits that were of very large size, with an unusual perivascular arrangement, and evenly exhibited the tinctorial, optical and ultrastructural characteristics of amyloid. Moreover, all Aβ deposits contained Aβ40 as the lesions labeled by immunoreagents specific for this Aβ species matched exactly those revealed by Aβ42 or by antibodies to total Aβ. Finally, Aβ deposition largely spared the neostriatum while deeply affected the thalamus, the cerebellum and the brainstem, and therefore did not conform with the hierarchical topographical sequence of involvement identified in sporadic AD[30]. This scenario differs from any other cerebral Aβ amyloidosis reported so far.

Mutations of the APP gene, although rare, have been the first genetic cause of cerebral Aβ amyloidosis to be indentified[16].

The phenotypic variability of FAD linked to APP mutations is very broad. Some of the APP mutations – such as the K670M/N671L, T714I, V717I[10,14,15]- are associated with pure, typical Alzheimer

disease, others are associated with a phenotype indicated as HCHWA where CAA is striking and neurofibrillary changes are absent (E693Q, E693K, G705C), and another group exhibits full-expressed AD accompanied by unusually severe CAA (A692G, E693G, D694N, A713T and duplication of APP gene) . Overall, CAA appears to be more frequent and severe in APP-FAD than in sporadic AD or in FAD linked to mutations of presenilins.

The present report further widens the phenotypic variability of APP-FAD. In the patient homozygous for the A673V APP mutation, the Aβ deposits were largely related to the vascular system, and mostly represented by amyloid built up in the neuropil immediately surrounding the vessel wall ("drusige Entartung"), pointing to the Virchow-Robin spaces as the predilection site of Aβ deposition.

The morphology of SP was different from all the subtypes described so far. In many instances, SP displayed a large compact core surrounded by a ring of amyloid bundles assuming a radial aspect and resembling long fringes. Such "fringed plaques" exhibited some similarities but also substantial differences compared to another specific type of SP, the "cotton-wool plaque", that have been described in cases of FAD linked to PSEN1 mutations[17]. These two types of SP are similarly very large and can be visualized even at H&E. However, cotton wool plaques are poorly fluorescent after thioflavine S, often lack a central amyloid core and contain Aβ40 only at the periphery. Radiating bundles of amyloid indicated as "spicules", "spikes", "wisps" or "stars" have been described previously in SP of familial forms of AD or CAA and in sporadic AD, sometimes indicated as "kuru-like" plaques, However, the "fringed" plaques of

our patient differ from them in being much larger, irregularly shaped and made up of amyloid bundles that appear long, wavy, intermingled each other rather than .short and straight as in “kuru-like” plaques.

It is now widely accepted that Aβ deposits in the brains of AD patients and aged nondemented subjects are heterogeneous regarding both their tinctorial and structural properties and the length of the Aβ species. Immunohistochemical studies have established that Aβ is deposited in amyloid plaques, either cored or with less-defined boundaries, that are fluorescent after thioflavine S, as well as in poorly circumscribed immunoreactive lesions that lack the properties of amyloid and have been indicated as diffuse plaques or preamyloid deposits, to underline the likelihood that they represent immature lesions and early phases of SP formation[28].

At least two distinct species of Aβ with different C-termini, Aβ x-42 (Aβ42) and Aβ x-40 (Aβ40), are deposited in AD brains, with the former being far predominant in parenchymal deposits, the latter in CAA. In vitro experiments have demonstrated that Aβ42 polymerizes in fibrils much faster than Aβ40, pointing to the C-terminal tail of Aβ as crucial to determine its aggregation potential. Using specific immunoreagents for the two species, it emerged that in the AD cortex all the Aβ deposits contain Aβ42, while less than one third are Aβ40 positive[13]. In nondemented aged individuals the percentage of Aβ40 positive deposits is even lower, reflecting the fact that diffuse plaques and preamyloid deposits are consistently Aβ42 positive but Aβ40 negative[9]. The deviation between the amount of Aβ42- and Aβ40-labeled plaques is pronounced in FAD linked to

PSEN1 mutation, especially those lying in the N-terminal half of PSEN1[18].

The properties of Aβ deposits of the patient reported here appear unprecedented for the high content of Aβ40-positive deposits in the parenchyma and of Aβ42-positive in the vessel walls as well as for the absence of preamyloid deposits.

Aβ40 and Aβ42 differ significantly regarding their biochemical and fibrillogenic properties. In vitro, Aβ42 exhibit lower solubility and higher propensity to form fibrillary aggregates compared to Aβ40. Accordingly, and despite the preponderance of Aβ40 in physiologic conditions, that represents about 90% of the Aβ species in human CSF as well as in conditioned media of APP expressing cells, the major constituent of SP is Aβ42, suggesting that its aggregation plays a critical role in the process of amyloid formation[26].

The formation of Aβ-amyloid in the brain of the patient homozygous for the A673V APP mutation may be explained considering that Aβ synthetic peptides bearing the corresponding amino acid substitution have striking increased ability to aggregate in vitro compared to wild type peptides[7]. The overrepresentation of Aβ40 in the brain suggests that this modification may be more pronounced for Aβ40 than for Aβ42 that is intrinsically highly amyloidogenic.

It remains to be explained why in this patient all the Aβ assumes fibrillary amyloid form and significant preamyloid deposits do not arise. The large quantity of Aβ40 species deposited in the brain with a distribution largely matching Aβ42 suggests that the N-terminal end of Aβ is crucial for fibrillogenesis in this setting and that Aβ aggregates very efficiently involving both species. The

neuropathology of this case was characterized by a relatively low density of amyloid plaques of large dimensions, as the growth of the amyloid assemblies was a more active phenomenon than the nucleation of new Aβ deposits.

Accordingly, in vitro studies on the effects of the A673V mutation on the aggregation and amyloidogenic properties of Aβ showed that the assemblies formed by the mutated peptides are much larger and more stable than those formed by wild-type peptides. Moreover, the aggregation kinetic of the mutant Aβ species is much faster than that of wild-type peptides suggesting that, once triggered, the nucleation of Aβ species proceeds very rapidly towards the formation of large amyloid assemblies[7].

A final comment concerns the topographic distribution of Aβ deposits that spares the striatum. This is surprising also in consideration of the following facts: i) in cases of familial AD the striatum has been identified as initial site of Aβ deposition by neuroimaging studies using PIB as amyloid-ligand[32]; ii) a hierarchical scheme in which the striatum precedes the cerebellum and the brainstem in the temporal sequence of progressive involvement of the brain by Aβ accumulation has been reported[21]. It is intriguing that the only striatal areas in which Aβ is present is the nucleus accumbens. Whether this differential involvement depends on structural variation between these brain areas or is related to other factors such as their connectivity may be a relevant issue in AD pathogenesis.

In summary, the presence of the Alzheimer hallmark lesions in the patient homozygous for the APP A673V mutation indicates that the basic pathologic features are comparable to those of the sporadic

late onset AD and of autosomal dominant FAD. However, our findings indicate that differences in the molecular processes involved in the deposition of Aβ intervene, as reflected by several relevant peculiarities both in the structural and antigenic characteristics of Aβ deposits and in their topographic distribution.

Future analyses of the biochemical properties and the distribution in cellular compartments of Aβ in this unique recessive AD subtype and the comparison with those of the sporadic and the autosomal dominant forms of the disease linked to other APP mutations or to mutations of presenilin genes may help to understand the molecular mechanisms of Aβ deposition in Alzheimer disease.

6. Acknowledgements

This work was supported by grants from the Italian Ministry of Health (grant RFPS 2007/02), from Fondazione CARIPLO, from ERA-Net Neuron (grant nEUROsyn) and from Telethon Italy.

The authors thank Mrs. Francesca Cacciatore and Mrs. Sonia Spinello for skillful technical assistance.

7. References

1. Basun H, Bogdanovic N, Ingelsson M et al (2008) Clinical and neuropathological features of the Arctic APP gene mutation causing early-onset Alzheimer disease. Arch Neurol 65:499-505.

2. Braak H, Braak E (1991) Neuropathological stageing of Alzheimer-related changes. Acta Neuropathol 82:239-259.

3. Bruni AC, Bernardi L, Colao R et al (2010) Worldwide distribution of PSEN1 Met146Leu mutation: A large variability for a founder mutation Neurology 74:798-806.

4. Bugiani O, Giaccone G, Rossi G et al (2010) Hereditary cerebral hemorrhage with amyloidosis associated with E693K mutation of APP. Arch Neurol 67:987-995.

5. Cras P, van Harskamp F, Hendriks L et al (1998) Presenile Alzheimer dementia characterized by amyloid angiopathy and large amyloid core type senile plaques in the APP 692Ala→Gly mutation. Acta Neuropathol 96:253-260.

6. Cupidi C, Capobianco R, Goffredo D et al (2010) Neocortical variation of Aβ load in fully expressed, pure Alzheimer disease. J Alzheimers Dis 19:57–68.

7. Di Fede G, Catania M, Morbin M et al (2009) A recessive mutation in the APP gene with dominant-negative effect on amyloidogenesis. Science 323:1473-1477.

8. Duyckaerts C, Delatour B, Potier M-C (2009) Classification and basic pathology of Alzheimer disease. Acta Neuropath 118:5-36.

9. Fukumoto H, Asami-Odaka A, Suzuki N, Shimada H, Ihara Y, Iwatsubo T (1996) Amyloid β protein deposition in normal aging has the same characteristics as that in Alzheimer's disease. Predominance of Aβ42(43) and association of Aβ40 with cored plaques. Am J Pathol 148:259-265.

10. Goate A, Chartier-Harlin MC, Mullan M et al (1991) Segregation of a missense mutation in the amyloid precursor protein gene with familial Alzheimer's disease. Nature 349:704-706.

11. Grabowski TJ, Cho HS, Vonsattel JP, Rebeck GW, Greenberg SM (2001) Novel amyloid precursor protein mutation in an Iowa family with dementia and severe cerebral amyloid angiopathy. Ann Neurol 49:697-705.

12. Hardy GA, Higgins GA (1992) Alzheimer's disease: the amyloid cascade hypothesis. Science 286:184-185.

13. Iwatzubo T, Odaka A, Suzuki N, Mizusawa H, Nukina N, Ihara Y (1994) Visualization of Aβ42(43) and Aβ40 in senile plaques with

end-specific Aβ monoclonals: evidence that an initially deposited species is Aβ42(43). Neuron 13:45-53.

14. Kumar-Singh S, De Jonghe C, Cruts M et al (2000) Nonfibrillar diffuse amyloid deposition due to a gamma(42)-secretase site mutation points to an essential role for N-truncated Abeta(42) in Alzheimer's disease. Hum Mol Gen 9: 2589-2598.

15. Lannfelt L, Bogdanovic N, Appelgren H et al (1994) Amyloid precursor protein mutation causes Alzheimer's disease in a Swedish family. Neurosci Lett 168:254-256.

16. Levy E, Carman MD, Fernandez-Madrid IJ et al (1990) Mutation of the Alzheimer's disease amyloid gene in hereditary cerebral hemorrhage, Dutch type. Science 248:1124-1126.

17. Mann DM, Takeuchi A, Sato S et al (2001, a) Cases of Alzheimer's disease due to deletion of exon 9 of the presenilin-1 gene show an unusual but characteristic beta-amyloid pathology known as 'cotton wool' plaques. Neuropathol Appl Neurobiol 27:189 –196.

18. Mann DMA, Pickering-Brown SM, Takeuchi A et al (2001, b) Amyloid angiopathy and variability in amyloid β deposition is determined by mutation position in Presenilin-1-linked Alzheimer's disease. Am J Pathol 158:2165-2175.

19. Marcon G, Giaccone G, Cupidi C et al (2004) Neuropathological and clinical phenotype of an Italian Alzheimer family with M239V mutation of presenilin 2 gene. J Neuropathol Exp Neurol 63:199-209.

20. Mirra SS, Heyman A, McKeel D et al (1991) The Consortium to Establish a Registry for Alzheimer's Disease (CERAD). Part II. Standardization of the neuropathological assessment of Alzheimer's disease. Neurology 41:479-486.

21. Obici L, Demarchi A, de Rosa G et al (2005) A novel AbetaPP mutation exclusively associated with cerebral amyloid angiopathy. Ann Neurol 58:639-644.

22. Piscopo P, Marcon G, Piras MR et al (2008) A novel PSEN2 mutation associated with a peculiar phenotype. Neurology 70:1549-1554.

23. Rossi G, Giaccone G, Maletta R et al. (2004) A family with Alzheimer disease and strokes associated with A713T mutation of the APP gene. Neurology 63:910-912.

24. Rovelet-Lecrux A, Hannequin D, Raux G et al (2006) APP locus duplication causes autosomal dominant early-onset Alzheimer disease with cerebral amyloid angiopathy. Nat Genet 38:24-26.

25. Scholz W (1938) Studien zur Pathologie der Hirngefäße II: die drusige Entartung der Hirnarterien und Capillaren. Z gesamte Neurol Psychiatr 162:694-715.

26. Seubert P, Vigo-Pelfrey C, Esch F et al (1992) Isolation and quantification of soluble Alzheimer's β-peptide from biological fluids. Nature 359:325-327.

27. Shepherd C, McCann Heather, Halliday GM (2009) Variations in the neuropathology of familial Alzheimer's disease. Acta Neuropath 118:37-52.

28. Tagliavini F, Giaccone G, Frangione B, Bugiani O (1988) Preamyloid deposits in the cerebral cortex of patients with Alzheimer's disease and nondemented individuals. Neurosci Lett 93:191-196.

29. Takao M, Ghetti B, Murrel JR et al (2001) Ectopic white matter neurons, a developmental abnormality that may be caused by the PSEN1 S169L mutation in a case of familial AD with myoclonus and seizures. J Neuropathol Exp Neurol 60:1137-1152.

30. Thal DR, Rűb U, Orantes M, Braak H (2002) Phases of Aβ-deposition in the human brain and its relevance for the development of AD. Neurology 58:1791-1800.

31. Van Duinen SG, Castaño EM, Prelli F, Bots GT, Luyendijk W, Frangione B (1987) Hereditary cerebral hemorrhage with amyloidosis in patients of Dutch origin is related to Alzheimer disease. Proc Natl Acad Sci USA 84:5991-5994.

32. Villemagne VL, Ataka S, Mizuno T et al (2009) High striatal amyloid β-peptide deposition across different autosomal Alzheimer disease mutation types. Arch Neurol 66:1537-1544.

Chapter 3

Biochemical features of the amyloidosis associated with the APP A673V mutation

1. Introduction

The APP A673V mutation[1] represents a new scenario in the AD field, since it induces the disease only in the homozygous state, while heterozygous carriers are never affected, neither in advanced age, consisting with a recessive mendelian trait of inheritance. Nonetheless, the mutation is very aggressive when occurring in homozygosity and shows a double pathogenic mechanism: it enhances the fibrillogenic properties of Aβ and shifts the APP processing towards the amyloidogenic pathway, causing an increase in the production of Aβ1-40, Aβ1-42, N-terminally truncated Aβ isoforms and the APP fragments sAPPβ and C99, generated along the amyloidogenic pathway.

The neuropathological picture showed several distinctive hallmarks compared to sporadic or familial AD inherited as a dominant trait. Beside the marked severity of the lesions, peculiar features were the configuration of the Aβ deposits, that were often of large size and perivascular, and exhibited a complete correspondence between the pattern elicited by amyloid stainings and the labeling obtained with immunoreagents specific for Aβ. Moreover, the topographic distribution of Aβ deposition was not in compliance with the hierarchical regional sequence of involvement documented in sporadic AD, since it spared the neostriatum while deeply affecting

the cerebellum and the brainstem. Finally, the use of antibodies which specifically recognize Aβ1-40 or Aβ1-42 showed that the plaques are composed by both the isoforms, without the predominance of the longer peptide that is usually seen in AD brains[2].

These findings demonstrated that the presence of the A673V substitution on both alleles causes a severe form of early-onset AD with distinctive neuropathological features; however, the molecular basis underlying such a peculiar picture are still unclear.

In order to clarify the role played by the APP A673V mutation in determining the neuropathologic changes described above, we characterized the brain of the homozygous carrier from a biochemical point of view. We studied the distribution of the Aβ peptides in brain fractions enriched in proteins with different solubility and we compared it with the distribution in sporadic AD brains or in brains from familial AD patients carrying mutations in APP or PS1 genes. Moreover, we described the profile of Aβ isoforms in the patient's CSF, in comparison with sporadic AD, and paralleled it with the composition of amyloid extracted from the patient's leptomeningeal vessels.

2. Materials and methods

2.1 Samples collection

The brains were obtained at autopsy. The right cerebral hemisphere, the cerebellum and the brainstem were fixed in 10% formalin, while the left cerebral hemisphere was dissected and partly fixed in Alcolin (a non-linking alcohol-based fixative, Diapath) and

partly frozen at -80°C. Biochemical analysis was performed on three familial AD, carrying either the homozygous A673V or the heterozygous A713T mutations in the APP gene and the heterozygous P117A substitution in PS1 gene. Five sporadic AD were also included in the study. The ApoE genotype was determined for all other cases included in the study (Table 1).

Patient	ApoE genotype
Control	ε3/ε4
sAD 1	ε3/ε3
sAD 2	ε3/ε3
sAD 3	ε3/ε4
sAD 4	ε3/ε3
sAD 5	ε3/ε4
APP A673V	ε3/ε3
APP A673T	ε3/ε3
PS1 P117A	ε2/ε3

Table 1. ApoE genotypes. The ApoE genotype was determined for all the sporadic and familial AD cases included in the study of biochemical characterization of the APP A673V brain fractions.

Amyloid was extracted from the leptomeningeal vessels from the three familial AD cases and of a sporadic AD patient carrying the homozygous ApoE ε4 allele and showing a massive congophilic angiopathy upon the histological analysis.

CSF from the A673V homozygous carrier was collected at four different time-points along the progression of the disease (T1, T2, T3, T4) and the results of CSF analysis were compared with those obtained from 20 sporadic AD (sAD) and 20 age-matched non demented controls.

2.2 Brain homogenates preparation and fractionation

Brains were processed using a four-step extraction in order to obtain fractions defined by their biochemical properties and, in particular, by their solubility in different buffers and detergents [3]. Briefly, samples from frontal cortices were homogenized in 7 volumes of Tris buffer (20mM Tris-HCl pH=7.4), sonicated and centrifuged 1 hour, 100,000xg, 4°C using a TL100 Ultracentrifuge (Beckman Coulter). The supernatant was called Tris-soluble fraction and stored at -80°C. The pellet was homogenized in 7 volumes of Triton buffer (20mM Tris-HCl pH=7.4, 0.1% Triton X-100), sonicated and centrifuged 1 hour, 100,000xg, 4°C. The supernatant was retained as the Triton-soluble fraction and stored at -80°C. The remaining pellet was homogenized in 7 volumes of SDS buffer (20mM Tris-HCl pH=7.4, 2% SDS), sonicated and centrifuged 1 hour, 100,000xg, 4°C. The supernatant was called SDS-soluble fraction and stored at -80°C. The pellet was extracted in 70% formic acid, sonicated and neutralized with 1M Tris pH=11.0. The last represented the insoluble fraction.

All the buffers used were added with Complete Mini protease inhibitors (Roche).

2.3 Aβ quantification

Levels of Aβ1-40, Aβ1-42 and aggregated Aβ in each fraction were measured by enzyme-linked immunosorbent assay (ELISA) (Aβ40 Human ELISA kit, Aβ42 Human ELISA kit, Aggregated Aβ Human ELISA kit, Invitrogen), according to manifacturer's instructions.

At least five replicates were performed for each measurement.

2.4 Immunoblot analysis

2.4.1 Analysis of C-terminal fragments

100µg proteins from SDS-soluble fractions were loaded on 12.5% tris-tricine polyacrilamide gels, transferred to polyvinylidene fluoride membranes and probed with the polyclonal anti APP C-terminal fragment A8717 antibody (1:4000, Sigma). The immunoreactions were visualized by enhanced chemiluminescence system (GE Healthcare).

2.4.2 Aβ oligomers detection

Samples from frontal cortices were homogenized in 9 volumes of lysis buffer (100mM sodium chloride, 10mM EDTA, 0.5% NonidetP40, 0.5% sodium deoxycholate in 10mM tris-HCl pH=7.4) and cleared by centrifugation at 3,000xg, 5 minutes.

100µg of the clarified homogenates were loaded on 12.5% tris-tricine polyacrilamide gels, transferred to polyvinylidene fluoride membranes and probed with the monoclonal 4G8 (1:2000, Signet) or 6E10 (1:2000, Signet) antibodies. The immunoreactions were visualized by enhanced chemiluminescence system (GE Healthcare).

2.5 Amyloid extraction from leptomeningeal vessels

About 12g of leptomeninges were carefully separated from the parenchyma and frozen at -80°C; 4.5g were used for amyloid extraction following a modified Pras' protocol[4]. Briefly, the leptomeninges were homogenized in 9 volumes of 150mM NaCl,

sonicated using a Ultrasonic homogenizer Sonopuls-series HD2070 and centrifuged 30 minutes, 30,000xg, 4°C. OD_{280} was measured in the supernatant. The pellet was homogenized again in 9 volumes of 150mM NaCl and all the steps previously described were repeated until OD_{280} in the supernatant was lower than 0.2. The pellet was digested with Collagenase type I (Sigma) for 18 hours at 37°C and centrifuged 30 minutes, 30,000xg, 4°C. The pellet was homogenized in 9 volumes H_2O, sonicated and centrifuged 1 hour, 50,000xg, 4°C. OD_{280} was measured in the supernatant. The pellet was homogenized again in 9 volumes of H_2O and all the steps previously described were repeated until OD_{280} in the supernatant was lower than 0.2. The supernatants contained amyloid; they were collected, pooled, precipitated with 150mM NaCl and centrifuged 1 hour, 50,000xg, 4°C. Amyloid was extracted with 80% formic acid, dried and resuspended in H_2O for further analysis. The presence of amyloid was confirmed by DOT-BLOT using the monoclonal antibody 4G8 (1:2000, Signet), electron microscopy and atomic force microscopy.

2.6 SELDI-TOF MS analysis

Amyloid extracted from leptomeninges and CSF were analyzed by an immunoproteomic assay for Aβ peptide detection using SELDI-TOF MS in collaboration with Dr.ssa Roberta Ghidoni from IRCCS-Foundation-Fatebenefratelli in Brescia as previously described [5]. Specifically, 3µl of a 0.125 mg/ml monoclonal antibody solution (6E10 and 4G8, Signet) was incubated for 2 h at room temperature in a humidity chamber to allow covalent binding to the PS20 ProteinChip Array (Bio-Rad Laboratories.Inc.). Unreacted sites were

blocked for 30 min at room temperature with 0.5 M Tris-HCl, pH=8, in a humid chamber. Each spot was washed three times with PBS containing 0.5% (v/v) TritonX-100 and then twice with PBS alone. Spots were coated with 5µl of sample, incubated overnight in a humid chamber and then washed three times with PBS containing 0.1% (v/v) TritonX-100, twice with PBS alone and finally with deionized water. One microliter of α-cyano-4-hydroxy cinnamic acid (Bio-Rad Laboratories, Inc.) was added to each spot and mass identification was made using the ProteinChip SELDI System, Enterprise Edition (Bio-Rad Laboratories Inc.).

3. Results

3.1 Analysis of APP processing and distribution of Aβ peptides in brain homogenates

3.1.1 C-terminal fragments

The Western Blot analysis of APP C-terminal fragments showed a strong increase in the amyloidogenic C99 fragment and a high C99:C83 ratio in the APP A673V carrier, indicating that the mutation shifts the APP processing towards the amyloidogenic pathway. In sporadic AD, the non amyloidogenic fragment C83 is the most abundant, while in controls only a weak immunoreactivity corresponding to C83 is detectable (Fig. 1).

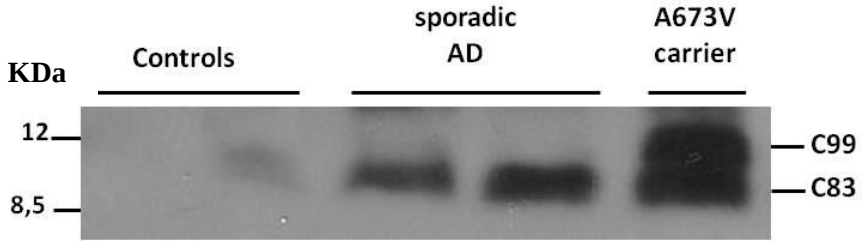

Figure 1. Western blot analysis of APP C-teminal fragments. The blot was probed with the anti-APP C-terminal fragment A8717 antibody. The APP A673V carrier showed a strong increase in the production of C99 amyloidogenic peptide.

3.1.2 Aβ levels by ELISA

Measurement of the Aβ40 and Aβ42 monomers on different fractions of brain homogenates by ELISA showed that the A673V mutated patient exhibits a distinct pattern of distribution of Aβ peptides in comparison with sporadic AD cases and control subjects. In particular, both the peptides were much more abundant than in sporadic AD brains. Aβ40 was by far the prevalent Aβ species in all the brain fractions of the A673V case (particularly SDS and formic acid extracts), and the Aβ1-42:Aβ1-40 ratio resulted to be much lower in comparison with sporadic AD cases, suggesting that a different representation of the two peptides occurs in the mutated patient (Table 2, Fig.2).

The measurement of Aβ in fractions of the APP A713T brain showed that Aβ40 is much more represented than in sporadic AD, while Aβ42 levels are not so high and appear to be similar to sAD. Indeed, Aβ42:Aβ40 ratio was very low in all compartments (Table 2, Fig. 2).

The PS1 P117A brain had the lower amounts of total Aβ as compared to the other mutated cases, not being so different than sporadic AD. Moreover, Aβ42 is more represented than Aβ40 in formic acid fraction, as expected for amyloid extracted from patients carrying a PS1 mutation (Table 2, Fig. 2).

Fraction	Patient	Aβ1-40	Aβ1-42	Aβ1-42/Aβ1-40 ratio	Aggregated Aβ
Tris	Control	1.27 ± 0.11	0.00	0.00	0.00
	sAD 1	12.46 ± 0.31	1.74 ± 0.16	0.14	0.00
	sAD 2	7.27 ± 0.29	0.35 ± 0.11	0.05	0.00
	sAD 3	5.85 ± 0.12	1.17 ± 0.40	0.20	0.00
	sAD 4	6.76 ± 0.31	0.87 ± 0.09	0.13	0.00
	sAD 5	34.47 ± 6.49	4.70 ± 0.29	0.14	1.81 ± 0.08
	APP A673V	834.61 ± 73.14	32.87 ± 13.23	0.04	4.67 ± 0.14
	APP A673T	167.39 ± 3.53	1.32 ± 0.05	0.01	1.35 ± 0.01
	PS1 P117A	11.53 ± 0.72	0.29 ± 0.03	0.03	0.00
Triton	Control	1.30 ± 0.11	0.00	0.00	0.00
	sAD 1	13.58 ± 0.64	1.00 ± 0.12	0.07	0.00
	sAD 2	9.97 ± 0.58	0.42 ± 0.13	0.04	0.00
	sAD 3	5.67 ± 0.28	1.20 ± 0.21	0.21	0.00
	sAD 4	7.56 ± 0.29	0.53 ± 0.05	0.07	0.00
	sAD 5	12.15 ± 1.13	2.45 ± 0.17	0.20	0.00
	APP A673V	233.68 ± 8.82	6.39 ± 0.63	0.03	6.02 ± 0.73
	APP A673T	104.14 ± 4.19	0.90 ± 0.09	0.01	2.94 ± 0.54
	PS1 P117A	8.29 ± 0.27	0.23 ± 0.10	0.03	0.00
SDS	Control	1.33 ± 0.11	0.00	0.00	0.00
	sAD 1	53.78 ± 1.86	1.18 ± 0.13	0.02	0.00
	sAD 2	18.82 ± 1.23	0.13 ± 0.02	0.01	0.00
	sAD 3	7.79 ± 0.16	1.83 ± 0.29	0.24	0.00
	sAD 4	15.81 ± 3.20	0.38 ± 0.08	0.02	0.00
	sAD 5	52.18 ± 3.58	1.88 ± 0.79	0.04	0.00
	APP A673V	59086.46 ± 4970.59	0.26 ± 0.02	0.00	1.31 ± 0.19
	APP A673T	6124.09 ± 386.21	2.00 ± 0.00	0.00	0.00
	PS1 P117A	46.12 ± 2.05	0.26 ± 0.01	0.01	0.00
Formic Acid	Control	1.62 ± 0.31	0.00	0.00	0.00
	sAD 1	143.99 ± 40.02	67.45 ± 4.52	0.47	0.00
	sAD 2	40.69 ± 4.17	19.05 ± 2.32	0.47	0.00
	sAD 3	10.77 ± 0.26	55.07 ± 11.35	5.11	0.00
	sAD 4	13.30 ± 1.52	8.94 ± 5.89	0.67	0.00
	sAD 5	253.45 ± 25.72	91.11 ± 7.16	0.36	0.00
	APP A673V	277731.10 ± 28404.74	131.08 ± 3.20	0.00	429.08 ± 10.25
	APP A673T	29717.97 ± 3347.72	42.22 ± 9.80	0.00	17.52 ± 2.11
	PS1 P117A	15.65 ± 2.61	21.84 ± 5.11	1.40	0.00

Table 2. Aβ levels in fractionated brain homogenates. The values are expressed as ng/g of tissue ± standard deviation. At least 5 measurements have been performed for each sample.

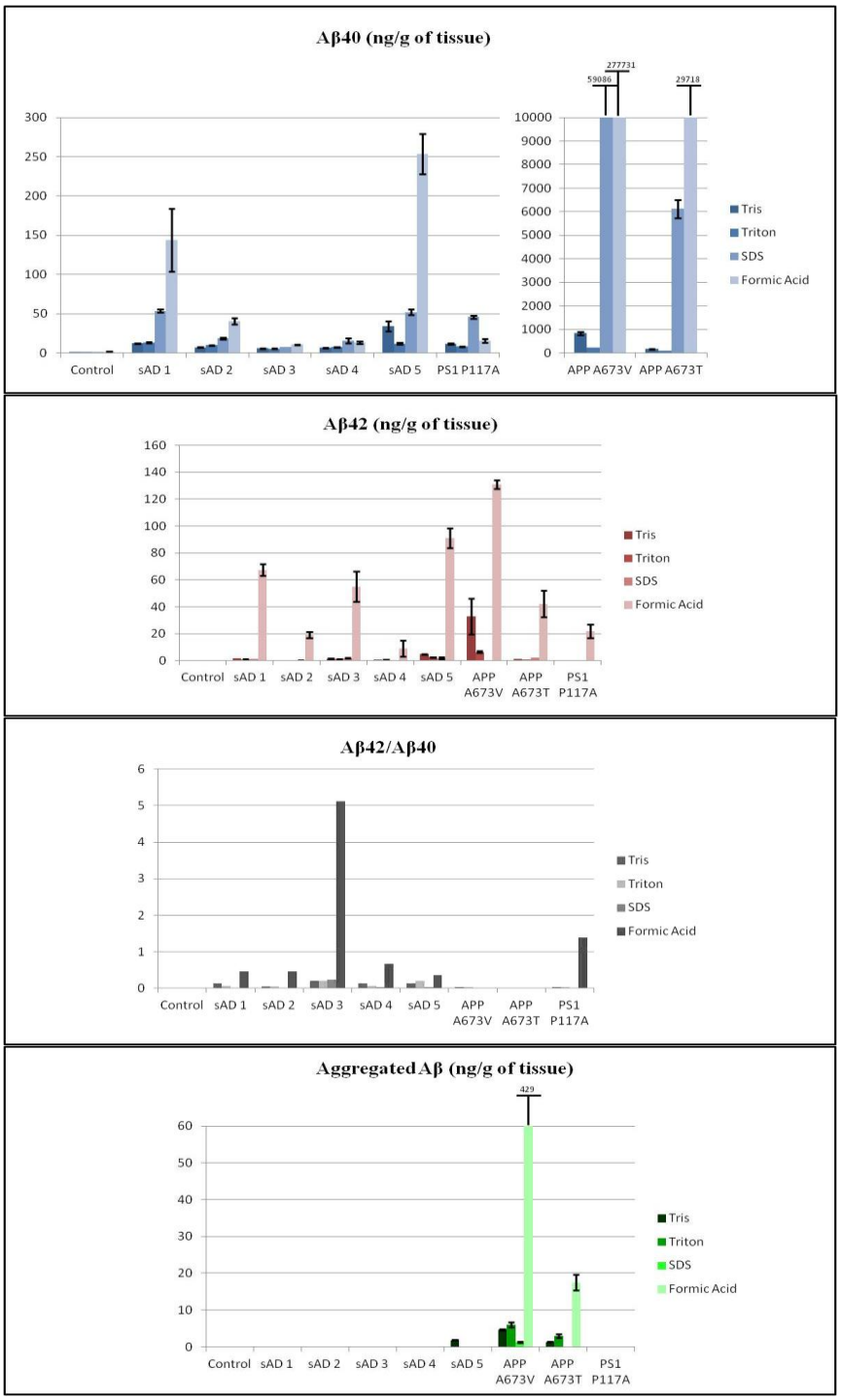

Figure 2. Graphical representation of Aβ levels in fractionated brain homogenates.

3.1.3 Aβ assemblies

Immunoblot analysis of brain homogenates showed the presence of several oligomeric assemblies in the homozygous APP A673V carrier (Fig. 3). Oligomers are not detectable in sporadic AD brains without a previous immunoprecipitation of the Aβ peptides (data not shown).

The propensity of A2V Aβ peptide to form aggregates was confirmed by the measurement of such assemblies by ELISA: the aggregated Aβ was markedly represented in all brain fractions from the A673V homozygous carrier, especially in formic acid extracts (>50 folds more than in sporadic AD cases) (Table 2, Fig. 2).

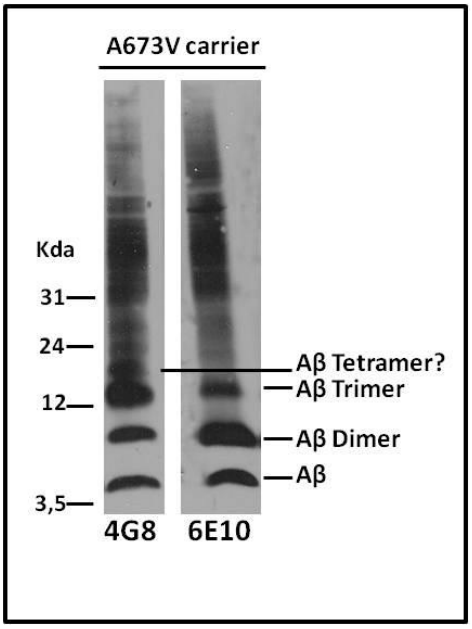

Figure 3. Oligomeric assemblies in brain homogenates from the APP A673V carrier. The blot was probed with 4G8 or 6E10 antibodies and showed a massive presence of the oligomeric forms in APP A673V brain.

3.2 Aβ pattern in CSF

The analysis by SELDI-TOF MS showed the presence of a set of Aβ fragments besides the full-length Aβ1-40 and Aβ1-42 in CSF samples. The measurement of Aβ levels showed a 10-fold decrease of total Aβ amount in CSF from the subject carrying the APP A673V substitution as compared to both controls and SAD patients. Aβ1-42 levels were 10- and 5-fold decreased than in controls and SAD cases, respectively; however, Aβ1-40 showed the strongest reduction, being 40-fold less abundant than in both controls and SAD patients. Moreover, we found low levels of all C-terminally truncated fragments, especially Aβ1-36, Aβ1-37, Aβ1-38 and Aβ1-39 in CSF from A673V mutated patient (Table 3) while the N-terminal truncated fragments that did not contained the A2V substitution were not changed.

Longitudinal analysis of A673V mutated CSF pattern along the disease progression showed a decrease of the C-terminally truncated Aβ isoforms between the first and the fourth time-points (T1-T4) (Table 3).

Mean signal intensity (uA) ± SE						
Peptides	CTR	AD	APP A673V T1	APP A673V T2	APP A673V T3	APP A673V T4
Aβ1-17	3.3 ± 0.2	3.8 ± 0.3	1.7 ± 0.1	1.4 ± 0.1	1.3 ± 0.2	1.8 ± 0.1
Aβ1-18	6.0 ± 0.6	6.3 ± 0.8	1.7 ± 0.1	0.6 ± 0.3	0.3 ± 0.3	1.5 ± 0.1
Aβ1-19	1.8 ± 0.1	1.9 ± 0.1	nd	nd	nd	nd
Aβ11-40	1.5 ± 0.1	1.8 ± 0.1	5.0 ± 0.3	2.2 ± 0.4	nd	nd
Aβ10-40	4.3 ± 0.6	5.0 ± 0.8	0.8 ± 0.1	4.9 ± 1.2	11.7 ± 2.6	6.8 ± 0.5
Aβ11-42	1.6 ± 0.1	1.7 ± 0.1	nd	0.6 ± 0.3	nd	nd
Aβ1-33	5.5 ± 0.3	5.1 ± 0.5	2.6 ± 0.3	2.3 ± 0.5	0.6 ± 0.2	0.6 ± 0.1
Aβ1-34	5.6 ± 0.4	5.3 ± 0.5	2.7 ± 0.3	2.4 ± 0.5	0.8 ± 0.1	0.7 ± 0.0
Aβ1-35	1.6 ± 0.1	2.1 ± 0.2	nd	1.8 ± 1.1	1.0 ± 0.5	nd
Aβ1-36	2.7 ± 0.1	2.8 ± 0.2	nd	nd	nd	nd
Aβ1-37	19.6 ± 1.5	20.0 ± 2.2	4.1 ± 0.3	2.1 ± 0.1	2.9 ± 0.3	2.7 ± 0.2
Aβ1-38	69.6 ± 6.2	71.5 ± 8.5	4.5 ± 0.4	3.5 ± 0.6	5.7 ± 0.5	3.6 ± 0.3
Aβ2-40	nd	nd	nd	nd	nd	nd
Aβ1-39	15.1 ± 1.2	15.6 ± 1.3	4.7 ± 0.4	1.9 ± 0.2	0.6 ± 0.6	0.7 ± 0.4
Aβ1-40	180.1 ± 16.5	183.1 ± 20.5	3.6 ± 0.6	4.6 ± 1.1	7.1 ± 0.9	4.3 ± 0.6
Aβ1-42	10.9 ± 0.9	5.8 ± 0.6	1.1 ± 0.2	1.0 ± 0.1	1.6 ± 0.2	1.4 ± 0.3
Total Aβ	*329.1*	*331.7*	*32.4*	*29.1*	*33.7*	*24.0*

Table 3. Aβ levels in CSF. CSF was collected from the APP A673V patient at 4 different time-points. The results were compared to CSF from 20 controls and 20 sporadic AD.

3.3 Aβ pattern in amyloid

The analysis of amyloid from the patient carrying the APP A673V mutation showed a strong deposition of Aβ1-40 (792.0±4.4uA), which was the predominant species in the leptomeningeal compartment (75.4±0.1% of total Aβ). Conversely, Aβ1-42 was less abundant (22.6±0.4uA, corresponding to 2.2±0.1% of total Aβ).

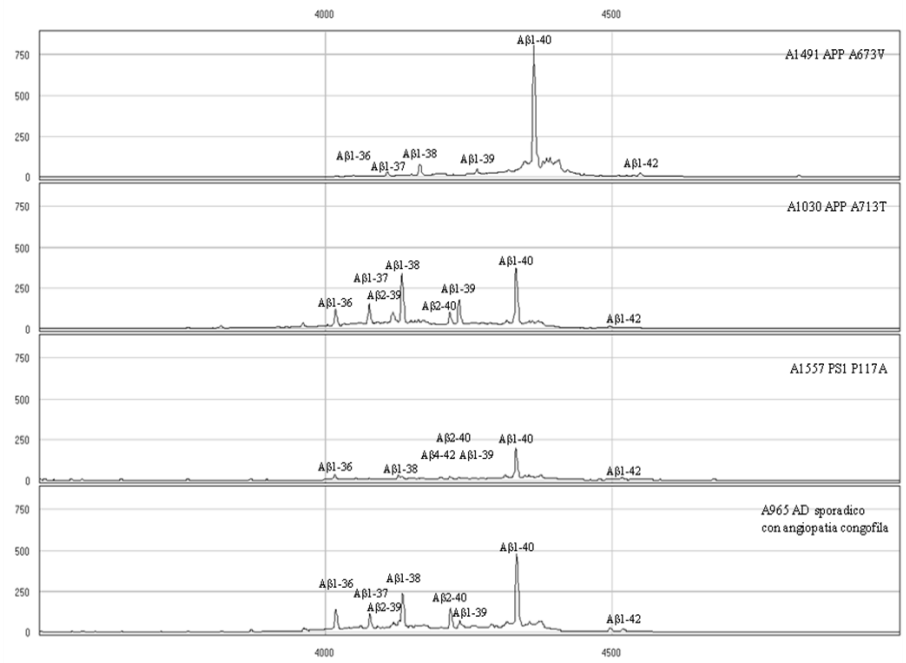

Figure 4. SELDI-TOF MS spectra of amyloid extracted from leptomeningeal vessels. In the APP A673V patient all the isoforms are shifted towards higher molecular weights because of the amino-acid substitution.

A panel of C-terminally truncated Aβ fragments contributed to amyloid composition; in particular, we found high levels of Aβ1-36 (10.6±0.1uA), Aβ1-37 (30.9±1.2uA), Aβ1-38 (73.7±2.5uA) and Aβ1-39 (47.5±1.6uA). Among N-terminally truncated fragments, only low levels of Aβ11-40 were detected (3.8±0.1uA) (Tables 4a, 4b).

Analyzing the SELDI-TOF spectra it was possible to observe a shifting of all the peptides carrying the APP A673V mutation towards higher molecular weights, due to the amino-acid substitution (Fig. 4, 5).

The analysis of amyloid from the patient carrying the A to T transition at codon 713 of APP, corresponding to position 42 of Aβ, showed high levels of Aβ1-40 (370.7±0.7uA), which is the most

abundant species (25.9% of total Aβ), while Aβ1-42 was almost undetectable (6.4±0.2uA, corresponding to 0.4% of total Aβ).

Very high amounts of C-terminally truncated peptides were measured; among them, Aβ1-36 (117.0±1.0uA), Aβ1-37 (149.3±0.9uA), Aβ1-38 (332.3±1.9uA) and Aβ1-39 (98.0±0.5uA) were the most abundant. Isoforms truncated at position 2 were also highly represented; in particular, Aβ2-37 (34.0±0.6uA), Aβ2-39 (98.0±0.5uA) and Aβ2-40 (99.3±0.3uA) were detected (Fig. 4, 5; Tables 4a, 4b).

In leptomeninges from the patient carrying the PS1 P117A mutation the total Aβ amount was lower compared to the other cases analyzed. Aβ1-40 was the most represented peptide (189.0±1.2uA, corresponding to 55.0% of total Aβ), but Aβ1-42 was also detected (16.0±1.2uA) and showed the highest relative percentage of total Aβ (4.6%), compared to the other AD cases.

Both N- and C-terminally truncated fragments were also present (Fig. 4, 5; Tables 4a, 4b). In this case an additional fragment, Aβ4-42 was detected.

The sporadic AD with ApoE ε4/ε4 genotype showed a profile very similar to APP A713T, with high amounts of Aβ1-40 (472.0±2.5uA, corresponding to 36.7% of total Aβ), C-terminally truncated isoforms Aβ1-36 (133.7±2.0uA), Aβ1-37 (107.7±0.9uA), Aβ1-38 (230.7±0.7) and Aβ1-39 (69.1±0.1), and peptides truncated at position 2 Aβ2-37 (25.5±0.4), Aβ2-39 (57.0±0.3) and Aβ2-40 (145.3±0.6) (Fig. 4, 5; Tables 4a, 4b) .

leptomeninges

Mean signal intensity (uA) ± SE					
Aβ peptide	MW	APP A673V	APP A713T	PS1 P117A	Sporadic AD
Aβ1-17	2068	0.0	17.2 ± 0.3	1.0 ± 0.0	6.4 ± 0.2
Aβ1-18	2166	0.0	30.6 ± 0.6	8.2 ± 0.1	20.1 ± 0.5
Aβ1-19	2314	0.0	2.1 ±0.1	1.7 ± 0.1	0.7 ±0.0
Aβ11-40	3151	3.8 ± 0.1	0.0	0.0	0.0
Aβ2-37	3957	0.0	34.0 ± 0.6	0.0	25.5 ±0.4
Aβ1-36	4017	10.6 ±0.1	117.0 ± 1.0	37.7 ± 0.4	133.7 ±2.0
Aβ1-37	4074	30.9 ± 1.2	149.3 ± 0.9	9.7 ± 0.4	107.7 ±0.9
Aβ2-39	4114	0.0	98.0 ± 0.5	0.0	57.0 ±0.3
Aβ1-38	4131	73.7 ± 2.5	332.3 ± 1.9	23.9 ± 0.4	230.7 ±0.7
Aβ4-42	4197	0.0	0.0	19.2 ± 0.3	0.0
Aβ2-40	4213	0.0	99.3 ± 0.3	21.4 ± 0.4	145.3 ± 0.6
Aβ1-39	4230	47.5 ± 1.6	175.3 ± 0.9	15.9 ± 0.2	69.1 ± 0.1
Aβ1-40	4329	792.0 ± 4.4	370.7 ±0.7	189.0 ± 1.2	472.0 ±2.5
Aβ1-42	4515	22.6 ±0.4	6.4 ± 0.2	16.0 ± 1.2	19.2 ±0.3

Table 4a. Aβ levels in amyloid extracted from leptomeningeal vessels.

leptomeninges

Relative Percentage (%)					
Aβ peptide	MW	APP A673V	APP A713T	PS1 P117A	Sporadic AD
Aβ1-17	2068	0.0	1.2	0.3	0.5
Aβ1-18	2166	0.0	2.1	2.4	1.6
Aβ1-19	2314	0.0	0.1	0.5	0.1
Aβ11-40	3151	0.4	0.0	0.0	0.0
Aβ2-37	3957	0.0	2.4	0.0	2.0
Aβ1-36	4017	1.1	8.2	11.0	10.4
Aβ1-37	4074	3.1	10.4	2.8	8.4
Aβ2-39	4114	0.0	6.8	0.0	4.4
Aβ1-38	4131	7.5	23.2	6.9	17.9
Aβ4-42	4197	0.0	0.0	5.6	0.0
Aβ2-40	4213	0.0	6.9	6.2	11.3
Aβ1-39	4230	4.9	12.2	4.6	5.4
Aβ1-40	4329	80.7	25.9	55.0	36.7
Aβ1-42	4515	2.3	0.4	4.6	1.5

Table 4b. Aβ levels in amyloid extracted from leptomeningeal vessels. Values are expressed as relative percentage of total Aβ.

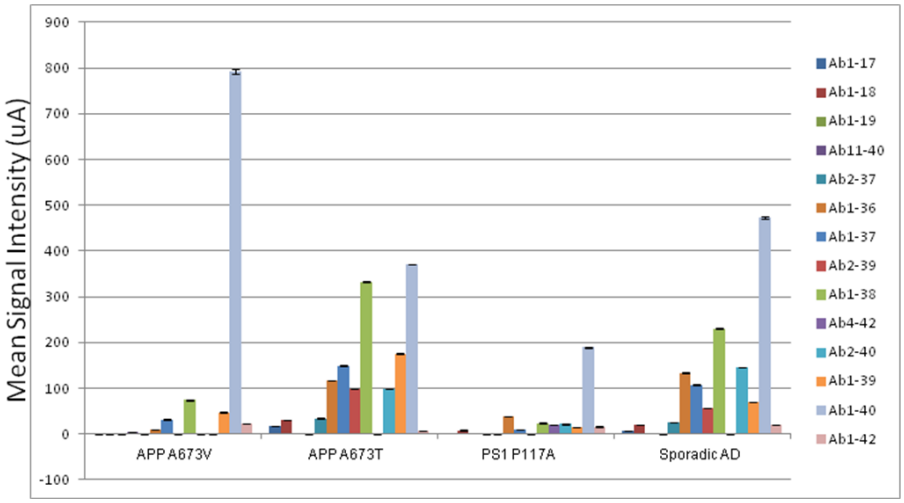

Figure 5. Graphical representation of Aβ levels in leptomeningeal amyloid.

4. Discussion

The neuropathological assessment of the brain from the patient carrying the homozygous APP A673V mutation revealed a distinctive pattern as compared to sporadic and familial AD. In fact, the amyloid deposits were larger than usual and had a peculiar localization, deeply affecting areas usually spared in AD, such as the cerebellum and the brainstem. Moreover, diffuse pre-amyloid plaques were absent, since there was a complete correspondence between the staining with antibodies specific to Aβ and the labeling of amyloid. This is probably due to the high propensity of mutated Aβ to aggregate, suggesting that the peptides that are released in the extracellular space are immediately captured and settle into plaques.

This peculiar picture induced us to determine how the A673V mutation causes the pathologic changes observed in the brain of the mutated patient. The study of brain fractions enriched with proteins with different solubility to detergents showed much higher levels of both Aβ40 and Aβ42 compared to sporadic AD, with a predominance of the shorter isoform and, as a consequence, a significant reduction in the Aβ42:Aβ40 ratio. These data agree with the neuropathological finding that the plaques are composed by both the isoforms, without the prevalence of Aβ42 that is usually observed in sporadic AD, and are also confirmed by SELDI TOF MS analysis on amyloid extracted from leptomeningeal vessels. SELDI TOF MS allowed us to extend the Aβ quantification to other isoforms, including N- and C-terminally truncated peptides. The APP A673V amyloid showed a peculiar composition, with high levels of the forms containing the mutation Aβ1-36, Aβ1-37, Aβ1-38, Aβ1-39, besides Aβ1-40, which is the most abundant peptide. Aβ1-42 is also represented, even if at lower levels. The accumulation of such fragments could be charged to the presence of the mutation, which makes the peptides more prone to aggregate. Interestingly, the isoforms starting at codon 2 are absent, probably because the mutation at the same residue inhibit the cleavage by the enzymes involved in Aβ degradation.

The APP A673V brain was compared to sporadic AD, and also to two familial cases, carrying APP A713T or PS1 P117A mutations. Both the ELISA measurements on brain fractions and SELDI TOF MS analysis of leptomeningeal amyloid showed that not only the APP A673V, but also the other familial brains, are characterized by a

distinctive amyloid composition, suggesting that, at least for familial AD, different types of amyloid exist.

The characterization of the APP A673V case was extended to CSF. SELDI TOF MS analysis showed a reduction of exactly the same fragments that accumulate in the patient's amyloid, including Aβ1-40 which doesn't change in sporadic AD, and the shorter C-terminally truncated species. CSF Aβ1-42 reduction is always observed in sporadic AD and is thought to be caused by sequestration of the peptide in senile plaques, which prevents the transport of soluble Aβ1-42 from the brain to the CSF. Previous studies found an inverse association between Aβ1-42 levels in CSF and amyloid deposition in the brain [6-8]; our observation validate this hypothesis showing that not only Aβ1-42, but all the isoforms which are reduced in CSF accumulate in the brain.

In summary, neuropathological changes observed in A673V homozygous carrier is paralleled by a peculiar biochemical profile, characterized by a distinctive distribution of Aβ in brain fractions and a composition of amyloid that differs from sporadic and familial AD.

The study confirmed that all the Aβ isoforms that accumulate in the brain are detracted from CSF pathway.

5. References

1. Di Fede G, Catania M, Morbin M, et al. A Recessive Mutation in the APP Gene with Dominant-Negative Effect on Amyloidogenesis. Science 2009;323:1473-7.

2. Giaccone G, Morbin M, Moda F, et al. Neuropathology of the recessive A673V APP mutation: Alzheimer disease with distinctive features. Acta Neuropathol 2010;120:803-12.

3. Steinerman JR, Irizarry M, Scarmeas N, et al. Distinct pools of beta-amyloid in Alzheimer disease-affected brain: a clinicopathologic study. Arch Neurol 2008;65:906-12.

4. Vidal RG, Ghiso J, Gallo G, Cohen M, Gambetti PL, Frangione B. Amyloidoma of the CNS. II. Immunohistochemical and biochemical study. Neurology 1992;42:2024-8.

5. Albertini V, Bruno A, Paterlini A, et al. Optimization protocol for amyloid-beta peptides detection in human cerebrospinal fluid using SELDI TOF MS. Proteomics Clin Appl 2010;4:352-7.

6. Strozyk D, Blennow K, White LR, Launer LJ. CSF Abeta 42 levels correlate with amyloid-neuropathology in a population-based autopsy study. Neurology 2003;60:652-6.

7. Fagan AM, Mintun MA, Mach RH, et al. Inverse relation between in vivo amyloid imaging load and cerebrospinal fluid Abeta42 in humans. Ann Neurol 2006;59:512-9.

8. Forsberg A, Engler H, Almkvist O, et al. PET imaging of amyloid deposition in patients with mild cognitive impairment. Neurobiol Aging 2008;29:1456-65.

Development of a novel therapy for AD based on the anti-amyloidogenic activity of the human A2V Aβ variant

1. Introduction

In vitro experiments with synthetic peptides showed that the APP A673V mutation has the peculiar feature of enhancing the fibrillogenic properties of the mutated peptide when it is incubated alone, but hindering amyloidogenesis when both wild-type and mutated Aβ are present in the mixture. Moreover, the co-existence of the two Aβ species reduces the toxicity of the wild-type peptide on human neuroblastoma cell cultures[1]. This finding has important implications for the development of a treatment for AD, based on the anti-amyloidogenic activity of this novel Aβ variant.

Adeno-associated viruses (AAV) are non pathogenic, single-stranded DNA Dependoiruses, which belong to Parvoviridae family [2]. They are able to transduce dividing as well as non-dividing cells, constituting a tool of choice for *in vivo* brain delivery. AAV vectors do not express any viral protein and are therefore devoid of inflammatory and immunogenic properties; as a consequence, cells transduced with AAV mantein the viral genome for long periods of time, ranging from several months to years [3]. Moreover, such vectors remain into the cell in episomal form, ensuring a long-term expression of the transgene without the problems associated with insertional mutagenesis.

More than 100 different AAV serotypes have been identified, displaying different biological properties in terms of vector yield and tropism for specific tissues, both *in vitro* and *in vivo* [4]. Among them, serotype 2 (AAV2) is the most prevalent in human population and is not associated with any known pathology [5]; different clinical trials are evaluating the therapeutic efficiency of engineered AAV2 for the treatment of Alzheimer's disease, Canavan's disease and Parkinson's disease (i.e., ES-008; UK-0181; US-0623; US-0930, from "Gene Therapy Clinical Trials Worldwide": http//www.abedia.com/wiley). However, more than 80% of humans may be exposed to AAV2, resulting in a pre-existing humoral immunity that limits the efficacy of the AAV2-based gene therapy [6]. Moreover, AAV2 has been demonstrated to have a limited distribution when injected into the brain. The recently studied non-human primate AAV serotypes 7, 8, 9 have shown to transduce higher amounts of cells and to have a massive spread in the brain, as compared to AAV2 [7]. Among them, it has been demonstrated that AAV9 has the highest *in vivo* intracerebral diffusion and transduction efficiency [8].

Previous studies in our laboratory showed that mouse brains injected with recombinant AAV9 expressing the β-galactosidase (AAV-βgal) reporter gene resulted in an abundant vector genome spread all over the brain (Fig. 1). The pattern of distribution suggested that the AAV-βgal was able to undergo axonal transport; in fact, although the injection was unilateral, βgal activity was also detected in the controlateral hemisphere, with potential benefits for the treatment of neurodegenerative diseases, which usually affect the whole brain.

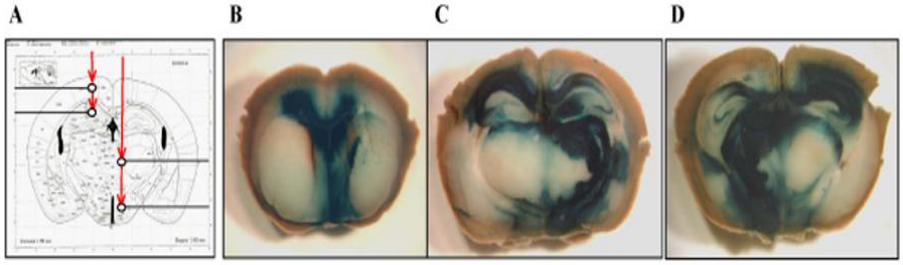

Figure 1. **Stereomicroscopic detection of βgal activity.** The brain are from mice sacrified one month after injection into the cerebral cortex, thalamus, hyppocampus and hypothalamus (A). Septum (B) and caudal diencephalon (C and D) are transduced.

APP23 mouse line is a very appropriate model for investigating pathogenic mechanisms of Alzheimer's disease involving APP and Aβ peptide because of the massive production of amyloid deposits in the brain of these mice. The first amyloid plaques appear at six months of age in the frontal cortex and rapidly extend to the entire neocortex and the hippocampus. In very old mice (24-36 months) all brain regions show the presence of at least some plaques, except for the cerebellum; the white matter and the cerebral vasculature are also involved[9].

In this work we investigated the ability of Aβ1-40 carrying the A2V substitution to interfere with amyloid deposition in the brain of a mouse model of AD. We injected the animals' brains with AAV9 engineered for the expression of the wild-type or the mutated Aβ peptide and we studied the effects resulting from the interaction between the transgene codified by AAV9 and the human Aβ peptide produced by the mouse. For the experiments we chose a novel line of transgenic mice that we generated by crossing APP23 with animals

lacking murine APP transcription (moAPPko), in order to obtain mice expressing high levels of human APP but not the endogenous murine gene (APP23/moAPPko).

2. Materials and Methods

2.1 Animal facility

Animal facility is licensed and inspected by the Italian Ministry of Health. Current animal husbandry and housing practices comply both with the Council of Europe Convention ETS123 (European convention for the protection of vertebrate animals used for experimental and other scientific purposes; Strasbourg, 18.03.1986) - Italian Legislative Decree 116/92, Gazzetta Ufficiale della Repubblica Italiana 10, 18.02.1992, and with the 86/609/EEC (Council Directive of 24.11.1986 on the approximation of laws, regulation and administrative previsions of the Member States regarding the protection of animals used for experimental and other scientific purposes).

Animals are housed in groups of 2-5 in individually ventilated cages taking into account their sociable compatibility (dominance, sex, ratio). Mice are daily fed with special diet food and water is provided *ad libitum*. Lighting is on an automatic 12 hours basis, including dawn and dusk steps. Changes are performed weekly and regular veterinary visits and consulting services are provided.

2.2 Animal strains

APP23, which express human APP carrying the double Swedish mutation at position 670/671, and APP knock-out mice were kindly

provided by Dr. Efrat Levy from Nathan Kline Institute in New York. Animals from the two transgenic lines were crossed and selected in order to obtain mice with hemizygous expression of human APP on a background knock-out for endogenous murine APP (APP23/moAPPko).

Mice were inoculated when they were ten months old and sacrificed one or three months after the injection.

2.3 AAV engineering

Four minigenes expressing human Aβ1-40, wild-type or carrying the A2V substitution, either with or without a mouse synthetic secretion signal peptide (SP) (MLPSLALLLLAAWTVRA), all including an artificial stop codon, were generated. The sequence codifying for wild-type human Aβ1-40 was amplified from amyloid precurson protein cDNA and cloned either alone or in frame with SP into pcDNA3.1(-) plasmid (Invitrogen). Aβ1-40 peptides lacking SP were added with an artificial methionine at their amino-terminus, in order to allow the transcription start. Aβ1-40 carrying the A to V substitution at position 2 was obtained by site-directed mutagenesis using Quickchange Site-Directed Mutagenesis Kit (Stratagene). The minigenes were recovered from pcDNA3.1(-) and subcloned into pAAV-MCS plasmid (AAV Helper Free System, Stratagene). These constructs were used to engineer AAV9 vector by the triple transfection method in HEK293A cells in collaboration with the International Centre for Genetic Engineering and Biotechnology (ICGEB) of Trieste. pAAV-MCS was co-transfected along with the Helper plasmid, containing either the wild-type AAV genome without

the viral inverted terminal repeat sequences (ITRs), and the ITR transgene cassette plasmid (pITR). Three days after transfection, cells were lysated and the AAV were isolated from the solution on a CsCl gradient centrifugation. Dialysis of CsCl fractions containing AAV against a physiological buffer was necessary before the in vivo analysis because CsCl can exert toxic effects on animals. To measure the physical titer (here defined as the number of packaged recombinant AAV genomes/ml), a small volume of each fraction was treated with DNase I in order to eliminate possible unpackaged DNA, followed by digestion with proteinase K to remove the capsid proteins. DNA quantification was performed by real-time PCR, using the TaqMan technology. The primers for PCR amplification and the fluorescent internal probe have been designed in order to recognize target sequences inside the CMV promoter.

2.4 Evaluation of the efficacy of engineered pAAV-MCS plasmid to synthesize Aβ1-40

The ability of pAAV-MCS-Aβ1-40 to express the transgenic protein was evaluated on a human neuroblastoma cell model. Briefly, SH-SY5Y cells were grown in DMEM/F12 (Gibco) supplied with 10% Fetal Bovine Serum (FBS, Gibco). 90% confluent cells were transiently transfected with the plasmids by using Lipofectamine 2000 (Invitrogen) in Optimem (Gibco) without serum. Six hours after transfection, the medium was replaced with fresh Optimem. 48h later, the medium was collected and added with Complete Protease Inhibitors Mini (Roche); cells were harvested and lysed in RIPA buffer (50mM Tris-HCl pH=7.5, 150mM NaCl, 1%Nonidet P40,

0.5%Sodium deoxycholat, 0.1%SDS, protease inhibitors). Aβ was measured in both medium and cell lysates by enzyme-linked immunosorbent assay (ELISA) (Aβ40 Human ELISA kit, Invitrogen), according to manifacture's instructions.

2.5 Surgical procedures for AAV injection

Mice were anaesthetized by intraperitoneal injection of tribromoethanol (Avertin®, 100µl/10g). Under sterile conditions, the subject was shaved and cleaned at the site of surgery and placed in position in a stereotaxic holder (Lab Standard Stereotaxic), using the appropriate mouse/neonatal rat holding platform (Cunningham, Lab Standard from 2 Biological Instrument) and ear bars. The body temperature was maintained by the use of a heat lamp positioned shining off to the side of the cage. A small incision was made in the skin and a swab soaked with a 5% hydrogen peroxide solution was used to clean the tissue from the skull. The position of the syringe's needle (Hamilton Syringes, G26S) was adjusted so that it lines up with the animal's bregma, the needle was adjusted to the coordinates relative to the bregma determined by using "The Mouse Brain, in Stereotaxic Coordinates" by Keith B. J. Franklin and George Paxinos, Academic Press. A micro-drill (Minicraft) was used to punch the skull and the needle was inserted through the incision. The engineered AAV was injected at a rate of 1µl/2min by manual pression of the syringe plunger. Before extracting the needle we waited several minutes (five or more). The incision was closed by autoclip wound closing system (2 Biological Instrument) and antibiotic cream as well as lidocaine was applied to the wound.

2.6 Stereotaxical coordinates

Mice were inoculated into the right hemisphere with 2µl of AAV9 engineered for the expression of one among the following peptides: wild-type Aβ1-40 with SP ($7.9X10^{11}$ U/ml), A2V Aβ1-40 with SP ($8.7X10^{11}$ U/ml), wild-type Aβ1-40 without SP ($7.2X10^{11}$ U/ml), A2V Aβ1-40 without SP ($9.0X10^{11}$ U/ml). Inoculations were carried out in four different areas following these stereotaxical coordinates: septum (0.38 caudal; 0.50 lateral; 3.50 depth) and overlying cortex (0.38 caudal; 0.50 lateral; 1.50 depth), hippocampus (1.94 caudal; 1.00 lateral; 2.00 depth) and overlying cortex (1.94 caudal; 1.00 lateral; 0.8 depth).

At least 5 transgenic and 2 non transgenic animals were injected for each group. Control mice were treated with void vector. A group of mice did not receive any treatment.

2.7 Post surgical care

Initial post surgical care included observing the animals to ensure uneventful recovery from the anesthesia and surgery. The incision site was closely monitored daily until the skin healed. If necessary, topical antibiotics were used.

2.8 Sacrifice

Mice were sacrificed one and three months after the injection. Animals were first anesthetized with Tiletamine-Zolazepam (0,5mg/10g), and then intracardiac injection of Embutramide (0,2ml) was performed. Each organ was collected and processed for histological analysis.

2.9 Histological and immunohistochemical analysis

The brains were collected, fixed in 3% Paraformaldehyde at room temperature for 48 hours, cut in 1mm coronal sections, dehydrated and embedded in paraplast. Five-µm thick serial sections from paraffin-embedded tissues were stained with hematoxylin-eosin (H&E) or probed with 4G8 antibody.

2.10 Immunohistochemical staining

Sections were pre-treated with 70% Formic Acid at room temperature for 10 minutes and immunostained with the monoclonal anti-Aβ antibody (Signet, 1:1000).

2.11 Images capture

Stained sections were examined on a Nikon Eclipse E800 microscope, images captured using a Nikon Digital Camera DXM1200 and analyzed with NIS-elements software.

3. Results

3.1 Temporal profile of amyloidosis in APP23/moAPPko mice

The immunohistochemical analysis showed that APP23/moAPPko mice develop intracellular Aβ deposits at 4-5 months of age and initial amyloid formation at 9-11 months. They exhibit extensive plaque deposits throughout the neocortex and hippocampus, as well as neuronal loss in the hippocampal CA1 region, at 13-15 months (Fig. 2).

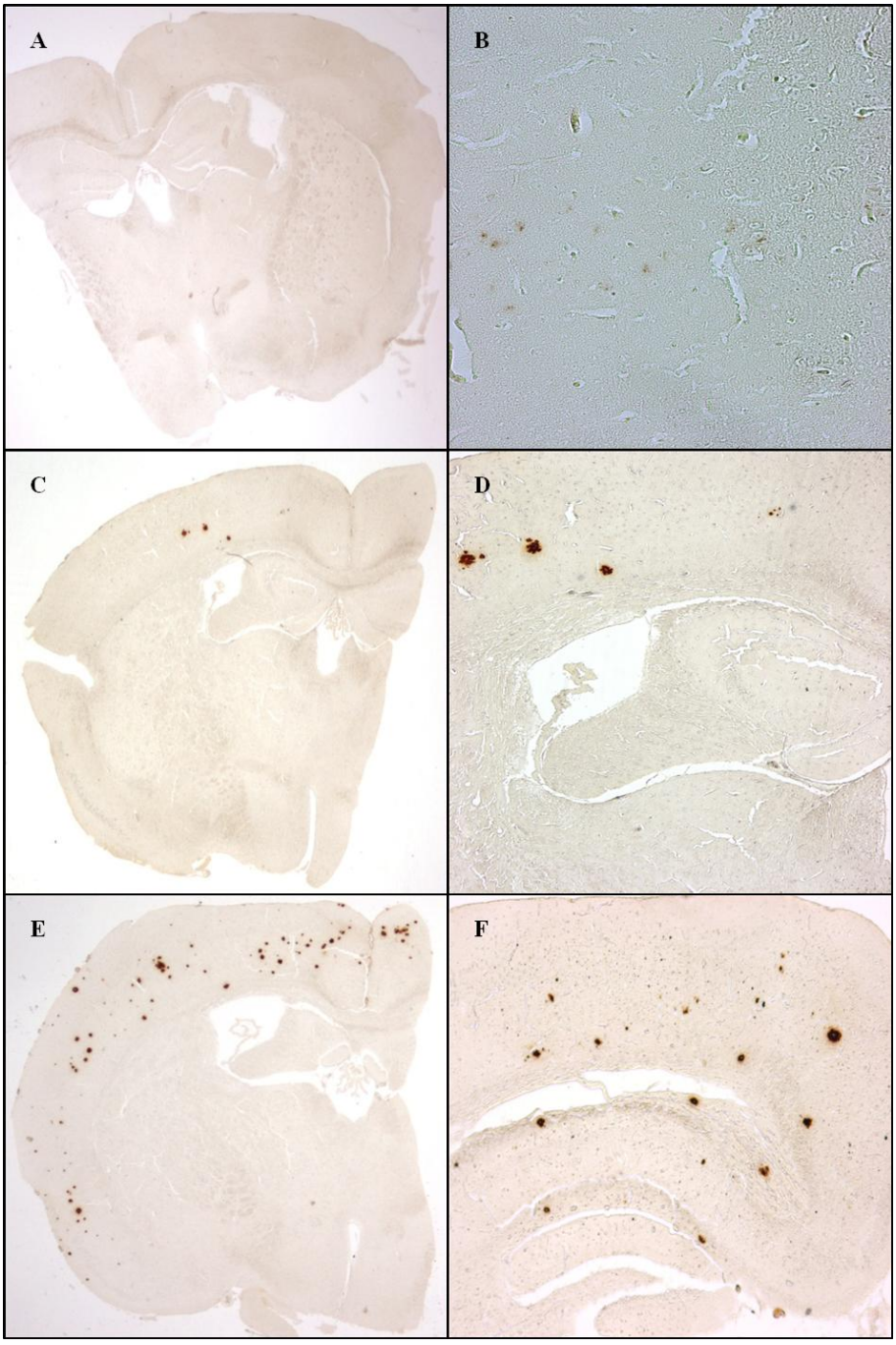

Figure 2. Neuropathologic assessment of APP23/moAPPko mice. A (1X) and B (4X): motor cortex from 4 months old mice; C (1X) and D (4X): motor cortex from 11 months old mice; E (1X) and F (20X): motor cortex from 13 months old mice.

3.2 Assessment of Aβ levels expressed by engineered AAV in cell models

The measurement of Aβ1-40 in media and cell lysates of transfected cells showed that in SH-SY5Y cells transfected with pAAV-MCS-Aβ1-40 with SP the transgenic protein accumulates in the media. Conversely, cells transfected with pAAV-MCS-Aβ1-40 without SP are enriched with Aβ in cell lysates (Fig. 3, Table 1). Non transfected cells have low levels of the protein both in the medium and in cell lysate (Table 1).

This result suggests that pAAV-MCS plasmid engineered for the expression of human Aβ is able to induce the expression of the peptide. Moreover, the presence of the signal peptide allows the transgenic protein to be secreted out of the cells. Indeed, the plasmids we have generated are suitable for being used in further experiments.

Plasmid		Medium (pg/200mg of proteins)	Cell lysate (pg/10000mg of proteins)
Non transfected cells		12.8	15.4
pAAV-MCS-SP-Aβ1-40	Wt	126.6	31.3
	A2V	178.4	16.0
pAAV-MCS-Met-Aβ1-40	Wt	22.8	155.0
	A2V	22.2	91.4

Table 1. Aβ1-40 measurement in media and cell lysates from transiently transfected SH-SY5Y cells.

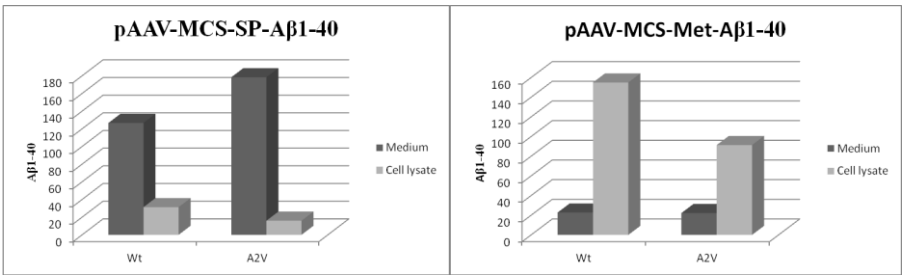

Figure 3. Graphical representation of Aβ levels in media and cell lysates from transfected SH-SY5Y cells. Aβ1-40 levels are expressed as pg/200mg of total proteins in the medium and as pg/10000mg of total proteins in cell lysates.

3.3 Inhibition of amyloidogenesis in APP23/moAPPko mice injected with AAV9-Aβ1-40

Immunohistochemical analysis of animals sacrificed 1 month after AAV9 injection showed no differences both between treated and untreated animals and among groups injected with different AAV9-Aβ1-40 (data not shown).

Among animals sacrificed 3 months after AAV9 injection, the groups treated with AAV9-Met-Aβ1-40 showed a very interesting behavior. Indeed, mice that had received wild-type Aβ1-40 peptide were similar to untreated animals, while those injected with A2V Aβ1-40 displayed a marked reduction in amyloid deposits compared to controls (Fig. 4).

Groups treated with AAV-SP-Aβ1-40 showed less amyloid deposits than untreated animals, with no substantial difference between injection of wild-type and A2V Aβ. However, the reduction of Aβ deposition was not so important as in mice treated with AAV9-Met-Aβ1-40.

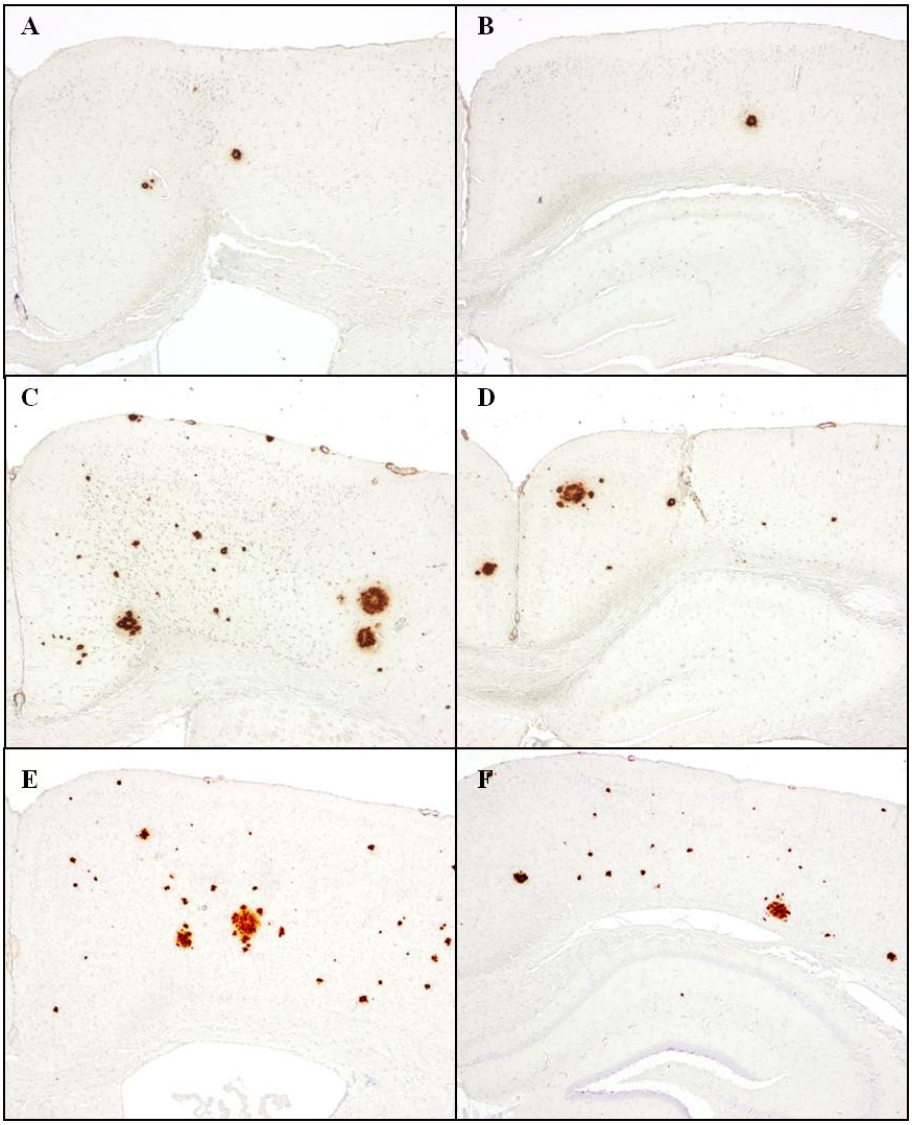

Figure 4. Immunohistochemical analysis of mice injected with AAV engineered for the expression of human Aβ1-40. Neocortex (A, C, E) and hippocampus and overlying cortex (B, D, F) from mice treated with A2V AAV-Aβ1-40 (A, B), with wt AAV-Aβ1-40 (C, D) or with the void vector (E, F) probed with 4G8 antibody. Treatment with A2V Aβ1-40 resulted in a remarkable reduction of Aβ deposits compared to mice treated with wt Aβ1-40 or the void vector.

4. Discussion

The histological and immunohistochemical analysis of aged APP23/moAPPko mice showed that in the brain of these animals the evolution of the changes associated with AD is slower than in APP23 mice previously described[9]. This result may be due to the lack of the endogenous murine APP, even if the modality is not clear, or to the obvious differences that can be found when the same mouse line is raised in different animal facilities. APP23/moAPPko line was used in the present work in order to avoid a possible interaction between the endogenous murine and the transgenic human APP, which could affect the interaction between human wild-type and mutated Aβ.

In this work 10 months old APP23/moAPPko mice, which show abundant intracellular assemblies and an initial extracellular amyloid deposition, were injected with AAV9 engineered for the expression of wild-type or A2V mutated human Aβ, preceded or not by a signal peptide whose task is to lead the secretion of the protein out of the cell. This double strategy allowed us to test the ability of the transgenic peptide to interfere either with the intracellular accumulation or with the extracellular plaque formation. In the animals injected with A2V Aβ1-40 without the signal peptide we observed a marked reduction of amyloid deposits, in comparison to both untreated animals and mice injected with wild-type Aβ.

Previous studies performed in our laboratory with synthetic peptides and cell models[1]had shown that the co-existence of wild-type and A2V Aβ is able to hinder amyloidogenesis and to reduce Aβ toxicity *in vitro*. Distinct from previous approaches based on

theoretical grounds, our strategy stems from the clinical observation that a naturally-occurring variant of Aβ protects from disease.

The inteference with amyloid deposition of A2V Aβ delivered by AAV may represent a "proof of concept", demonstrating that the anti-amyloidogenic activity of the mutated peptide occurs not only *in vitro*, but also *in vivo*. In fact, the mutated Aβ delivered by AAV9 interacts with the wild-type Aβ codified by the transgenic APP23/moAPPko mice and reduces its deposition in brain tissue under the form of amyloid plaques.

In mice treated with A2V-Aβ1-40 preceded by the signal peptide we observed a weak reduction of amyloid deposition, without significant differences between animals injected with wild-type or A2V Aβ. This finding suggests that the interaction of Aβ expressed by AAV and the endogenous protein is more efficient when occurring inside the cell than after Aβ secretion.

These results must be considered as preliminary; the study will be amplified including a larger number of animals to confirm the reduction of amyloid deposition due to A2V Aβ injection. Moreover, since Aβ toxicity is supposed to be caused not only by insoluble plaques but also, and probably primarily, by soluble oligomers[10-12], the amount and pattern of oligomeric assemblies will be evaluated in treated and untreated mice. If confirmed, the finding here described may pave the way for the exploitment of the A2V Aβ anti-amyloidogenic activity in order to develop a novel disease-modifying treatment for Alzheimer's disease.

5. References

1. Di Fede G, Catania M, Morbin M, et al. A Recessive Mutation in the APP Gene with Dominant-Negative Effect on Amyloidogenesis. Science 2009;323:1473-7.

2. Mayor HD, Melnick JL. Small deoxyribonucleic acid-containing viruses (picodnavirus group). Nature 1966;210:331-2.

3. Athanasopoulos T, Fabb S, Dickson G. Gene therapy vectors based on adeno-associated virus: characteristics and applications to acquired and inherited diseases (review). Int J Mol Med 2000;6:363-75.

4. Gao G, Vandenberghe LH, Wilson JM. New recombinant serotypes of AAV vectors. Curr Gene Ther 2005;5:285-97.

5. Chirmule N, Propert K, Magosin S, Qian Y, Qian R, Wilson J. Immune responses to adenovirus and adeno-associated virus in humans. Gene Ther 1999;6:1574-83.

6. Mastakov MY, Baer K, Symes CW, Leichtlein CB, Kotin RM, During MJ. Immunological aspects of recombinant adeno-associated virus delivery to the mammalian brain. J Virol 2002;76:8446-54.

7. Mandel RJ, Manfredsson FP, Foust KD, et al. Recombinant adeno-associated viral vectors as therapeutic agents to treat neurological disorders. Mol Ther 2006;13:463-83.

8. Otto M, Cepek L, Ratzka P, et al. Efficacy of flupirtine on cognitive function in patients with CJD: A double-blind study. Neurology 2004;62:714-8.

9. Sturchler-Pierrat C, Staufenbiel M. Pathogenic mechanisms of Alzheimer's disease analyzed in the APP23 transgenic mouse model. Ann N Y Acad Sci 2000;920:134-9.

10. Lambert MP, Barlow AK, Chromy BA, et al. Diffusible, nonfibrillar ligands derived from Abeta1-42 are potent central nervous system neurotoxins. Proc Natl Acad Sci U S A 1998;95:6448-53.

11. Gong Y, Chang L, Viola KL, et al. Alzheimer's disease-affected brain: presence of oligomeric A beta ligands (ADDLs) suggests a molecular basis for reversible memory loss. Proc Natl Acad Sci U S A 2003;100:10417-22.

12. Shankar GM, Bloodgood BL, Townsend M, Walsh DM, Selkoe DJ, Sabatini BL. Natural oligomers of the Alzheimer amyloid-beta protein induce reversible synapse loss by modulating an NMDA-type glutamate receptor-dependent signaling pathway. J Neurosci 2007;27:2866-75.

Summary, conclusions and future perspectives

We have recently identified a novel APP mutation, the A to V substitution at codon 673 (APP 770 numbering), which differs from all the other genetic defects associated to AD, as it causes the disease only in the homozygous state, while heterozygous carriers are never affected, neither in advanced age. This is consistent with a recessive trait of inheritance.

In vitro studies showed that the mutation has a double pathogenic effect: it shifts the APP processing towards the amyloidogenic pathway and it enhances the fibrillogenic properties of Aβ.

The histological and immunohistochemical analysis of the brain from the patient carrying the homozygous A673V mutation in the APP gene revealed a distinctive neuropathological picture. In particular, Aβ deposits differ from both sporadic and familial cases, since they are of large size and perivascular, and they deeply affect areas usually spared in AD, such as the cerebellum and the brainstem. The staining with antibodies specific to Aβ and the labeling of amyloid showed a complete correspondence, suggesting that diffuse, pre-amyloid plaques are absent, and confirming the high propensity to aggregate of the mutated peptide. Moreover, the staining with antibodies that specifically recognize either Aβ40 or Aβ42 showed that the senile plaques are composed by both the isoforms, without the prevalence of Aβ42 that is usually observed in AD brains.

The biochemical study performed on brain homogenates and amyloid extracted from leptomeningeal vessels indicated that the molecular profile of the patient carrying the A673V mutation is

different from both sporadic and familial AD cases. In fact, it shows a distinctive distribution of Aβ peptides in brain homogenate fractions, with a prevalence of Aβ40, especially in SDS-soluble and insoluble fractions, with a significant decrease of Aβ42:Aβ40 ratio. Moreover, the distribution of full-length and N- or C-terminally truncated Aβ isoforms is peculiar: Aβ1-40 is again the most abundant species and the shorter isoforms Aβ1-36, Aβ1-37, Aβ1-38, Aβ1-39, which include the mutation, are also well represented. This could be due to the high propensity of mutated peptides to aggregate and settle in amyloid plaques. Interestingly, the isoforms beginning at position 2 are absent, probably because the mutation inhibits the cleavage at this position.

Actually, the comparison of the biochemical profiles of sporadic and familial AD revealed that a wide heterogeneity is detected among familial and also among sporadic cases. This finding paralleles the phenotypic heterogeneity found in AD; it is known that AD clinical and neuropathological phenotype, as well as the progression of disease, are not the same for all patients and that different subjects show different responses to therapeutic treatments.

If confirmed, our findings could contribute to unveil the molecular basis of such phenotypic variability. In order to achieve this goal, we planned to extend the analysis of amyloid profile to a large number of sporadic and familial AD brains, trying to identify sub-groups with similar profiles and to compare them with clinical features and drug responsiveness.

In vitro studies of electron microscopy with synthetic peptides showed that the incubation of an equimolar mixture of wild-type and

A2V Aβ resulted in a reduction of the peptide's polymerization. Laser-light scattering experiments demonstrated that the co-incubation of the two species generated very unstable aggregates, that could be easily dissolved. Moreover, the toxicity of the peptide mixture on human neuroblastoma cells was lower not only than the mutated, but also than the wild-type Aβ when incubated alone. All these findings could explain why A673V heterozygous carriers are not affected and indicate that the co-existence of A2V and wild-type Aβ could even be protective against AD.

To test if the inhibition by the mutated peptide on wild-type Aβ polymerization may be used as a novel therapeutic strategy to AD, we performed an *in vivo* experiment studying the effects of A2V Aβ1-40 when delivered to the brain of AD mouse models. We observed a marked reduction of amyloid deposits in animals injected with mutated Aβ, compared to untreated littermates. Interestingly, mice were treated at ten months of age, when amyloid plaques are already present. This suggests that the mutated peptide prevents endogenous Aβ deposition and is probably able also to disrupt Aβ aggregates.

To turn this finding into a therapeutic approach we are testing the anti-amyloidogenic activity of synthetic short peptides composed by D amino-acids and carrying the A2V substitution, in order to minimize the degradation of the protein during the delivery to the brain and to reduce the immune response elicited by the drug. Preliminary experiments allowed us to identify a six-residue peptide (Aβ1-6, D-isomer) that effectively hinders amyloidogenesis *in vitro*. Next step will be the selection of suitable carriers for the delivery to

the brain. Golden nanoparticles or TAT-peptides have been preliminary identified.

The characterization of the APP A673V mutation on the one side allowed us to shed light on pathogenic mechanisms involved in AD and, on the other side, offered the molecular basis to develop a novel disease-modifying therapy for AD.

Publications

A Recessive Mutation in the APP Gene with Dominant-Negative Effect on Amyloidogenesis

Giuseppe Di Fede, Marcella Catania, Michela Morbin, Giacomina Rossi, Silvia Suardi, Giulia Mazzoleni, Marco Merlin, Anna Rita Giovagnoli, Sara Prioni, Alessandra Erbetta, Chiara Falcone, Marco Gobbi, Laura Colombo, Antonio Bastone, Marten Beeg, Claudia Manzoni, Bruna Francescucci, Alberto Spagnoli, Laura Cantù, Elena Del Favero, Efrat Levy, Mario Salmona, Fabrizio Tagliavini

Science, 2009 Mar 13;323(5920):1473-7

Neuropathology of the recessive A673V APP mutation: Alzheimer disease with distinctive features

Giorgio Giaccone, Michela Morbin, Fabio Moda, Mario Botta, Giulia Mazzoleni, Andrea Uggetti, Marcella Catania, Maria Luisa Moro, Veronica Redaelli, Alberto Spagnoli, Roberta Simona Rossi, Mario Salmona, Giuseppe Di Fede, Fabrizio Tagliavini

Acta Neuropathol. 2010 Dec;120(6):803-12. Epub 2010 Sep 15.